

Performance of Quadrature Amplitude Modulation in Nakagami Fading Channels with Diversity

by

Furaih Fayiz Al-Shalan

A Thesis Presented to the

FACULTY OF THE COLLEGE OF GRADUATE STUDIES

KING FAHD UNIVERSITY OF PETROLEUM & MINERALS

DHAHRAN, SAUDI ARABIA

In Partial Fulfillment of the
Requirements for the Degree of

MASTER OF SCIENCE

In

ELECTRICAL ENGINEERING

March, 2000

INFORMATION TO USERS

This manuscript has been reproduced from the microfilm master. UMI films the text directly from the original or copy submitted. Thus, some thesis and dissertation copies are in typewriter face, while others may be from any type of computer printer.

The quality of this reproduction is dependent upon the quality of the copy submitted. Broken or indistinct print, colored or poor quality illustrations and photographs, print bleedthrough, substandard margins, and improper alignment can adversely affect reproduction.

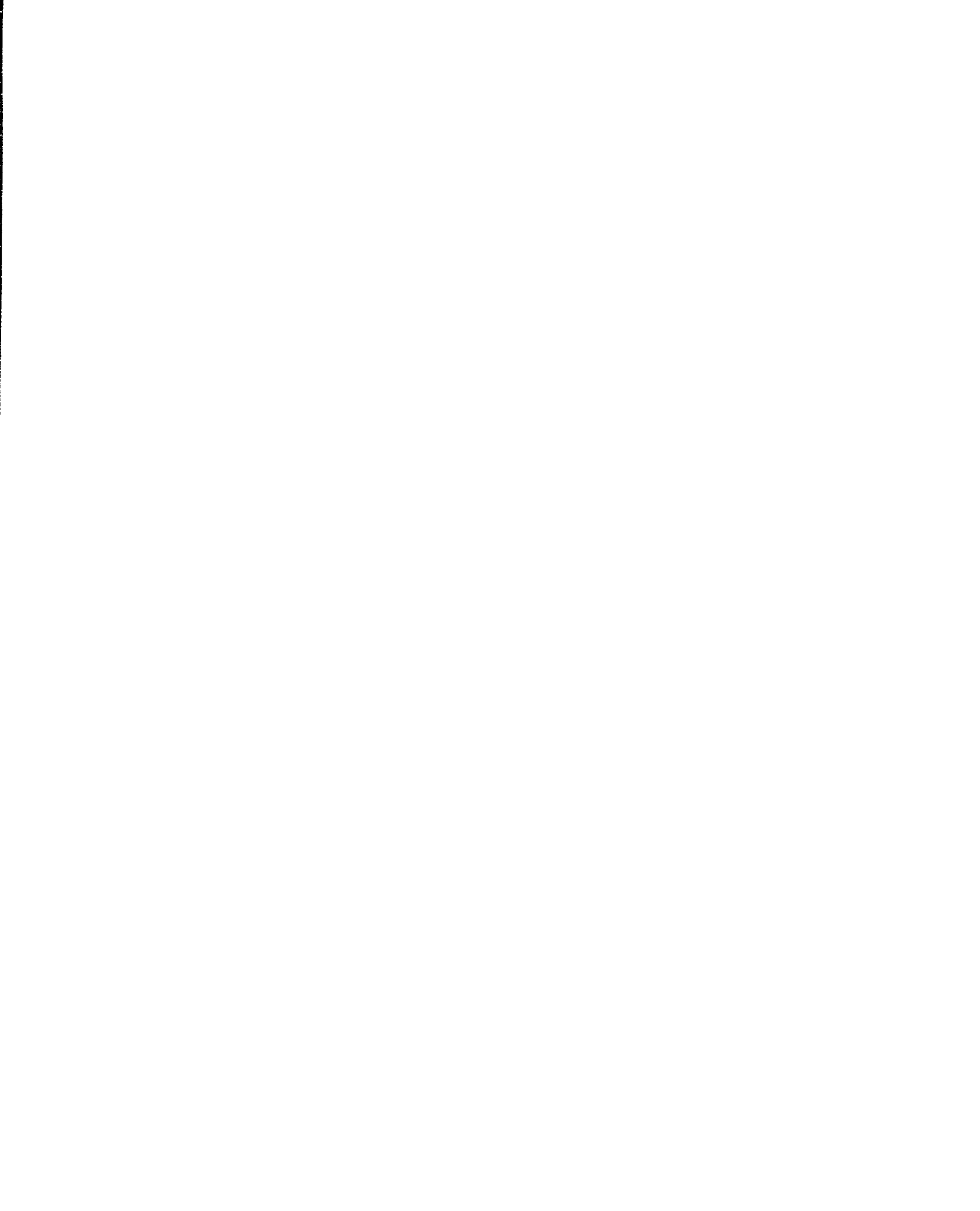
In the unlikely event that the author did not send UMI a complete manuscript and there are missing pages, these will be noted. Also, if unauthorized copyright material had to be removed, a note will indicate the deletion.

Oversize materials (e.g., maps, drawings, charts) are reproduced by sectioning the original, beginning at the upper left-hand corner and continuing from left to right in equal sections with small overlaps.

Photographs included in the original manuscript have been reproduced xerographically in this copy. Higher quality 6" x 9" black and white photographic prints are available for any photographs or illustrations appearing in this copy for an additional charge. Contact UMI directly to order.

**Bell & Howell Information and Learning
300 North Zeeb Road, Ann Arbor, MI 48106-1346 USA
800-521-0600**

UMI[®]



**PERFORMANCE OF QUADRATURE AMPLITUDE
MODULATION IN NAKAGAMI FADING
CHANNELS WITH DIVERSITY**

BY

FURAIH FAYIZ AL-SHALAN

A Thesis Presented to the
DEANSHIP OF GRADUATE STUDIES

KING FAHD UNIVERSITY OF PETROLEUM & MINERALS

DHAHRAN, SAUDI ARABIA

In Partial Fulfillment of the
Requirements for the Degree of

MASTER OF SCIENCE

In

ELECTRICAL ENGINEERING

MARCH 2000

UMI Number: 1399746

UMI[®]

UMI Microform 1399746

Copyright 2000 by Bell & Howell Information and Learning Company.

All rights reserved. This microform edition is protected against
unauthorized copying under Title 17, United States Code.

Bell & Howell Information and Learning Company
300 North Zeeb Road
P.O. Box 1346
Ann Arbor, MI 48106-1346

KING FAHD UNIVERSITY OF PETROLEUM AND MINERALS

DHAHRAN, SAUDI ARABIA

DEANSHIP OF GRADUATE STUDIES


This thesis, written by

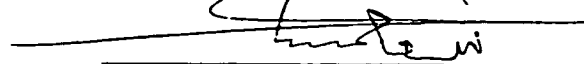
FURAIH FAYIZ AL-SHALAN

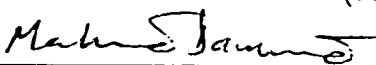
under the direction of his Thesis Advisor and approved by his Thesis Committee, has been presented to and accepted by the Dean of Graduate Studies, in partial fulfillment of the requirements for the degree of

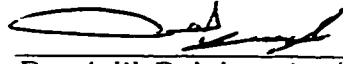
MASTER OF SCIENCE IN ELECTRICAL ENGINEERING


Thesis Committee

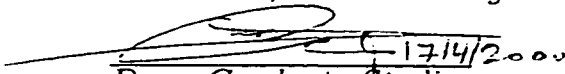

Dr. Maan A. Kousa (Chairman)


Dr. Saud A. Al-Semari (Member)


Dr. Mahmoud M. Dawoud (Member)


Dr. Adil Balghonaim (Member)


Chairman, Electrical Engineering


Dean, Graduate Studies



Dedicated To

His Royal Highness, Prince Sultan ibn Khalid Al-Faisal

Acknowledgement

Praise be to God, the most gracious and the most merciful. Without his blessing and guidance my accomplishments would never have been possible. Acknowledgment is due to King Fahd University of Petroleum and Minerals for support of this research. I would like to thank my thesis adviser, Dr. Maan Kousa for his guidance and patience. I am also grateful to Dr. Saud A. Al-Semari for his full support and constant encouragement and advice both in technical and non-technical matters. I would also like to thank the other members of the thesis committee, Dr. Mahmoud M. Dawoud and Dr. Adil Balghonaim for their constructive criticisms, helpful suggestions and kind cooperation.

I would like to thank Dr. Abdullah Al-Shehri the Dean of Graduate studies for his support and encouragement. I am thankful to Mr. Adinoyi for his comments and valuable discussions and I am also thankful to my friends Mr. Lahouari and Chenaoua for what they did.

I am grateful to Saudi Telecom Company for giving me the opportunity to pursue my Master degree and in particular, his excellency Gaddah A. Hassousah the general manager of Al-Jouf district for his support, encouragement and patience.

Last, but not the least, I would like to thank my parents, my wife, and all my family members for their support. In reality this thesis is theirs too.

LIST OF SYMBOLS

$\varphi_n(t)$	Angle of incidence of nth plane wave.
$a_n(t)$	Amplitude of nth plane wave.
$\tau_n(t)$	Arrival time of plane wave.
$f_{D,n}$	Doppler shift.
R_c	Delay power spectrum.
T_m	Multipath spread of the channel.
$R_c(\Delta f)$	Spaced-frequency correlation function.
$(\Delta f)_c$	Coherence bandwidth of the fading channel.
T_s	Symbol time duration.
W	Signal bandwidth.
$S(\lambda)$	Doppler power spectrum.
$R_c(\Delta t)$	Spaced-time correlation function.
$(\Delta t)_c$	Coherence time of the fading channel.
$S_c(\tau; \lambda)$	Scattering function.
$\alpha(t)$	Envelop of the fading channel.
$\theta(t)$	Phase of the fading channel.
Ω	Average power of the envelop.
K	Rician factor.
m	Nakagami parameter.
GMSK	Gaussian Minimum Shift Keying.
FM	Frequency Modulation.
GSM	Global System for Mobile.
DECT	Digital European Cordless Telephone.
QAM	Quadrature Amplitude Modulation.
MRC	Maximum Ratio Combiner.
EGC	Equal Gain Combiner.
SC	Selection Combiner.
GSC	Generalized Selection Combiner.
M	Modulation size.
AWGN	Additive White Gaussian Noise.
L	Number of diversity channels.
SNR	Signal to Noise ratio.
γ	Instantaneous signal to noise ratio.
$\bar{\gamma}$	Average signal to noise ratio.
γ_{mrc}	Instantaneous SNR for MRC.
γ_{egc}	Instantaneous SNR for EGC.
γ_{sc}	Instantaneous SNR for SC.

Contents

Abstract(English)	xiv
Abstract(Arabic)	xv
1 INTRODUCTION	1
1.1 Multipath Fading Channels	1
1.1.1 Mathematical Model of the Fading Channel	2
1.1.2 Statistical Channel Correlation Functions	3
1.1.3 Statistical Models of Flat Fading Channels	6
1.2 Modulation	10
1.2.1 Quadrature Amplitude Modulation (QAM)	11
1.3 Principles of Diversity Combining	13
1.3.1 Microscopic Diversity Techniques	14
1.3.2 Predetection Diversity Combining Schemes	14
1.4 Literature Review	16
1.4.1 Performance of Different Modulation Schemes over Nak- agami Fading Channels	16

1.4.2	Performance of Different Modulation Schemes in Nakagami Fading Channel with Different Diversity Combining Schemes	17
1.4.3	Performance of M-ary Quadrature Amplitude Modulation Scheme in Different Channels	20
1.5	Proposed Work	21
2	PERFORMANCE ANALYSIS OF QUADRATURE AMPLITUDE MODULATION IN NAKAGAMI FADING CHANNELS	22
2.1	Introduction	22
2.2	System and Channel Models	23
2.2.1	Transmitted QAM Signals	23
2.2.2	Multilink Channel Model	24
2.3	Performance of QAM in Nakagami Fading Channel	25
2.4	Performance of QAM in Nakagami Fading Channels with Diversity Schemes	32
2.4.1	MRC Diversity	32
2.4.2	EGC Diversity	34
2.4.3	SC Diversity	36
3	Simulation and Discussion	44
3.1	Study Cases	44
3.1.1	Nakagami-m Distribution	44
3.1.2	Performance of M-QAM in Nakagami Fading Channel	44

3.1.3	Performance of M-QAM with MRC in Nakagami Fading Channels	45
3.1.4	Performance of M-QAM with EGC in Nakagami Fading Channels	45
3.1.5	Performance of M-QAM with SC in Nakagami Fading Channels	45
3.1.6	Performance of M-QAM with Generalized Selection combining Scheme in Nakagami Fading Channels	46
3.2	Simulation Results	46
3.3	Observations and Discussion	83
3.3.1	Matching between Theoretical and Simulation	83
3.3.2	General Observation	83
3.3.3	Comparison of MRC, EGC, SC, and GSC	91
4	CONCLUSIONS AND RECOMMENDATION FOR FUTURE WORK	94
4.1	Conclusions	94
4.2	Recomendations for Future work	96

List of Figures

1.1	Classification of the modulation schemes [23]	12
2.1	16-QAM signal constellation	26
2.2	Multilink Channel Model	27
3.1	Different Nakagami- m distributions a- $m = \frac{1}{2}$ one sided gaussian distribution b- $m = 1$ Rayleigh distribution c- $m = 4$ which corresponds to Ricean distribution with $K = 6.4775$	47
3.2	Performance of 4-QAM in Nakagami fading channel with different Nakagami parameter ($m = 1, 2, 4$)	48
3.3	Performance of 16-QAM in Nakagami fading channel with different Nakagami parameter ($m = 1, 2, 4$)	49
3.4	Performance of 64-QAM in Nakagami fading channel with different Nakagami parameter ($m = 1, 2, 4$)	50
3.5	Performance of 4-QAM with MRC in Nakagami fading channels, ($m = 1$)	51
3.6	Performance of 4-QAM with MRC in Nakagami fading channels, ($m = 2$)	52

3.7	Performance of 4-QAM with MRC in Nakagami fading channels, ($m = 4$)	53
3.8	Performance of 16-QAM with MRC in Nakagami fading channels, ($m = 1$)	54
3.9	Performance of 16-QAM with MRC in Nakagami fading channels, ($m = 2$)	55
3.10	Performance of 16-QAM with MRC in Nakagami fading channels, ($m = 4$)	56
3.11	Performance of 64-QAM with MRC in Nakagami fading channels, ($m = 1$)	57
3.12	Performance of 64-QAM with MRC in Nakagami fading channels, ($m = 2$)	58
3.13	Performance of 64-QAM with MRC in Nakagami fading channels, ($m = 4$)	59
3.14	Performance of 4-QAM with EGC in Nakagami fading channels, ($m = 1$)	60
3.15	Performance of 4-QAM with EGC in Nakagami fading channels, ($m = 2$)	61
3.16	Performance of 4-QAM with EGC in Nakagami fading channels, ($m = 4$)	62
3.17	Performance of 16-QAM with EGC in Nakagami fading channels, ($m = 1$)	63
3.18	Performance of 16-QAM with EGC in Nakagami fading channels, ($m = 2$)	64

3.19 Performance of 16-QAM with EGC in Nakagami fading channels, ($m = 4$)	65
3.20 Performance of 64-QAM with EGC in Nakagami fading channels, ($m = 1$)	66
3.21 Performance of 64-QAM with EGC in Nakagami fading channels, ($m = 2$)	67
3.22 Performance of 64-QAM with EGC in Nakagami fading channels, ($m = 4$)	68
3.23 Performance of 4-QAM with SC in Nakagami fading channels, ($m = 1$)	69
3.24 Performance of 4-QAM with SC in Nakagami fading channels, ($m = 2$)	70
3.25 Performance of 4-QAM with SC in Nakagami fading channels, ($m = 4$)	71
3.26 Performance of 16-QAM with SC in Nakagami fading channels, ($m = 1$)	72
3.27 Performance of 16-QAM with SC in Nakagami fading channels, ($m = 2$)	73
3.28 Performance of 16-QAM with SC in Nakagami fading channels, ($m = 4$)	74
3.29 Performance of 64-QAM with SC in Nakagami fading channels, ($m = 1$)	75
3.30 Performance of 64-QAM with SC in Nakagami fading channels, ($m = 2$)	76

3.31 Performance of 64-QAM with SC in Nakagami fading channels, ($m = 4$)	77
3.32 Performance of 4-QAM with GSC in Nakagami fading channels, ($m = 1, L = 4$) a- $L_c = 3$, b- $L_c = 2$	78
3.33 Performance of 4-QAM with GSC in Nakagami fading channels, ($m = 2, L = 4$) a- $L_c = 3$, b- $L_c = 2$	79
3.34 Performance of 4-QAM with GSC in Nakagami fading channels, ($m = 4, L = 4$) a- $L_c = 3$, b- $L_c = 2$	80
3.35 Performance of 4-QAM with different diversity Schemes in Nakagami fading channels, ($m = 1, L = 4$)	81
3.36 Performance of 4-QAM with different diversity Schemes in Nakagami fading channels, ($m = 2, L = 4$)	82
3.37 Performance of 4-QAM with different diversity Schemes in Nakagami fading channels, ($m = 4, L = 4$)	84
3.38 Performance of 4-QAM with MRC and EGC over Nakagami fading channels, ($m = 1$)	85
3.39 Performance of 4-QAM with MRC and EGC over Nakagami fading channels, ($m = 2$)	86
3.40 Performance of 4-QAM with MRC and EGC over Nakagami fading channels, ($m = 4$)	87
3.41 Performance of 4-QAM with MRC and GSC over Nakagami fading channels, ($m = 1$)	88
3.42 Performance of 4-QAM with MRC and GSC over Nakagami fading channels, ($m = 2$)	89

3.43 Performance of 4-QAM with MRC and GSC over Nakagami fading channels, ($m = 4$)	90
---	----

THESIS ABSTRACT

Name: AL-SHALAN, FURAIH FAYIZ
Title: Performance of QAM in Nakagami Fading
Channels with Diversity
Degree: Master of Science
Major Field: Electrical Engineering
Date of Degree: March, 2000

In mobile communication systems, multipath fading seriously degrades the performance. However, if the multipath medium is well characterized, transmitter and receiver can be designed to match the channel and to reduce the effect of these disturbances. Nakagami fading channel which is considered to be a good model for this channel is presented. The performance of M-ary Quadrature Amplitude Modulation (M-QAM) scheme which has high spectral efficiency is analyzed and the use of different diversity schemes to mitigate the effects of fading is investigated.

The goal of this thesis is to provide closed formulas for the performance of M-QAM without and with different diversity combining schemes over Nakagami fading channels which can be used by system designers and engineers. Computer simulations are performed to confirm the theoretical formulas derived and also to study the effects of changing some parameters on the performance of the system.

King Fahd University of Petroleum and Minerals
Dhahran, Saudi Arabia

خلاصة الرسالة

تقييم أداء طريقة تضمين المقدار العمودي QAM عند استخدامها في القنوات المضمحلة بوجود التباين

إن وجود المسارات المتعددة المضحلة في الاتصالات اللاسلكية يقلل من كفاءة جهاز الاتصالات . ولكن إذا تم وضع نموذج مناسب للوسط الذي يتم فيه الإرسال فإنه يقلل من الآثار السلبية لوجود هذه المسارات المضمحلة .

إن نموذج Nakagami يعتبر مناسباً ليمثل قناة الاتصالات اللاسلكية .

سوف يتم دراسة تقييم أداء طريقة تضمين المقدار العمودي QAM والتي تملك كفاءة عالية من الناحية الطيفية وكذلك يتم دراسة استخدام عدة أنواع من طريق التباين لتحسين كفاءة جهاز الاتصالات اللاسلكية .

الهدف من الرسالة هو إيجاد معادلات أو صيغ لتقييم أداء QAM عند استخدامها في أنظمة أجهزة الاتصالات اللاسلكية وذلك بوجود عدة أنواع من التباين أو عدمه .

تم عمل المحاكاة للنظام المذكور باستخدام الكمبيوتر لإثبات الصيغ (المعادلات) المشتقة وكذلك دراسة تغيير بعض العوامل على أداء نظام الاتصالات .

Chapter 1

INTRODUCTION

1.1 Multipath Fading Channels

In mobile communication systems, the incoming radio wave arrives at the receiver in multiples with different propagation delays and attenuation levels due to reflection, refraction and scattering caused by natural and man-made structures. This phenomenon is referred to as *multipath* effect. These waves having randomly distributed amplitudes, phases and angles of arrival combine vectorially at the receiving antenna and cause the received signal to experience fading. As a result of the relative motion between a mobile and a base station, each multipath wave experiences an apparent frequency shift which is called Doppler spread and is directly proportional to the velocity and direction of motion of the mobile with respect to the direction of arrival of the received multipath wave. **Fading** is used to describe the rapid fluctuation of the amplitude of a radio signal over a short period of time and it is due to time variant multipath characteristics of the channel. In the following subsections, first the mathematical model of the fading channel is

presented then, statistical channel correlation functions is described lastly, the important statistical models of flat fading channels are discussed.

1.1.1 Mathematical Model of the Fading Channel

Let the transmitted signal arrives at the mobile station (MS) from N paths, and each path has its own angle of incidence $\varphi_n(t)$, amplitude $a_n(t)$ and time delay $\tau_n(t)$, for $n = 1, 2, \dots, N$.

The **doppler shift** is given by [13]

$$f_{D,n}(t) = f_m \cos \varphi_n(t) \quad (1.1)$$

where $f_m = \frac{v}{\lambda_c}$, v is the velocity of the mobile station and λ_c is the wavelength of the electromagnetic wave.

Consider the transmission of the band-pass signal,

$$s(t) = \Re\{u(t) \exp(j2\pi f_c t)\} \quad (1.2)$$

where $u(t)$ is the complex low-pass signal and f_c is the carrier frequency. The received band-pass waveform is

$$x(t) = \Re\{r(t) \exp(j2\pi f_c t)\} \quad (1.3)$$

where the received complex low-pass signal is given by

$$r(t) = \sum_{n=1}^N a_n(t) e^{-j2\pi[(f_c + f_{D,n}(t))\tau_n(t) - f_{D,n}(t)]} u(t - \tau_n(t)) \quad (1.4)$$

which can be simplified to

$$r(t) = \sum_{n=1}^N a_n(t) e^{-j\phi_n(t)} u(t - \tau_n(t)) \quad (1.5)$$

where $\phi_n(t) = 2\pi[(f_c + f_{D,n}(t))\tau_n(t) - f_{D,n}(t)]$ is the phase associated with the n^{th} path.

From Equation 1.5, the channel can be modeled by a time-variant linear filter having the complex low-pass impulse response [1]

$$c(\tau, t) = \sum_{n=1}^N a_n(t) e^{-j\phi_n(t)} \delta(\tau - \tau_n(t)) \quad (1.6)$$

where t is the observation time and τ is the application time of the impulse, $a_n(t)$, $\tau_n(t)$, $\phi_n(t)$ are the random time-varying amplitude, arrival time and phase sequences respectively.

Since $f_c + f_{D,n}(t)$ is very large, a small change in the path delay $\tau_n(t)$ causes a large change in the phase $\phi_n(t)$. At any time t these random phases may result in a constructive or destructive addition of the components. On the other hand, the amplitudes $a_n(t)$, which depend on the scatterers medium, do not change significantly over small spatial distance. Therefore **fading** is primarily due to time variations in the random phases $\phi_n(t)$ that are caused by doppler shifts $f_{D,n}(t)$.

1.1.2 Statistical Channel Correlation Functions

Bello [2] proposed the notion of wide-sense stationary uncorrelated scattering (WSSUS) to model fading phenomenon. WSSUS implies that the attenuation and phase shift of the channel associated with one path delay τ_1 is uncorrelated with that of another path delay τ_2 . With such a model of fading channels, Bello was able to define functions that apply for all times and all frequencies. Four functions are used to model the mobile channel and

they are discussed below.

The first function is the autocorrelation function of the impulse response of the channel

$$R_c(\tau_1, \tau_2; \Delta t) = \frac{1}{2} E[c(\tau_1; t)c^*(\tau_2; t + \Delta t)] \quad (1.7)$$

Under the assumption of WSSUS, Equation 1.7 [1] can be simplified to

$$R_c(\tau_1, \tau_2; \Delta t) = R_c(\tau_1; \Delta t)\delta(\tau_1 - \tau_2) \quad (1.8)$$

where $R_c(\tau; \Delta t) = \frac{1}{2} E[c(\tau; t)c^*(\tau; t + \Delta t)]$

An important quantity is the value of $R_c(\tau; \Delta t)$ at $\Delta t = 0$. $R_c(\tau; 0) = R_c(\tau)$ is referred to as **Multipath intensity profile (or delay power spectrum)**. It represents the average power of the channel at a relative path delay of τ . For a single transmitted impulse, the time T_m between the first and last received component represents the Maximum excess delay (or Multipath spread of the channel).

The second function is the Spaced-frequency correlation function $R_c(\Delta f)$, which is the Fourier transform of the Multipath intensity profile of the channel $R_c(\tau)$.

The range of frequencies over which the channel passes all spectral components with approximately equal gain and linear phase is referred to as **coherence bandwidth** $(\Delta f)_c$ of the channel and is approximately inversely proportional to T_m , i.e. $(\Delta f)_c \simeq \frac{1}{T_m}$ [1]

The above two functions describe the *selectivity* of the channel. The channel is referred to as **frequency non selective** when $T_s \gg T_m$, otherwise it

is **frequency selective**, where T_s is the symbol time duration. Frequency selectivity occurs whenever the received multipath components of a symbol extend beyond the symbol time duration T_s causing intersymbol interference (ISI). The equivalent condition for $T_s \gg T_m$ as viewed in frequency domain is $(\Delta f)_c \gg W$ where $(\Delta f)_c$ is the coherence bandwidth of the channel and W is the signal bandwidth. Consequently, a channel is frequency non selective when $(\Delta f)_c \gg W$; otherwise it is frequency selective. Frequency non selective is referred to as flat fading.

The other two functions describe the time variations of the channel and they are the **doppler power spectrum** $S(\lambda)$ and the **spaced-time correlation function** $R_c(\Delta t)$. The Doppler power spectrum gives knowledge about the spectral spreading of a transmitted sinusoid (impulse frequency) in the doppler shift domain. **Doppler spread** is the width of the doppler power spectrum denoted by f_D and it usually ranges from 20 Hz to 100 Hz. The Fourier transform of doppler power spectrum $S(\lambda)$ is Spaced-time correlation function $R_c(\Delta t)$. This function specifies the extent to which there is correlation between the channel's response to a sinusoid sent at time t_1 and the response to similar sinusoid sent at time $t_1 + \Delta t$. The **coherence time** $(\Delta t)_c$ is a measure of the expected time duration over which the channel's response is essentially time invariant and it is related to **doppler spread** by $(\Delta t)_c \simeq \frac{1}{f_d}$. Slow fading happens if the condition $(\Delta t)_c \gg T_s$ is satisfied, otherwise it is fast fading.

A function that combines both frequency and time effects is called the **Scattering function** $S_c(\tau; \lambda)$ of the channel. It provides a measure of the

average power output of the channel as a function of the time delay and the doppler frequency. The Scattering function is defined as

$$S_c(\tau; \lambda) = \int_{-\infty}^{\infty} R_c(\tau; \Delta t) e^{-j2\pi\lambda\Delta t} d(\Delta t) \quad (1.9)$$

Doppler power spectrum is related to the Scattering function by

$$S(\lambda) = \int_{\tau} S_c(\tau; \lambda) d\tau \quad (1.10)$$

1.1.3 Statistical Models of Flat Fading Channels

In flat (frequency non-selective) fading the channel affects the transmitted signal by introducing a fading envelope and a random phase. In slow fading it is assumed that the phase and the fading envelope are constants over at least one symbol duration. Depending on the nature of the radio propagation environment, there are different models which describe the statistical behavior of the fading envelope $\alpha(t) = |r(t)|$ where $r(t)$ is the received signal.

- **Rayleigh Model**

The Rayleigh distribution is frequently used to model multipath fading with no direct line-of-sight (LOS) path. For an unmodulated carrier, the received complex low-pass signal at any time t is

$$r = \sum_{n=1}^N a_n e^{j\phi_n} = \alpha e^{j\theta} = X + jY. \quad (1.11)$$

In analyzing the amplitude of the received signal r , the following approximations are usually assumed to be valid [3, 4]

- The received signal consists of a large number of plane waves.
 - There is no correlation between the plane waves.
 - There is no correlation between the phase and the amplitude of one plane wave.
- The phase, ϕ_n , is uniformly distributed in $[0, 2\pi]$. With these assumptions and using the central limit theorem, r becomes a complex Gaussian process, and X and Y are Gaussian RVs with

$$E[X] = E[Y] = 0, \sigma_X^2 = \sigma_Y^2 = \frac{\Omega}{2}, E[XY] = 0 \quad (1.12)$$

where $\Omega = E[\alpha^2(t)]$.

In this case, the channel fading amplitude is distributed according to

$$p(\alpha) = \frac{2\alpha}{\Omega} \exp\left(-\frac{\alpha^2}{\Omega}\right), \alpha \geq 0 \quad (1.13)$$

It follows that the instantaneous SNR per symbol of the channel γ , is distributed according to the exponential distribution

$$p_\gamma = \frac{1}{\bar{\gamma}} \exp\left(-\frac{\gamma}{\bar{\gamma}}\right), \gamma \geq 0 \quad (1.14)$$

where $\bar{\gamma}$ is the average SNR per symbol. The amount of fading (AF) associated with any fading pdf was introduced by Charash [5, 6] as a unified measure of the severity of the fading

$$AF = \frac{\text{var}(\alpha^2)}{\Omega^2} \quad (1.15)$$

The Rayleigh distribution therefor has an AF equal to 1 and typically agrees very well with experimental data for mobile systems where no LOS path exists between the transmitter and receiver antennas [1]. It also applies to the propagation of reflected and refracted paths through the troposphere [7] and ionosphere [8], [9] and to ship-to-ship [10, 11, 12] radio links.

- **Rician Model**

The Rice distribution is often used to model propagation paths consisting of one strong direct LOS component and many random weaker components. Here the channel fading amplitude follows the distribution

$$p(\alpha) = \frac{2\alpha(1+K)}{\Omega} e^{-K - \frac{\alpha^2(1+K)}{\Omega}} I_0\left(2\alpha\sqrt{\frac{K(K+1)}{\Omega}}\right), \alpha \geq 0 \quad (1.16)$$

where K is the Rician fading parameter which ranges from 0 to ∞ and I_0 is the Bessel function of the first kind of order zero .

The AF of the Rician distribution is given by [13]

$$AF = \frac{1+2K}{(1+2K)^2}, K \geq 0 \quad (1.17)$$

Hence the amount of fading ranges from 0 to 1. The Rician distribution spans the range from Rayleigh fading ($K=0$) to no fading (constant amplitude) ($K = \infty$). This type of fading is typically observed in the

first resolvable LOS paths of microcellular urban and suburban land mobile [14], picocellular indoor [15], and factory [16] environments. It also applies to the dominant LOS path of satellite [17, 18] and ship-to-ship [10] radio links.

- **Nakagami Model**

The Nakagami distribution is proposed by Nakagami [19] to fit empirical data and is often used to model multipath fading for the following reasons:

1- Flexibility in matching experimental data more than Rayleigh and Rician distributions [20].

2- Nakagami distribution can model fading conditions that are either more or less severe than the Rayleigh fading. When $m = 1$, the Nakagami distribution reduces to the Rayleigh distribution, when $m = \frac{1}{2}$, it becomes a one-sided Gaussian distribution, and when $m \rightarrow \infty$, the distribution approaches that of an impulse, thus representing the no fading AWGN channel.

3- Rice distribution can be approximated by Nakagami using the following relations:

$$K = \frac{\sqrt{m^2 - m}}{m - \sqrt{m^2 - m}}, m > 1 \quad (1.18)$$

This is accurate for small values of SNR [21].

The Nakagami distribution is given by

$$p(\alpha) = \frac{2m^m \alpha^{2m-1}}{\Gamma(m) \Omega^m} \exp\left(-\frac{m\alpha^2}{\Omega}\right), m \geq \frac{1}{2} \quad (1.19)$$

The Nakagami distribution is defined by two parameters which are $\Omega = E[\alpha^2(t)]$ and $m = \frac{\Omega^2}{\text{var}(\alpha^2)}$.

The reciprocal of m is the amount of fading, that is $AF = \frac{1}{m}$. So, large m models the case of less fading. The Nakagami distribution spans the widest range of AF (from 0 to 2). The instantaneous SNR per symbol of the channel γ has the Gamma distribution [13]

$$p(\gamma) = \left(\frac{m}{\Omega}\right)^m \frac{\gamma^{m-1}}{\Gamma(m)} \exp\left(-\frac{m\gamma}{\Omega}\right) \quad (1.20)$$

More on the use and derivation of the Nakagami fading model can be found in the paper by Braun and Derush [3]

1.2 Modulation

The adoption of the modulation techniques is very crucial for the design of an efficient mobile communication system. Modulation techniques are adopted based on the following requirements [22]:

- High spectral efficiency, to accommodate a number of subscribers over a limited spectrum.
- High power efficiency. Since small battery size is usually used, the power efficiency for the transmitter amplifier should be high.
- High fading immunity. Terminals for mobile communication systems are located in multipath fading environments. Therefore, they should be operated under time-varying multipath conditions.
- Low carrier-to-cochannel interference power ratio (CCI)
- Low out-of-band radiation

- Constant or near constant envelope
- Low cost and ease of implementation

Figure 1.1 shows classification of the common modulation schemes based on these three requirements. During late 70's and early 80's, constant envelope digital modulation schemes using a nonlinear amplifier were studied. As a result of these studies, Gaussian filtered minimum shift keying (GMSK) [24, 25], Phase-locked loop quaternary phase shift keying, PLL-QPSK [26], 4-level frequency modulation, FM [27] and tamed FM [28] were developed. Among these, GMSK was selected as the modulation scheme for the European digital cellular system GSM and the DECT system [23].

In the mid-1980's when the capacity became a limiting factor, developments of linear modulation having a 2 bits/s/Hz transmission ability were started [29]. Feher's QPSK (FQPSK) and FQAM [30] are two modulation schemes which have their spectra compact even if they are amplified by a nonlinear amplifier. $\pi/4$ -QPSK [29] was applied to Japanese [31] and North American digital cellular standards [32].

1.2.1 Quadrature Amplitude Modulation (QAM)

Since the late 80's there has been development of modulation schemes with spectral efficiency greater than 2 bits/s/Hz such as 16-QAM [33, 34]. 16-QAM or multi-carrier 16QAM (M16QAM) have been applied to the Japanese multichannel access (MCA) system [35], the Japanese public PMR systems [36] and the ESMR system in the US [37]. A 64 kbit/s 16-QAM modem using a digital pilot aided technique with fade compensation has been

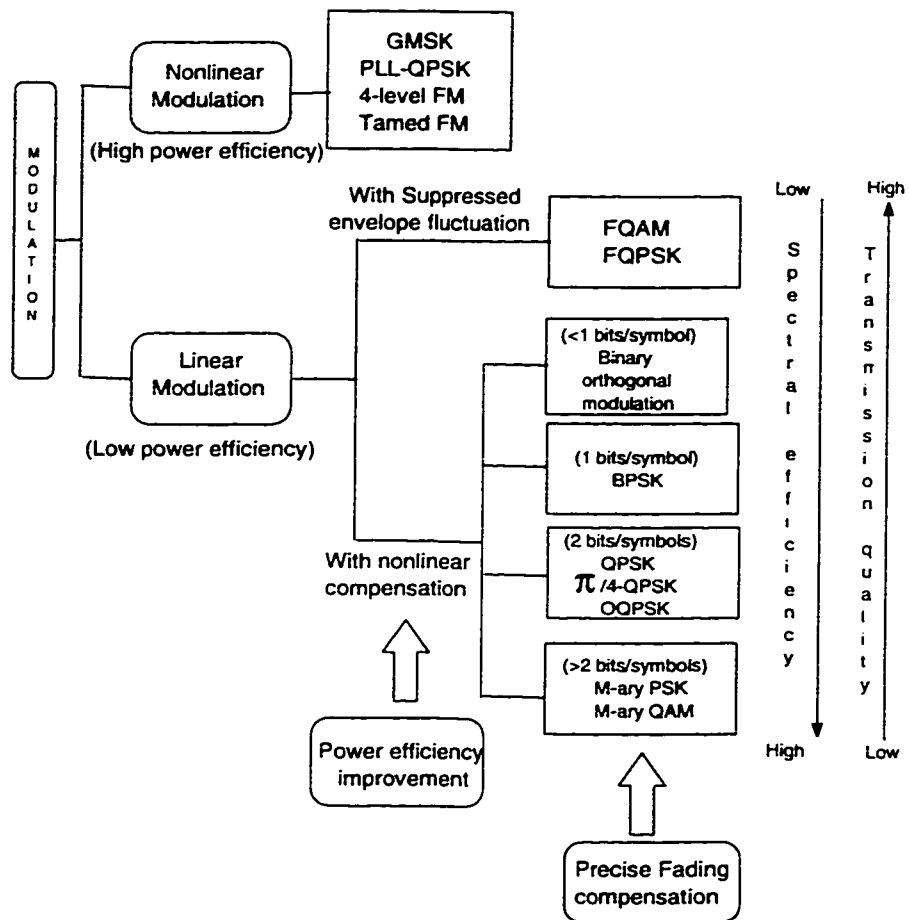


Figure 1.1: Classification of the modulation schemes [23]

reported by Sampei [38]. This modem gives about three times better capacity than that of GMSK. Sampei [39] has proposed a 6-channel trellis-coded 16-QAM/TDMA system. He has shown that the channel capacity of the proposed system is two times larger than that of $\pi/4$ QPSK. QAM modulation scheme will be presented in detail in Chapter 3.

1.3 Principles of Diversity Combining

In order to improve the reliability of communications on wireless radio channels, some techniques have to be employed to mitigate the effects of multipath fading. Diversity reception is one of the well known methods that can be used for that purpose. The idea behind diversity is to extract the information from signals received via multiple fading paths to improve the resultant SNR. Diversity systems can be classified into two broad categories. These are microscopic (micro) diversity systems and macroscopic (macro) diversity systems. Microdiversity techniques are used to compact the effects of short-term (multipath) fading [40]. The term micro is used because decorrelation between received signals occurs if the separation between the antennas is on the order of one-half of a wavelength [40]. Macrodiversity techniques are used to combat the effects of long-term fading (shadowing). The term macro is used because large spatial separation between the macro diversity ports is needed to achieve decorrelated shadowing [40]. Good references on the topic of diversity systems are [40, 41, 42]. In the following we discuss the microscopic diversity since we are interested in the short-term fading.

1.3.1 Microscopic Diversity Techniques

Microscopic diversity techniques can be further classified according to the method used to provide multiple fading signal paths. These include the use of different frequencies (frequency diversity), different time of transmission (time diversity), different antennas (space diversity) and different polarization (polarization diversity). In this thesis, the emphasis will be on the use of space diversity techniques. Space diversity techniques are very attractive because the diversity improvement can be achieved with no extra power or bandwidth, but at the expense of increase system complexity. Diversity receivers can also be classified as either pre detection or post detection. For coherent detection both of the classifications will offer the same performance. In the following, pre detection diversity reception is discussed in some detail.

1.3.2 Predetection Diversity Combining Schemes

In predetection diversity, the signals received by the different branches or antennas are combined at the IF level, and the resultant predetection signal is then demodulated. That is, combining is done before the detection or the demodulation process. Different forms of predetection combining schemes have been proposed in the literature. The most relevant space diversity combining schemes are maximal ratio combining (MRC), equal gain combining (EGC), and selection combining (SC).

The resultant signal at the output of an L-branch MR, EG, or SC predetection diversity combiner is given by

$$r_o(t) = \sum_{i=1}^L g_i[r_i(t) + n_i(t)] \quad (1.21)$$

where $n_i(t)$ is an additive Gaussian zero mean noise, and $r_i(t)$ is the signal received by the i^{th} branch and is given by

$$r_i(t) = \alpha_i(t)e^{j\theta_i(t)}e^{j(2\pi f_c t + \Phi_m(t))} \quad (1.22)$$

where f_c is the carrier frequency, $\Phi_m(t)$ is the desired information signal, $\alpha_i(t)$ is a random amplitude process, and $\theta_i(t)$ is a random phase process. The values of the gain factors, g_i , depend on the type of diversity combining schemes used. In MR combining, the signals received from the different branches are weighted in proportion to their voltage to noise power ratios, co-phased, and then summed. That is the MR gain factors are given by [40]

$$g_i = k \frac{\alpha_i e^{-j\theta_i(t)}}{N_i} \quad (1.23)$$

where k is an arbitrary complex constant, and N_i is the average noise power in the i^{th} branch. MRC is the optimum form of linear diversity combining schemes [43] since it gives the best performance improvement among all combining schemes. In MRC, the branch gains are continuously adjusted to give the maximum predetection SNR.

In EGC, the outputs of the different branches are co-phased, equally weighted and then summed. The EG gain factors are given by

$$g_i = e^{-j\varphi_i(t)}. \quad (1.24)$$

In selection diversity, the branch with largest SNR is selected and co-phasing of signals is not needed. Hence, the SC gain factors can be written as

$$g_i = \begin{cases} 1 & \text{if } i = s \\ 0 & \text{if } i \neq s \end{cases} \quad (1.25)$$

Where s is the index for the branch with highest SNR.

Recently Milstein [44, 45, 46] considered a new combining scheme called generalized selection combining scheme (GSC). GSC is a scheme in which we choose the L_c largest signals from L total diversity branches and then coherently combine them. When $L_c = L$ we have MRC and when $L_c = 1$ we have SC so MRC and SC are special cases of GSC.

1.4 Literature Review

The performance of different modulation schemes with and without diversity schemes has been analyzed, derived or simulated over Nakagami fading channels in many literature. In the following subsections, we present an up-to-date survey of the published work in this area. In the last subsection the proposed work is discussed.

1.4.1 Performance of Different Modulation Schemes over Nakagami Fading Channels

The performance of binary phase shift keying (BPSK) systems in Nakagami fading channels has been studied by Wojnar [47] in which closed formula for the bit error rate (BER) of binary systems for coherent and noncoherent

detection is derived. The performance of M-ary phase shift keying (MPSK) in Nakagami fading channel is derived in [48] based on an approximation. Aalo in [49] analyzed the error rate performance of coherent MPSK signals in Nakagami fading channel and derived a closed form expression for integer values of Nakagami parameter m . The performance of M-ary differential phase shift keying (MDPSK) and differential quaternary phase shift keying (DQPSK) are analyzed in [50] and [51] respectively.

1.4.2 Performance of Different Modulation Schemes in Nakagami Fading Channel with Different Diversity Combining Schemes

- **Maximum Ratio Combining Scheme**

The performance of binary signals with L-branch maximum ratio combining diversity (MRC) in Nakagami fading channel has been studied in [52] and a closed form for BER performance has been derived only for integer values of Nakagami parameter m and identical fading parameters across all diversity branches. The BER performance of MRC rake receiver in Nakagami fading channel has been derived in [53] for arbitrary values of the Nakagami parameter m but keeping this value identical for all diversity branches. In [54] the performance of binary signals with MRC has been derived for arbitrary parameters. A closed form expression for it has been obtained in [55] with arbitrary values of fading parameter and different averages across the diversity branches.

The effect of correlation between diversity channels on the performance

of MRC diversity reception system has been studied in [52] and [48] but the analysis has been limited to dual branch diversity systems. In [56] the performance of MRC with L correlated branches has been evaluated for two correlation models namely constant correlation model and exponential correlation model. Extension to a general correlation model has been given in [57] on the basis of L variant moment generating function MGF of the random input power vector. In [58] Zhang also analyzed the performance of MRC in a correlated Nakagami fading channel with arbitrary branch covariance matrix using the characteristic function for the SNR at MRC output avoiding the difficulties of obtaining the pdf of it.

- **Equal Gain Combining Scheme**

The analysis of equal gain combining diversity (EGC) in Nakagami fading has been first studied by [48]. Expressions for the outage rate for error probability and average error probability for M -ary phase shift keying (MPSK) at the output of a dual branch equal gain combiner have been derived in [48]. The analysis of equal gain combiner for $L > 2$ has been done lately by A.Abu-dayya [59] where he derived an infinite series of the complementary probability distribution function (cdf) of the signal to noise ratio (SNR) at the output of the EGC combiner. The analysis has been done by making use of the convergent infinite series for the complementary distribution function (cdf) and the probability density function (pdf) of a sum of independent random variables rv's which have been derived by [60]. Bit error rate perfor-

mance of coherent and noncoherent binary systems with L-branch EGC in Nakagami fading has been derived. The performance of MDPSK and DPSK with equal gain combining in Nakagami fading has been derived in [61] and [62] respectively.

- **Selection Combining Scheme**

The performance of selection diversity systems in Nakagami fading has been studied first by [63] but the analysis has been limited to binary signaling and two branches. The analysis has been extended in [64] to L-branch selection diversity of M-ary noncoherent frequency shift keying MNFSK signals and closed form formula for the symbol error probability has been derived. A formula for the performance over Rayleigh fading has been obtained as special case of Nakagami. In [65] BER performance of coherent and noncoherent binary systems with L-branch selection diversity have been derived.

The effect of correlation on the performance for dual branch selection diversity system with NFSK signaling has been examined first by [66]. The performance of L-branch selection diversity system in correlated Nakagami fading channels were studied in [67] where the joint distribution of L correlated variables was used based on a series expansion in terms of the Laguerre polynomials [68].

The most important contribution of evaluating error performance of digital communication systems over generalized fading channels has been done lately by alouini [69, 70, 71, 72]. The new approach does not attempt to compute or approximate the probability density function (pdf) of the signal to noise ratio (SNR) at the output of the combiner and then average

the conditional BER over that pdf. Instead, it takes advantage of an alternate form of the Gaussian Q-function [73] and the resulting alternate integral representation of the conditional BER as well as some known Laplace transforms and/or Gauss-Hermitte quadrature integration to independently average over the pdf of each channel that fades. In all cases this approach leads to expressions of the average BER that involve a single finite range integral whose integrand contains only elementary functions and which can be easily computed numerically.

1.4.3 Performance of M-ary Quadrature Amplitude Modulation Scheme in Different Channels

The performance of M-ary quadrature amplitude modulation in additive white Gaussian noise AWGN is available in many literature i.e [1]. In [74] the performance of M-QAM in Rayleigh fading channel with two-branch maximum ratio combining diversity (MRC) has been derived. Kim [75] derived the BER of M-QAM L-branch MRC diversity reception in Rayleigh fading channel using a series expansion of the complementary error function and the error rate expression is in the form of an infinite series rather than a closed form. Error probability performance of L-branch MRC and SC of M-QAM in Rayleigh fading channel have been derived in [76].

The bit error probability of M-QAM in Rician fading channel has been derived in [77].

1.5 Proposed Work

The aim of this Thesis is to evaluate the performance of M-ary Quadrature Amplitude Modulation (M-QAM) scheme in slow Nakagami fading channel. we choose M-QAM because it is a very effective technique to increase channel capacity. If 16-QAM is used, it is possible to carry out $64kb/s$ transmission with almost the same channel spacing as that of the present analog systems (less than 30 kHz). It gives about three times better capacity than that of GMSK [22]. Since Nakagami spans the widest range of fading conditions so it is a good model for fading channels. This combination (i.e M-QAM over Nakagami) has not been studied before. We will derive the performance of M-QAM over Nakagami fading channel without/with different diversity combining schemes (MRC,EGC, and SC) . Theoretical results will be verified by simulation. The performance of M-QAM over Nakagami fading channel will be simulated for different M, different branch diversity L and different Nakagami parameter m . In particular we will consider the values $m = 1, 2, 4$. The Thesis is organized as follows. In Chapter 2, performance of M-QAM over Nakagami fading channel without/with different diversity combining schemes (MRC,EGC, and SC) will be derived. Simulation results and observations are presented and discussed in Chapter 3. Conclusions and recommendation for future work are summarized in Chapter 4.

Chapter 2

PERFORMANCE ANALYSIS OF QUADRATURE AMPLITUDE MODULATION IN NAKAGAMI FADING CHANNELS

2.1 Introduction

In this chapter the performance of M-ary Quadrature Amplitude Modulation (M-QAM) in Nakagami fading channel is analyzed. Both diversity (MRC, EGC and SC) and nondiversity schemes are considered, and closed formulas for symbol error rate (SER) are derived for each case. In the next section the transmitted QAM signals and the multipath channel model are described. The performance of QAM in Nakagami fading channels without diversity is derived in section 2.3. The performance of the system under MRC, EGC, and SC is analyzed in section 2.4.

2.2 System and Channel Models

2.2.1 Transmitted QAM Signals

The M-ary QAM signal transmitted over one signaling interval may be represented as [13]

$$s_m(t) = A\Re[(x_m^I + jx_m^Q)g_{T_s}e^{-j2\pi f_c t}], \quad 0 \leq t \leq T_s, \quad m = 1, 2, \dots, M \quad (2.1)$$

where g_{T_s} is a rectangular pulse of duration T_s , f_c is the carrier frequency, and $\{x_m = x_m^I + jx_m^Q\}$ is the source symbol sequence that results from mapping successive k -bit blocks into one of $M = 2^k$ possible waveforms where k is an even number. The variables x_m^I, x_m^Q take the values $\{\bar{\mp}1, \bar{\mp}3, \dots, \bar{\mp}(N-1)\}$, where $N = \sqrt{M}$.

The quadrature representation of QAM signal is

$$s_m(t) = \sqrt{\frac{2E_A}{T_s}}x_m^I \cos(2\pi f_c t) + \sqrt{\frac{2E_A}{T_s}}x_m^Q \sin(2\pi f_c t) \quad (2.2)$$

$$0 \leq t \leq T_s, \quad m = 1, 2, \dots, M$$

Where E_A is the energy of the basic pulse g_{T_s} . The energy of the symbol x_m is E_m where $E_m = E_A|x_m|^2$. The average symbol energy E_{avs} is related to E_A [13] as :

$$E_{avs} = \frac{2(M-1)}{3}E_A. \quad (2.3)$$

The average energy per bit is

$$E_{avb} = \frac{E_{avs}}{\log_2(M)}. \quad (2.4)$$

The signal space constellation for 16-QAM is shown in Figure 2.1.

From equation 2.2 it is clear that QAM signal is equivalent to two PAM (Pulse Amplitude Modulation) signals. It implies that we can transmit $M = N^2$ independent symbols within the same bandwidth of one M-ary PAM scheme.

2.2.2 Multilink Channel Model

We consider a multilink channel where the transmitted signal is received over L independent slowly flat Nakagami fading channels, as shown in Figure 2.2. In this figure, $\{ r_l(t) \}_{l=1}^L$ is the set of received replicas of the transmitted signal $s_m(t)$ where l is the channel index, $\{ \alpha_l \}_{l=1}^L$, $\{ \theta_l \}_{l=1}^L$, and $\{ \tau_l \}_{l=1}^L$ are the random channel amplitudes, phases, and delays, respectively. It is assumed that the sets $\{ \alpha_l \}_{l=1}^L$, $\{ \theta_l \}_{l=1}^L$, and $\{ \tau_l \}_{l=1}^L$ are mutually independent. The first channel is assumed to be the reference channel with delay $\tau_1 = 0$. Without loss of generality, we assume that $\tau_1 < \tau_2 < \dots < \tau_L$. Because of the slow fading assumption, it is assumed that the $\{ \alpha_l \}_{l=1}^L$, $\{ \theta_l \}_{l=1}^L$, and $\{ \tau_l \}_{l=1}^L$ are all constant over a symbol interval. The fading amplitudes $\{ \alpha_l \}_{l=1}^L$ are assumed to be statistically independent identical Nakagami random variables (r.v.). Each Nakagami r.v. has a mean square value $\overline{\alpha_l^2}$ which is denoted by Ω_l and whose square is a Gamma random variable. After passing through the fading channel, each replica of the signal is corrupted by Additive White Gaussian Noise (AWGN) with a one-sided power spectral density $N_o W/H_z$. The AWGN is assumed to be statistically independent from channel to channel and independent of the fading amplitudes $\{ \alpha_l \}_{l=1}^L$. Hence,

the instantaneous SNR per symbol of the l^{th} channel is given by $\gamma_l = \frac{\alpha^2 E_s}{N_o}$, where E_s is the average energy of the symbol and the average SNR for all the channels is the same $\bar{\gamma} = \gamma_l$.

2.3 Performance of QAM in Nakagami Fading Channel

The probability of symbol error for M-ary QAM signals in AWGN channel can be expressed as [1]

$$P(e) = 4\left(1 - \frac{1}{\sqrt{M}}\right)Q\left(\sqrt{2g\alpha^2 \frac{E_s}{N_o}}\right) - 4\left(1 - \frac{1}{\sqrt{M}}\right)^2 Q^2\left(\sqrt{2g\alpha^2 \frac{E_s}{N_o}}\right) \quad (2.5)$$

where $g = \frac{3}{2(M-1)}$ and E_s is the received average energy per symbol and $\alpha = 1$ for AWGN.

The above expression can be viewed as the conditional error probability for a given value of received SNR ($\gamma = \alpha^2 \frac{E_s}{N_o}$) and thus can be rewritten as

$$P(e|\gamma) = 4\left(1 - \frac{1}{\sqrt{M}}\right)Q(\sqrt{2g\gamma}) - 4\left(1 - \frac{1}{\sqrt{M}}\right)^2 Q^2(\sqrt{2g\gamma}) \quad (2.6)$$

Since α is a Nakagami random variable α^2 is a Gamma random variable and so is γ . Therefore the pdf of γ is given by :

$$p(\gamma) = \left(\frac{m}{\bar{\gamma}}\right)^m \frac{\gamma^{m-1}}{\Gamma(m)} \exp\left(-\frac{m\gamma}{\bar{\gamma}}\right) \quad (2.7)$$

The average symbol error rate $P_{MQAM}(e)$ of M-QAM in Nakagami fading channel is obtained by averaging the conditional $P(e|\gamma)$ over the pdf of γ ,

$$P_{MQAM}(e) = \int_0^{\infty} P(e|\gamma)p(\gamma) d\gamma \quad (2.8)$$

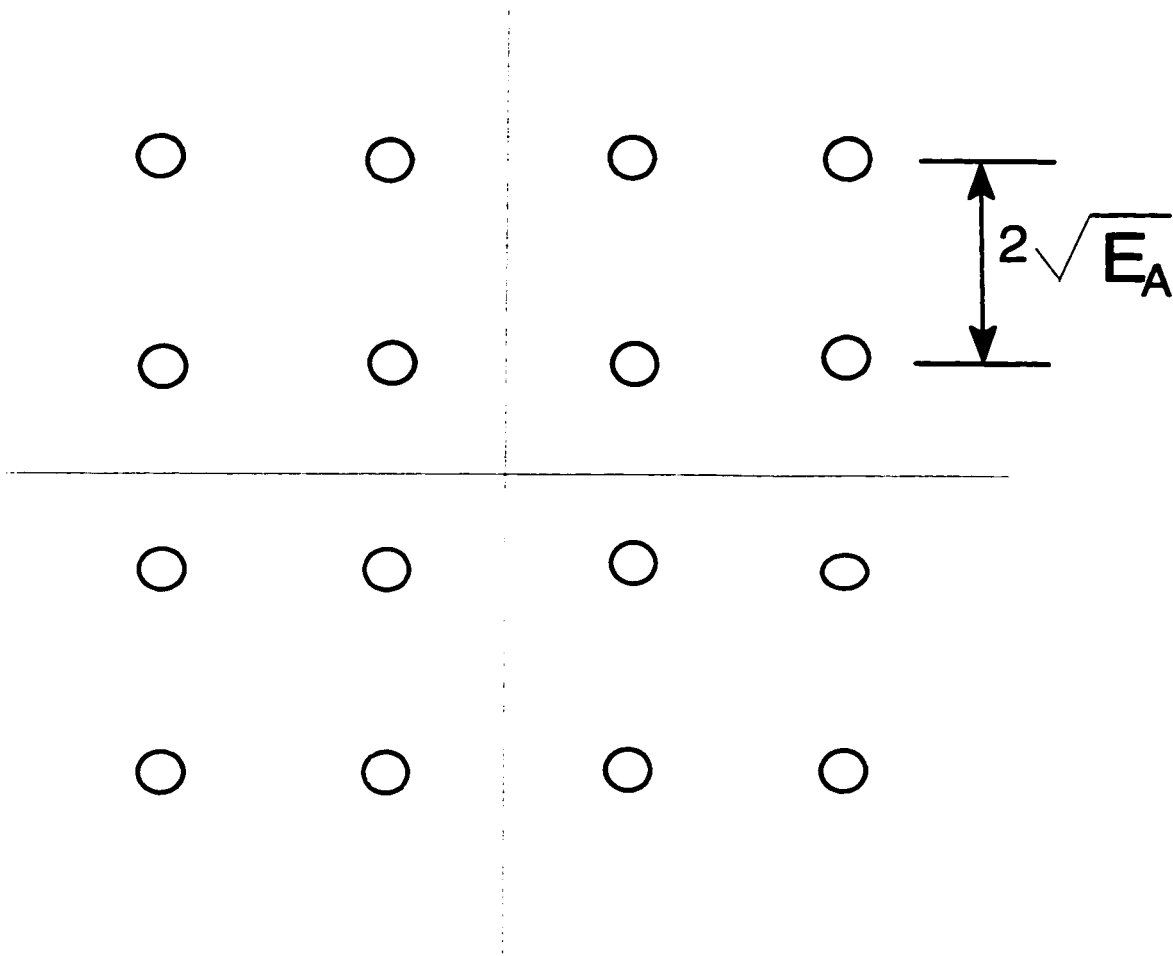


Figure 2.1: 16-QAM signal constellation

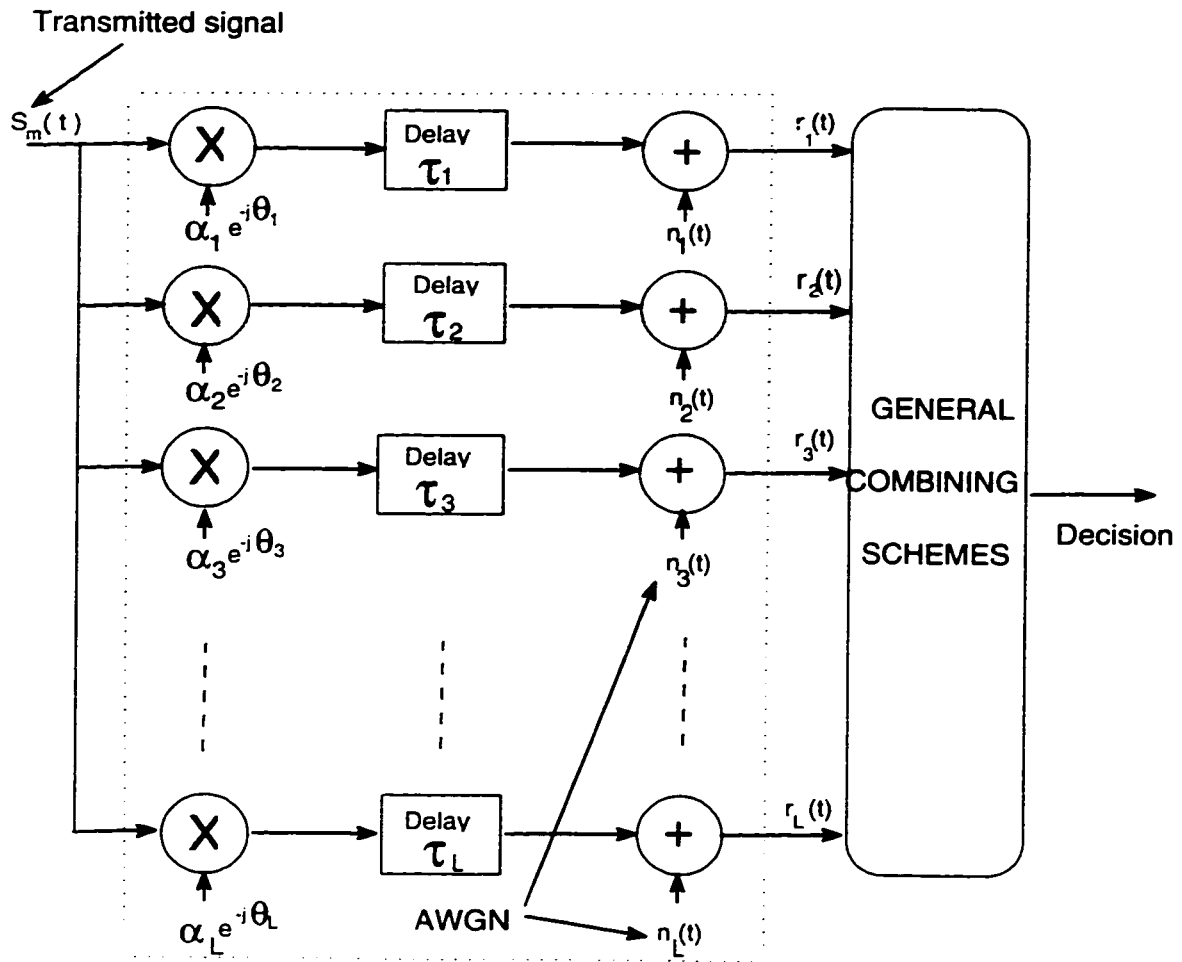


Figure 2.2: Multilink Channel Model

Substituting Equation 2.6 in Equation 2.8,

$$P_{MQAM}(e) = 4\left(1 - \frac{1}{\sqrt{M}}\right) \underbrace{\int_0^{\infty} p(\gamma)Q(\sqrt{2g\gamma})d\gamma}_{I_1} - 4\left(1 - \frac{1}{\sqrt{M}}\right) \underbrace{\int_0^{\infty} p(\gamma)Q^2(\sqrt{2g\gamma})d\gamma}_{I_2} \quad (2.9)$$

Equation 2.9 consists of two terms, I_1 and I_2 . Substitute Equation 2.7 in Equation 2.9 to obtain

$$I_1 = \int_0^{\infty} Q(\sqrt{2g\gamma}) \left(\frac{m}{\gamma}\right)^m \frac{\gamma^{m-1}}{\Gamma(m)} \exp\left(-\frac{m\gamma}{\gamma}\right) d\gamma \quad (2.10)$$

$$I_2 = \int_0^{\infty} Q^2(\sqrt{2g\gamma}) \left(\frac{m}{\gamma}\right)^m \frac{\gamma^{m-1}}{\Gamma(m)} \exp\left(-\frac{m\gamma}{\gamma}\right) d\gamma \quad (2.11)$$

Milstein [53] derived the following closed form integral,

$$J_m(a, b) = \frac{a^m}{\Gamma(m)} \int_0^{\infty} e^{-at} t^{m-1} Q(\sqrt{bt}) dt, m \geq 0 \quad (2.12)$$

$$J_m(c) = \frac{\sqrt{\frac{c}{\pi}}}{2(1+c)^{m+\frac{1}{2}}} \frac{\Gamma(m+\frac{1}{2})}{\Gamma(m+1)} ({}_2F_1(1, m+\frac{1}{2}, m+1; \frac{1}{1+c})) \quad (2.13)$$

Where $c = \frac{b}{2a}$ and ${}_2F_1(\cdot, \cdot, \dots; \cdot)$ is the Gauss hypergeometric function.

When m is a positive integer, the integral $J_m(a, b)$ reduces to [1]

$$J_m(a, b) = J_m(c) = [P(c)]^m \sum_{k=0}^{m-1} \binom{m-1+k}{k} [1-P(c)]^k \quad (2.14)$$

where

$$P(x) = \frac{1}{2}(1 - \sqrt{\frac{x}{1+x}})$$

To evaluate I_1 we let

$$a = \frac{m}{\gamma}$$

$$b = 2g$$

$$c = \frac{2g}{2\frac{m}{\gamma}} = \frac{g\bar{\gamma}}{m}$$

in Equation 2.14 then we have,

$$I_1 = \left[\frac{1}{2} \left(1 - \sqrt{\frac{g\bar{\gamma}}{m + g\bar{\gamma}}} \right) \right]^m \sum_{k=0}^{m-1} \binom{m-1+k}{k} \left[\frac{1}{2} \left(1 + \sqrt{\frac{g\bar{\gamma}}{m + g\bar{\gamma}}} \right) \right]^k \quad (2.15)$$

To evaluate I_2 , we will make use of available literature results. The symbol error probability for quadrature phase shift keying QPSK over AWGN channel is [1]

$$P_{QPSK}(e) = 2Q(\sqrt{2\gamma}) - Q^2(\sqrt{2\gamma}) \quad (2.16)$$

and that for BPSK is [1]

$$P_{BPSK}(e) = Q(\sqrt{2\gamma}) \quad (2.17)$$

From Equation 2.16 and 2.17, we can write

$$Q^2(\sqrt{2\gamma}) = 2P_{BPSK}(e) - P_{QPSK}(e) \quad (2.18)$$

Substituting Equation 2.18 in 2.11 yields,

$$I_2 = 2 \int_0^{\infty} P_{BPSK}(e)|_{\gamma=g\bar{\gamma}} p(\gamma) d\gamma - \int_0^{\infty} P_{QPSK}(e)|_{\gamma=g\bar{\gamma}} p(\gamma) d\gamma \quad (2.19)$$

$I_2 = I_3 - I_4$, where

$$I_3 = 2 \int_0^{\infty} P_{BPSK}(e)|_{\gamma=g\bar{\gamma}} \left(\frac{m}{\bar{\gamma}}\right)^m \frac{\gamma^{m-1}}{\Gamma(m)} \exp\left(-\frac{m\gamma}{\bar{\gamma}}\right) d\gamma \quad (2.20)$$

and

$$I_4 = \int_0^{\infty} P_{QPSK}(e)|_{\gamma=g\bar{\gamma}} \left(\frac{m}{\bar{\gamma}}\right)^m \frac{\gamma^{m-1}}{\Gamma(m)} \exp\left(-\frac{m\gamma}{\bar{\gamma}}\right) d\gamma \quad (2.21)$$

Sandeep [78] showed that the average symbol error rate of MPSK over N i.i.d Rayleigh fading channels, is given by

$$P_{MPSK} = \int_0^{\infty} P_{MPSK}(e) \frac{1}{\Gamma_N} \frac{\gamma^{N-1}}{\bar{\gamma}^N} e^{-\frac{\gamma}{\bar{\gamma}}} d\gamma \quad (2.22)$$

has the closed form

$$P_{MPSK} = \frac{M-1}{M} - \beta \left\{ \left(\frac{1}{2} + \frac{\tan^{-1}(\alpha)}{\pi} \right) \sum_{k=0}^{N-1} \binom{2k}{k} \frac{1}{[4(\mu^2+1)]^k} + \frac{\sin(\tan^{-1}(\alpha))}{\pi} \sum_{k=1}^{N-1} \sum_{i=1}^k \frac{T_{ik}}{(\mu^2+1)^k} [\cos(\tan^{-1}(\alpha))]^{2(k-i)+1} \right\} \quad (2.23)$$

in which

$$\mu = \sqrt{a\bar{\gamma}} \sin\left(\frac{\pi}{M}\right),$$

$$\beta = \frac{\mu}{\sqrt{\mu^2+1}}$$

$$\alpha = \frac{\sqrt{a\bar{\gamma}} \cos\left(\frac{\pi}{M}\right)}{\sqrt{\mu^2+1}}$$

$$a = \log_2(M)$$

$$T_{ik} = \frac{\binom{2k}{k}}{\binom{2(k-i)}{k-i} 4^{(2(k-i)+1)}}$$

Equation 2.22 can be used to evaluate I_3 and I_4 by letting $M = 2$ for I_3 and $M = 4$ for I_4 and $a = g \log_2(M)$, $N = m$, $\bar{\gamma} = \frac{\bar{\gamma}}{m}$

\Rightarrow

$$I_3 = [1 - \sqrt{\frac{g\bar{\gamma}}{m+g\bar{\gamma}}} \sum_{k=0}^{m-1} \binom{2k}{k} \frac{1}{[4(\mu_1^2+1)]^k}] \quad (2.24)$$

Where

$$\begin{aligned} \mu_1 &= \sqrt{\frac{g\bar{\gamma}}{m}} \\ \beta_1 &= \sqrt{\frac{g\bar{\gamma}}{m+g\bar{\gamma}}} \\ \alpha_1 &= 0 \end{aligned}$$

and

$$\begin{aligned} I_4 &= \frac{3}{4} - \beta_2 \left\{ \left(\frac{1}{2} + \frac{\tan^{-1}(\alpha_2)}{\pi} \right) \sum_{k=0}^{m-1} \binom{2k}{k} \frac{1}{[4(\mu_2^2+1)]^k} \right. \\ &\quad \left. + \frac{\sin(\tan^{-1}(\alpha_2))}{\pi} \sum_{k=1}^{m-1} \sum_{i=1}^k \frac{T_{ik}}{(\mu_2^2+1)^k} [\cos(\tan^{-1} \alpha_2)]^{2(k-i)+1} \right\} \quad (2.25) \end{aligned}$$

Where

$$\begin{aligned} \mu_2 &= \sqrt{\frac{2g\bar{\gamma}}{m}} \cdot \frac{\sqrt{2}}{2} = \sqrt{\frac{g\bar{\gamma}}{m}} \\ \alpha_2 &= \sqrt{\frac{g\bar{\gamma}}{m+g\bar{\gamma}}} \\ \beta_2 &= \sqrt{\frac{g\bar{\gamma}}{m+g\bar{\gamma}}} \end{aligned}$$

since $I_2 = I_3 - I_4$

$\mu_1 = \mu_2 = \mu$ and

$\beta_1 = \beta_2 = \beta$

we obtain

$$\begin{aligned} I_2 &= \left[\frac{1}{4} - \beta \left\{ \left(\frac{1}{2} - \frac{\tan^{-1}(\alpha_2)}{\pi} \right) \sum_{k=0}^{m-1} \binom{2k}{k} \frac{1}{[4(\mu^2+1)]^k} \right. \right. \\ &\quad \left. \left. - \frac{\sin(\tan^{-1}(\alpha_2))}{\pi} \sum_{k=1}^{m-1} \sum_{i=1}^k \frac{T_{ik}}{(\mu^2+1)^k} [\cos(\tan^{-1} \alpha_2)]^{2(k-i)+1} \right\} \right] \quad (2.26) \end{aligned}$$

The values of I_1 and I_2 will be utilized to evaluate the performance of MQAM over Nakagami fading channels using Equation 2.9, repeated her for convenience

$$P_{MQAM} = 4\left(1 - \frac{1}{\sqrt{M}}\right)I_1 - 4\left(1 - \frac{1}{\sqrt{M}}\right)^2 I_2 \quad (2.27)$$

The performance of MQAM over Rayleigh fading channel can be obtained by substituting $m = 1$ in I_1 and I_2 then Equation 2.27 becomes

$$P_{MQAM} = q\left(\frac{1 - \mu}{2}\right) - \frac{q^2}{16}\left[1 - \frac{4\mu}{\pi}\left(\tan^{-1}\left(\frac{1}{\mu}\right)\right)\right] \quad (2.28)$$

where $q = 4\left(1 - \frac{1}{\sqrt{M}}\right)$ and $\mu = \sqrt{\frac{g\bar{\gamma}}{1+g\bar{\gamma}}}$.

Equation 2.27 matches the result obtained by [79, Eqn.(4.38)] and it also matches the result obtained by [77, Eqn.(44)] for $M = 16$.

2.4 Performance of QAM in Nakagami Fading Channels with Diversity Schemes

2.4.1 MRC Diversity

MRC is the optimal diversity scheme since it results in a maximum likelihood receiver [13]. The output of the MRC combiner is given by [13]

$$\gamma_{mrc} = \sum_{l=1}^L \gamma_l. \quad (2.29)$$

For MRC diversity, the conditional error probability of M-QAM is

$$P(e|\gamma_{mrc}) = 4\left(1 - \frac{1}{\sqrt{M}}\right)Q(\sqrt{2g\gamma_{mrc}}) - 4\left(1 - \frac{1}{\sqrt{M}}\right)^2 Q^2(\sqrt{2g\gamma_{mrc}}) \quad (2.30)$$

which is conditioned at a fixed value of SNR γ_{mrc} where $\gamma_{mrc} = \sum_l^L \gamma_l = \sum_l^L \alpha_l^2 \frac{E_s}{N_0}$ and γ_l is the instantaneous SNR for each channel.

To get the average symbol error probability of M-QAM in Nakagami fading channel we average the conditional $P(e|\gamma_{mrc})$ over the pdf of γ_{mrc}

$$P_{MQAM,mrc}(e) = \int_0^{\infty} P(e|\gamma_{mrc}) p_{\gamma_{mrc}}(\gamma_{mrc}) d\gamma_{mrc} \quad (2.31)$$

Since each γ_l is a Gamma random variable and the analysis is done where we have i.i.d Nakagami fading channels the pdf of γ_{mrc} is also a gamma rv [19],

$$p_{\gamma_{mrc}}(\gamma_{mrc}) = \frac{m_{\gamma_{mrc}}}{\overline{\gamma_{mrc}}} \frac{\gamma_{mrc}^{m_{\gamma_{mrc}}-1} \exp(-\frac{\gamma_{mrc}}{\overline{\gamma_{mrc}}})}{\Gamma(m_{\gamma_{mrc}})} \quad (2.32)$$

With the parameters $\overline{\gamma_{mrc}} = L\overline{\gamma}$, $m_{\gamma_{mrc}} = Lm$ where $\overline{\gamma}$ is the average SNR for each channel we can rewrite Equation 2.32 as

$$p_{\gamma_{mrc}}(\gamma_{mrc}) = \frac{m}{\overline{\gamma}} \frac{\gamma_{mrc}^{Lm-1} \exp(-\frac{\gamma_{mrc}}{\overline{\gamma}})}{\Gamma(Lm)} \quad (2.33)$$

Following the same steps in evaluating the performance of M-QAM in Nakagami fading channels without diversity Equation 2.27 and noting that

$$p_{\gamma_{mrc}}(\gamma_{mrc}) = p_{\gamma}(\gamma)|_{m=Lm, \overline{\gamma}=L\overline{\gamma}, \gamma=\gamma_{mrc}}$$

The performance of M-QAM in Nakagami fading channels with MRC can be expressed as

$$P_{MQAM,mrc} = 4(1 - \frac{1}{\sqrt{M}})I_1 - 4(1 - \frac{1}{\sqrt{M}})^2 I_2 \quad (2.34)$$

where

$$I_1 = \left[\frac{1}{2} \left(1 - \sqrt{\frac{g\bar{\gamma}}{m+g\bar{\gamma}}} \right) \right]^{Lm} \sum_{k=0}^{Lm-1} \binom{Lm-1+k}{k} \left[\frac{1}{2} \left(1 + \sqrt{\frac{g\bar{\gamma}}{m+g\bar{\gamma}}} \right) \right]^k$$

and

$$I_2 = \left[\frac{1}{4} - \beta \left\{ \left(\frac{1}{2} - \frac{\tan^{-1}(\alpha_2)}{\pi} \right) \sum_{k=0}^{Lm-1} \binom{2k}{k} \frac{1}{[4(\mu^2+1)]^k} - \frac{\sin(\tan^{-1}(\alpha_2))}{\pi} \sum_{k=1}^{Lm-1} \sum_{i=1}^k \frac{T_{ik}}{(\mu^2+1)^k} [\cos(\tan^{-1}\alpha_2)]^{2(k-i)+1} \right\} \right]$$

and

$$\mu = \sqrt{2\frac{g\bar{\gamma}}{m}} \cdot \frac{\sqrt{2}}{2} = \sqrt{\frac{g\bar{\gamma}}{m}}$$

$$\alpha_2 = \sqrt{\frac{g\bar{\gamma}}{m+g\bar{\gamma}}}$$

$$\beta = \sqrt{\frac{g\bar{\gamma}}{m+g\bar{\gamma}}}$$

$$T_{ik} = \frac{\binom{2k}{k}}{\binom{2(k-i)}{k-i} 4^{i(2(k-i)+1)}}$$

For Rayleigh fading with $m = 1$, Equation 2.34 matches the result obtained by [79, Eqn.(4.39)].

2.4.2 EGC Diversity

Equal gain combiner EGC equally weights each branch before combining and therefore does not require estimation of the channel fading amplitude. The output SNR of the EGC is

$$\gamma_{egc} = \left(\sum_l^L \alpha_l \right)^2 \frac{E_s}{LN_o} \quad (2.35)$$

Although there is no known closed-form exact expression for the pdf of the sum of L i.i.d. Nakagami rvs, Nakagami [19] showed that a sum can be accurately approximated by another Nakagami distribution with a parameter

m_o and average power Ω_o given by

$$m_o = Lm$$

$$\Omega_o = L\Omega(1 + (L - 1) \frac{\Gamma^2(m + \frac{1}{2})}{m\Gamma^2(m)})$$

equivalently γ_{egc} is a Gamma rv with the following parameters

$$\bar{\gamma}_{egc} = \Omega(1 + (L - 1) \frac{\Gamma^2(m + \frac{1}{2})}{m\Gamma^2(m)}) \frac{E_s}{N_o}$$

$$m_{\gamma_{egc}} = Lm$$

This implies that the pdf of the output SNR of EGC is

$$p_{\gamma_{egc}}(\gamma_{egc}) = \frac{Lm}{\bar{\gamma}_{egc}} \frac{\gamma_{egc}^{Lm-1}}{\Gamma(Lm)} \exp\left(-\frac{Lm\gamma_{egc}}{\bar{\gamma}_{egc}}\right) \quad (2.36)$$

For EGC diversity, the conditional error probability of MQAM is

$$P(e|\gamma_{egc}) = 4\left(1 - \frac{1}{\sqrt{M}}\right)Q(\sqrt{2g\gamma_{egc}}) - 4\left(1 - \frac{1}{\sqrt{M}}\right)^2Q^2(\sqrt{2g\gamma_{egc}}) \quad (2.37)$$

which is conditioned at a fixed value of SNR γ_{egc} . To get the average symbol error probability $p(e)$ of M-QAM with EGC in Nakagami fading channel we average the conditional $P(e|\gamma_{egc})$ over the pdf of γ_{egc}

$$P_{MQAM,egc}(e) = \int_0^{\infty} P(e|\gamma_{egc})p_{\gamma_{egc}}(\gamma_{egc}) d\gamma_{egc} \quad (2.38)$$

Following the same steps in evaluating the performance of M-QAM in Nakagami fading channels without diversity but noting that

$$p_{\gamma_{egc}}(\gamma_{egc}) = p_{\gamma}(\gamma)|_{m=Lm, \bar{\gamma}=\bar{\gamma}_{egc}, \gamma=\gamma_{egc}}$$

the performance of M-QAM in Nakagami fading channels with EGC is

$$P_{MQAM,egc} = 4\left(1 - \frac{1}{\sqrt{M}}\right)I_1 - 4\left(1 - \frac{1}{\sqrt{M}}\right)^2I_2 \quad (2.39)$$

where

$$I_1 = \left[\frac{1}{2}\left(1 - \sqrt{\frac{g\bar{\gamma}_{egc}}{Lm+g\bar{\gamma}_{egc}}}\right)\right]^{Lm} \sum_{k=0}^{Lm-1} \binom{Lm-1+k}{k} \left(\frac{1}{2}\left[1 + \sqrt{\frac{g\bar{\gamma}_{egc}}{Lm+g\bar{\gamma}_{egc}}}\right]\right)^k$$

and

$$I_2 = \left[\frac{1}{4} - \beta \left\{ \left(\frac{1}{2} - \frac{\tan^{-1}(\alpha_2)}{\pi} \right) \sum_{k=0}^{Lm-1} \binom{2k}{k} \frac{1}{[4(\mu^2+1)]^k} - \frac{\sin(\tan^{-1}(\alpha_2))}{\pi} \sum_{k=1}^{Lm-1} \sum_{i=1}^k \frac{T_{ik}}{(\mu^2+1)^k} [\cos(\tan^{-1}\alpha_2)]^{2(k-i)+1} \right\} \right]$$

and

$$\begin{aligned} \mu &= \sqrt{\frac{g\bar{\gamma}_{egc}}{Lm}} \\ \alpha_2 &= \sqrt{\frac{g\bar{\gamma}_{egc}}{Lm+g\bar{\gamma}_{egc}}} \\ \beta &= \sqrt{\frac{g\bar{\gamma}_{egc}}{Lm+g\bar{\gamma}_{egc}}} \\ T_{ik} &= \frac{\binom{2k}{k}}{\binom{2(k-i)}{k-i} 4^{i(2(k-i)+1)}} \end{aligned}$$

2.4.3 SC Diversity

With SC the branch with the largest SNR per symbol is selected so the instantaneous symbol energy-to-noise ratio is

$$\gamma_{sc} = \max\{\gamma_1, \gamma_2, \dots, \gamma_L\} = \alpha_{\max}^2 \frac{E_s}{N_0} \quad (2.40)$$

where L is the number of diversity branches. The instantaneous symbol energy-to-noise ratio on the l^{th} diversity branch has Gamma pdf

$$p\gamma_l = \frac{m^m}{\bar{\gamma}_l} \frac{\gamma_l^{m-1}}{\Gamma(m)} \exp\left(-\frac{m\gamma_l}{\bar{\gamma}_l}\right) \quad (2.41)$$

where $\bar{\gamma}_l$ is the average received symbol energy-to-noise ratio for the l^{th} diversity branch and since the channels are independent identical Nakagami distributed (i.i.d) so $\bar{\gamma}_l = \bar{\gamma}$ for each diversity channel. The cumulative dis-

tribution function (cdf) at the output of the SC combiner $F_{\gamma_{sc}}$ is

$$F_{\gamma_{sc}}(\gamma_{sc}) = Pr[\gamma_1 \leq \gamma_{sc} \cap \gamma_2 \leq \gamma_{sc} \cap \dots \cap \gamma_L \leq \gamma_{sc}] = [F_{\gamma}(\gamma_{sc})]^L \quad (2.42)$$

The pdf of the SNR at the output of the SC combiner is obtained by differentiating Equation 2.42

$$p_{\gamma_{sc}}(\gamma_{sc}) = L[F_{\gamma}(\gamma_{sc})]^{L-1} p_{\gamma}(\gamma_{sc}) \quad (2.43)$$

where

$$F_{\gamma}(\gamma_{sc}) = \int_0^{\gamma_{sc}} p_{\gamma}(y) dy \quad (2.44)$$

and

$$p(\gamma) = \frac{m^m \gamma^{m-1}}{\bar{\gamma} \Gamma(m)} \exp\left(-\frac{m\gamma}{\bar{\gamma}}\right) \quad (2.45)$$

Substitute Equation 2.45 in Equation 2.44 we obtain

$$F_{\gamma}(\gamma_{sc}) = \frac{\gamma(m, \frac{m\gamma_{sc}}{\bar{\gamma}})}{\Gamma(m)}, \quad \gamma_{sc} \geq 0 \quad (2.46)$$

with $\gamma(., .)$ denoting the incomplete Gamma function [80].

Substituting Equation 2.45 and 2.46 in Equation 2.43 we obtain

$$p_{\gamma_{sc}}(\gamma_{sc}) = L \left[\frac{\gamma(m, \frac{m\gamma_{sc}}{\bar{\gamma}})}{\Gamma(m)} \right]^{L-1} \frac{m^m \gamma_{sc}^{m-1}}{\bar{\gamma} \Gamma(m)} \exp\left(-\frac{m\gamma_{sc}}{\bar{\gamma}}\right) \quad (2.47)$$

Fedele [81] showed that when m is an integer the pdf of the SC output $p_{\gamma_{sc}}(\gamma_{sc})$ (Equation 2.47) can be rewritten in terms of a finite series expressions as

$$p_{\gamma_{sc}}(\gamma_{sc}) = \frac{L}{\Gamma(m)} \sum_{l=0}^{L-1} (-1)^l \binom{L-1}{l} \exp\left(-\frac{m\gamma_{sc}}{\bar{\gamma}}\right) \sum_{k=0}^{l(m-1)} b_k^l \left(\frac{m}{\bar{\gamma}}\right)^{m+k} \gamma_{sc}^{m+k-1} \quad (2.48)$$

where the coefficients b_k^l can be recursively computed as $b_0^l = 1$, $b_1^l = l$, $b_{l(m+1)}^l = \frac{1}{((m-1)!)^l}$ and for $2 \leq k \leq l(m-1) - 1$, b_k^l can be computed by the following equation

$$b_k^l = \frac{1}{k} \sum_{j=1}^{j_o} \frac{j(l+1) - k}{j!} b_{k-j}^l \quad (2.49)$$

with $j_o = \min(k, m-1)$. For SC diversity, the conditional error probability of M-QAM is

$$P(e|\gamma_{sc}) = 4\left(1 - \frac{1}{\sqrt{M}}\right)Q(\sqrt{2g\gamma_{sc}}) - 4\left(1 - \frac{1}{\sqrt{M}}\right)^2 Q^2(\sqrt{2g\gamma_{sc}}) \quad (2.50)$$

which is conditioned at a fixed value of SNR γ_{sc} where $\gamma_{sc} = \alpha_{max}^2 \frac{E_s}{N_0}$ and α_{max} is the maximum fading amplitude. So the average symbol error probability of M-QAM in Nakagami fading channel with SC is

$$P_{MQAM,sc}(e) = \int_0^\infty P(e|\gamma_{sc}) p_{\gamma_{sc}}(\gamma_{sc}) d\gamma_{sc} \quad (2.51)$$

Substitute Equation 2.50 in 2.51 to get

$$\begin{aligned} P_{MQAM,sc} &= 4\left(1 - \frac{1}{\sqrt{M}}\right) \underbrace{\int_0^\infty p(\gamma_{sc}) Q(\sqrt{2g\gamma_{sc}}) d\gamma_{sc}}_{I_1} \\ &\quad - 4\left(1 - \frac{1}{\sqrt{M}}\right)^2 \underbrace{\int_0^\infty p(\gamma_{sc}) Q^2(\sqrt{2g\gamma_{sc}}) d\gamma_{sc}}_{I_2} \end{aligned} \quad (2.52)$$

Substituting Equation 2.48 in Equation 2.52 we obtain

$$\begin{aligned} I_1 &= \frac{L}{\Gamma(m)} \sum_{l=0}^{L-1} (-1)^l \binom{L-1}{l} \sum_{k=0}^{l(m-1)} b_k^l \int_0^\infty Q(\sqrt{2g\gamma_{sc}}) \\ &\quad \left(\frac{m}{\bar{\gamma}}\right)^{m+k} \exp\left(-\frac{m\gamma_{sc}}{\bar{\gamma}}\right) \gamma_{sc}^{m+k-1} d\gamma_{sc} \end{aligned} \quad (2.53)$$

$$I_2 = \frac{L}{\Gamma(m)} \sum_{l=0}^{L-1} (-1)^l \binom{L-1}{l} \sum_{k=0}^{l(m-1)} b_k^l \int_0^\infty Q^2(\sqrt{2g\gamma_{sc}}) \left(\frac{m}{\bar{\gamma}}\right)^{m+k} \exp(-l+1) \frac{m\gamma_{sc}}{\bar{\gamma}} \gamma_{sc}^{m+k-1} d\gamma_{sc} \quad (2.54)$$

Modify the integrand of I_1 so that it can be of the same form as the integrand of Equation 2.12

$$I_1 = \frac{L}{\Gamma(m)} \sum_{l=0}^{L-1} (-1)^l \binom{L-1}{l} \sum_{k=0}^{l(m-1)} b_k^l \frac{\Gamma(m+k)}{(l+1)^{m+k}} \int_0^\infty Q(\sqrt{2g\gamma_{sc}}) \left(\frac{(l+1)m}{\bar{\gamma}}\right)^{m+k} \exp(-l+1) \frac{m\gamma_{sc}}{\bar{\gamma}} \frac{1}{\Gamma(m+k)} \gamma_{sc}^{m+k-1} d\gamma_{sc} \quad (2.55)$$

Let

$$a = \frac{m(l+1)}{\bar{\gamma}} \text{ and}$$

$$b = 2g \text{ this implies } c = \frac{b}{2a}$$

so the result will be the same as the result of Equation 2.14, that is

$$I_1 = \frac{L}{\Gamma(m)} \sum_{l=0}^{L-1} (-1)^l \binom{L-1}{l} \sum_{k=0}^{l(m-1)} b_k^l \frac{\Gamma(m+k)}{(l+1)^{m+k}} [P_l(c)]^{m+k} \sum_{h=0}^{m+k-1} \binom{m+k-1+h}{h} [1 - P_l(c)]^h \quad (2.56)$$

where

$$P_l(c) = \frac{1}{2}(1 - \mu_l) \text{ and } \mu_l = \sqrt{\frac{g\bar{\gamma}}{g\bar{\gamma} + m(l+1)}}$$

To evaluate I_2 we substitute Equation 2.18 in Equation 2.54 so $I_2 = I_3 - I_4$

where

$$I_3 = \frac{L}{\Gamma(m)} \sum_{l=0}^{L-1} (-1)^l \binom{L-1}{l} \sum_{k=0}^{l(m-1)} b_k^l \int_0^\infty 2P_{MPSK}(e/\gamma)|_{M=2, \gamma=g\gamma_{sc}}$$

$$\left(\frac{m}{\bar{\gamma}}\right)^{m+k} \exp\left(-\left(l+1\right)\frac{m\gamma_{sc}}{\bar{\gamma}}\right) \gamma_{sc}^{m+k-1} d\gamma_{sc} \quad (2.57)$$

and

$$I_4 = \frac{L}{\Gamma(m)} \sum_{l=0}^{L-1} (-1)^l \binom{L-1}{l} \sum_{k=0}^{l(m-1)} b_k^l \int_0^\infty P_{MPSK}(e/\gamma)|_{M=4, \gamma=g\gamma_{sc}} \left(\frac{m}{\bar{\gamma}}\right)^{m+k} \exp\left(-\left(l+1\right)\frac{m\gamma_{sc}}{\bar{\gamma}}\right) \gamma_{sc}^{m+k-1} d\gamma_{sc} \quad (2.58)$$

We modify Equation 2.57 and 2.58 so that their integrands will be the same as the integrand of Equation 2.22

$$I_3 = \frac{L}{\Gamma(m)} \sum_{l=0}^{L-1} (-1)^l \binom{L-1}{l} \sum_{k=0}^{l(m-1)} b_k^l \frac{\Gamma(m+k)}{(l+1)^{m+k}} \int_0^\infty 2P_{BPSK}(e)|_{\gamma=g\gamma_{sc}} \left(\frac{(l+1)m}{\bar{\gamma}}\right)^{m+k} \exp\left(-\left(l+1\right)\frac{m\gamma_{sc}}{\bar{\gamma}}\right) \frac{1}{\Gamma(m+k)} \gamma_{sc}^{m+k-1} d\gamma_{sc} \quad (2.59)$$

$$I_4 = \frac{L}{\Gamma(m)} \sum_{l=0}^{L-1} (-1)^l \binom{L-1}{l} \sum_{k=0}^{l(m-1)} b_k^l \frac{\Gamma(m+k)}{(l+1)^{m+k}} \int_0^\infty P_{QPSK}(e)|_{\gamma=g\gamma_{sc}} \left(\frac{(l+1)m}{\bar{\gamma}}\right)^{m+k} \exp\left(-\left(l+1\right)\frac{m\gamma_{sc}}{\bar{\gamma}}\right) \frac{1}{\Gamma(m+k)} \gamma_{sc}^{m+k-1} d\gamma_{sc} \quad (2.60)$$

Using Equation 2.23 for Equation 2.59 and 2.60, we obtain

$$I_3 = \frac{L}{\Gamma(m)} \sum_{l=0}^{L-1} (-1)^l \binom{L-1}{l} \sum_{k=0}^{l(m-1)} b_k^l \frac{\Gamma(m+k)}{(l+1)^{m+k}} \left[1 - \beta_l \sum_{h=0}^{m+k-1} \binom{2h}{h} \frac{1}{[4(\mu_l^2 + 1)]^h}\right] \quad (2.61)$$

and

$$I_4 = \frac{L}{\Gamma(m)} \sum_{l=0}^{L-1} (-1)^l \binom{L-1}{l} \sum_{k=0}^{l(m-1)} b_k^l \frac{\Gamma(m+k)}{(l+1)^{m+k}}$$

$$\begin{aligned}
& \left[\frac{3}{4} - \beta_l \left\{ \frac{1}{2} + \frac{\tan^{-1}(\alpha_l)}{\pi} \right\} \sum_{h=0}^{m+k-1} \binom{2h}{h} \frac{1}{[4(\mu_l^2 + 1)]^h} \right. \\
& \left. + \frac{\sin(\tan^{-1}(\alpha_l))}{\pi} \sum_{h=1}^{m+k-1} \sum_{i=1}^h \frac{T_{ih}}{(\mu_l^2 + 1)^h} [\cos(\tan^{-1} \alpha_l)]^{2(h-i)+1} \right] \quad (2.62)
\end{aligned}$$

Then

$$\begin{aligned}
I_2 &= \frac{L}{\Gamma(m)} \sum_{l=0}^{L-1} (-1)^l \binom{L-1}{l} \sum_{k=0}^{l(m-1)} b_k^l \frac{\Gamma(m+k)}{(l+1)^{m+k}} \\
& \left\{ \frac{1}{4} - \beta_l \left\{ \frac{1}{2} - \frac{\tan^{-1}(\alpha_l)}{\pi} \right\} \sum_{h=0}^{m+k-1} \binom{2h}{h} \frac{1}{[4(\mu_l^2 + 1)]^h} \right. \\
& \left. - \frac{\sin(\tan^{-1}(\alpha_l))}{\pi} \sum_{h=1}^{m+k-1} \sum_{i=1}^h \frac{T_{ih}}{(\mu_l^2 + 1)^h} [\cos(\tan^{-1} \alpha_l)]^{2(h-i)+1} \right\} \quad (2.63)
\end{aligned}$$

with

$$\begin{aligned}
\alpha_l &= \beta_l = \sqrt{\frac{g\bar{\gamma}}{g\bar{\gamma} + m(l+1)}} \\
\mu_l &= \sqrt{\frac{g\bar{\gamma}}{m(l+1)}}
\end{aligned}$$

Finally, the values of I_1 and I_2 are substituted in Equation 2.52 to obtain $P_{MQAM,sc}$ and it is repeated here

$$P_{MQAM,sc} = 4 \left(1 - \frac{1}{\sqrt{M}}\right) I_1 - 4 \left(1 - \frac{1}{\sqrt{M}}\right)^2 I_2 \quad (2.64)$$

We show in the following the error probability performance of MQAM over Rayleigh fading channels with SC scheme and it is a special case of Equation 2.64. When $m = 1$, I_1 becomes as

$$I_1 = L \sum_{l=0}^{L-1} (-1)^l \binom{L-1}{l} \frac{1}{(l+1)} \left[\frac{1}{2} (1 - \mu_l) \right] \quad (2.65)$$

where

$$\mu_l = \sqrt{\frac{g\bar{\gamma}}{g\bar{\gamma} + (l+1)}}$$

We know that $L \binom{L-1}{l} \frac{1}{(l+1)} = \binom{L}{l+1}$ and we let $n = l + 1$ then Equation 2.65 can be rewritten as

$$I_1 = \sum_{n=1}^L (-1)^{n-1} \binom{L}{n} \left[\frac{1}{2}(1 - x_n) \right] \quad (2.66)$$

$$x_n = \mu_l|_{l+1=n} = \sqrt{\frac{c}{c+1}}$$

where $c = \frac{g\bar{\gamma}}{n} = \frac{3\bar{\gamma}}{2(M-1)n}$. We know that $\bar{\gamma} = \log_2 M\bar{\gamma}_c$ where $\bar{\gamma}_c$ is the average bit SNR per channel $\rightarrow c = \frac{3 \log_2 M\bar{\gamma}_c}{2(M-1)n} = \frac{\bar{\gamma}_c}{pn}$

then Equation 2.66 can be rewritten as

$$I_1 = \sum_{n=1}^L (-1)^{n-1} \binom{L}{n} \left[\frac{1}{2}(1 - \lambda_n) \right] \quad (2.67)$$

$$\text{where } \lambda_n = \sqrt{\frac{\bar{\gamma}_c}{pn + \bar{\gamma}_c}}$$

for I_2 when $m = 1$, $l + 1 = n$ and $\beta_l = \alpha_l = \lambda_n$ then

$$I_2 = L \sum_{n=1}^L (-1)^{n-1} \binom{L}{n} \left[\frac{1}{4} - \lambda_n \left(\frac{1}{2} - \frac{\tan^{-1}(\lambda_n)}{\pi} \right) \right] \quad (2.68)$$

$$I_2 = L \sum_{n=1}^L (-1)^{n-1} \binom{L}{n} \left[\frac{1}{4} - \frac{\lambda_n}{\pi} \left(\frac{\pi}{2} - \tan^{-1}(\lambda_n) \right) \right] \quad (2.69)$$

$$I_2 = L \sum_{n=1}^L (-1)^{n-1} \binom{L}{n} \frac{1}{4} \left[1 - \frac{4\lambda_n}{\pi} \left\{ \tan^{-1} \left(\frac{1}{\lambda_n} \right) \right\} \right] \quad (2.70)$$

Let $q = 4(1 - \frac{1}{\sqrt{M}})$ then Equation 2.64 can be rewritten as

$$P_{MQAM,sc} = L \sum_{n=1}^L (-1)^{n-1} \binom{L}{n} \left\{ q \left(\frac{1 - \lambda_n}{2} \right) - \frac{q^2}{16} \left[1 - \frac{4\lambda_n}{\pi} \left\{ \tan^{-1} \left(\frac{1}{\lambda_n} \right) \right\} \right] \right\} \quad (2.71)$$

Equation 2.71 is the same as [76, Eq.23] which is the performance of MQAM over Rayleigh fading channels with SC diversity scheme.

It is worth mentioning that when Gray mapping is used, the average bit error probability (BER) of MQAM is obtained by $BER = \frac{SER}{k}$. The various bit error rates of MQAM derived in this chapter are plotted in the following chapter. The equivalent system will be simulated, and simulation results will be used to verify the derivations.

The derivation of the symbol error rate of MQAM with GSC is very complicated. Therefore, only simulation is used to evaluate the performance of MQAM with this diversity scheme.

Chapter 3

Simulation and Discussion

3.1 Study Cases

3.1.1 Nakagami- m Distribution

As discussed in chapter 1, the Nakagami model is more general than any other fading channel model. Nakagami can model different fading conditions. Different family of Nakagami distribution is simulated and the results are illustrated in Figure 3.1.

3.1.2 Performance of M-QAM in Nakagami Fading Channel

The simulation results of the performance of M-QAM in Nakagami fading channel are presented. The simulation is performed for 4-QAM, 16-QAM and 64-QAM with different Nakagami parameters ($m = 1, 2, 4$). The effect of m is clear in Figure 3.2 - Figure 3.4. Large values of m model less fading channels. Consequently, the performance improves with increasing m .

3.1.3 Performance of M-QAM with MRC in Nakagami Fading Channels

Simulation results for 4-QAM with MRC in Nakagami fading channels for different fading conditions (different m) and different number of diversity branches are shown in Figure 3.5 - Figure 3.7. Figure 3.8 - Figure 3.10 show the simulation results for 16-QAM and Figure 3.11 - Figure 3.13 show the simulation results for 64-QAM.

3.1.4 Performance of M-QAM with EGC in Nakagami Fading Channels

The performance of M-QAM with EGC in Nakagami fading channels is simulated for different diversity branches and different fading conditions. The results for 4-QAM are shown in Figure 3.14 - Figure 3.16, for 16-QAM are shown in Figure 3.17 - Figure 3.19 and for 64-QAM are shown in Figure 3.20 - Figure 3.22.

3.1.5 Performance of M-QAM with SC in Nakagami Fading Channels

The performance of M-QAM with SC in Nakagami fading channels is simulated for different diversity branches and different fading conditions. The simulation results for 4-QAM are shown in Figure 3.23 - Figure 3.25. The simulation results for 16-QAM are shown in Figure 3.26 - Figure 3.28. The simulation results for 64-QAM are shown in Figure 3.29 - Figure 3.31.

3.1.6 Performance of M-QAM with Generalized Selection combining Scheme in Nakagami Fading Channels

Simulation results of the performance of 4-QAM with GSC over Nakagami fading channels are shown in Figure 3.32 - Figure 3.34 for different Nakagami parameter $m = 1, 2, 4$ respectively. The simulation is conducted for a system with number of diversity branches $L=4$. In these figures, the solid curve labeled (a) represents the performance of GSC with $L_c = 3$ (which is choosing the three largest signals out of the total number of diversity branches $L=4$) and the dashed curve labeled (b) represents the performance of GSC with $L_c = 2$.

3.2 Simulation Results

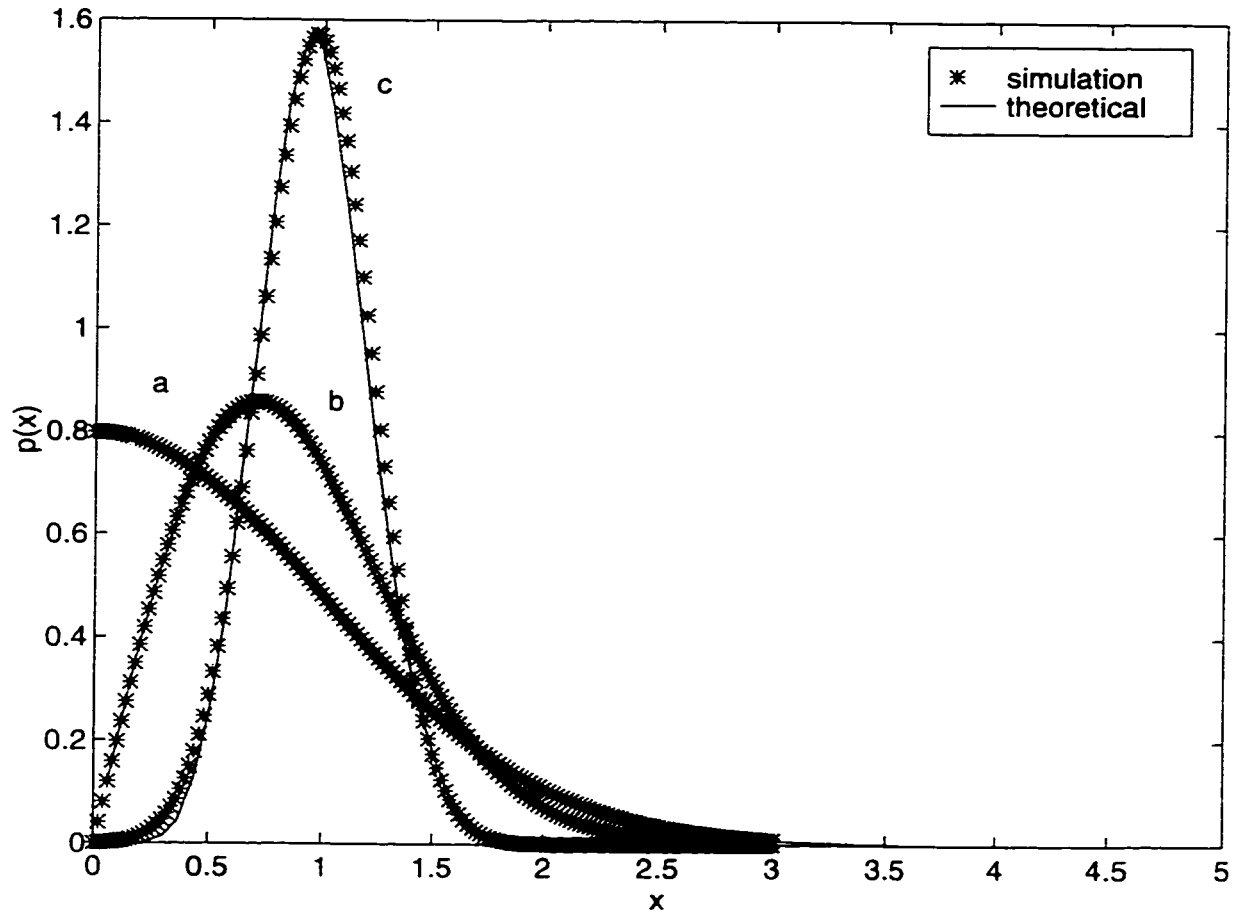


Figure 3.1: Different Nakagami- m distributions a- $m = \frac{1}{2}$ one sided gaussian distribution b- $m = 1$ Rayleigh distribution c- $m = 4$ which corresponds to Ricean distribution with $K = 6.4775$

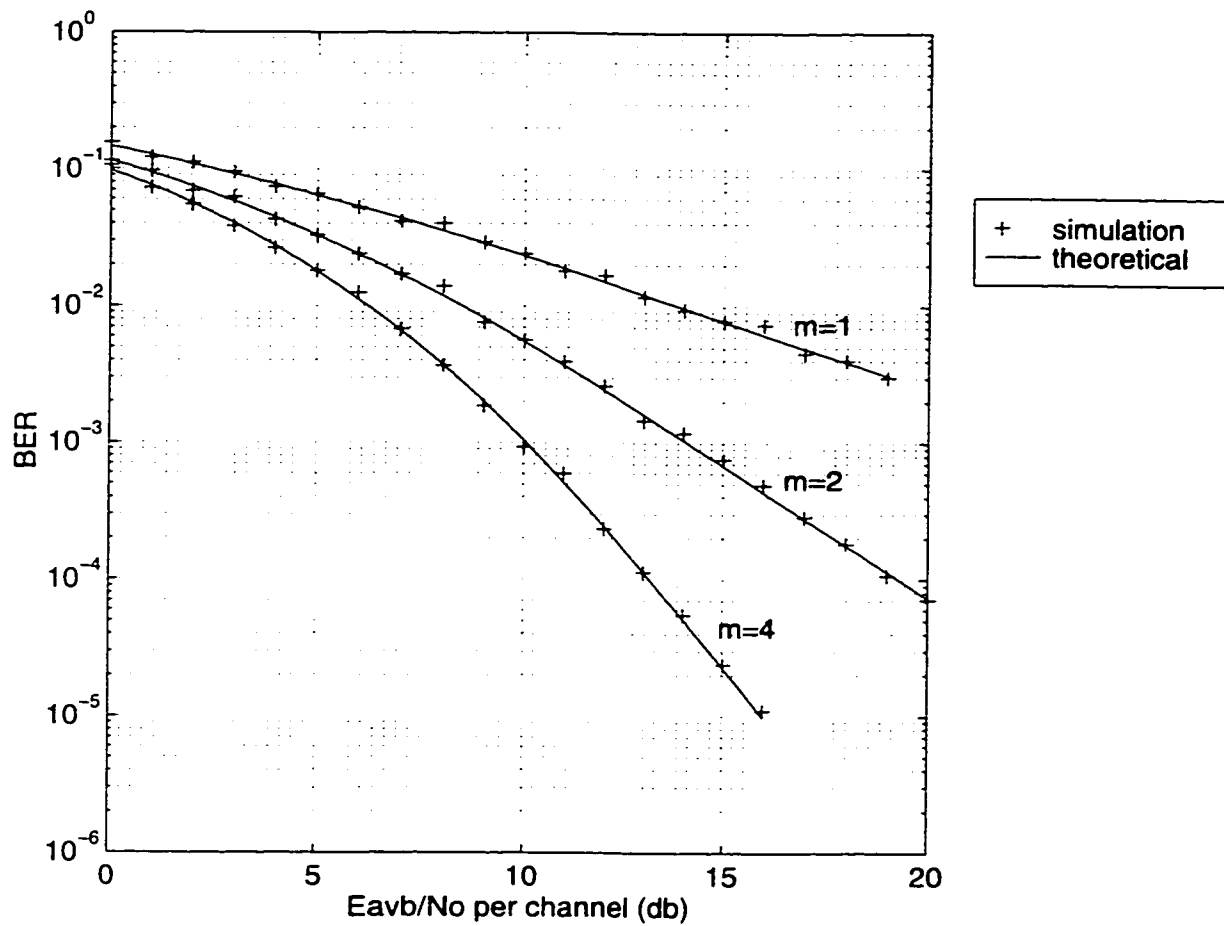


Figure 3.2: Performance of 4-QAM in Nakagami fading channel with different Nakagami parameter ($m = 1, 2, 4$)

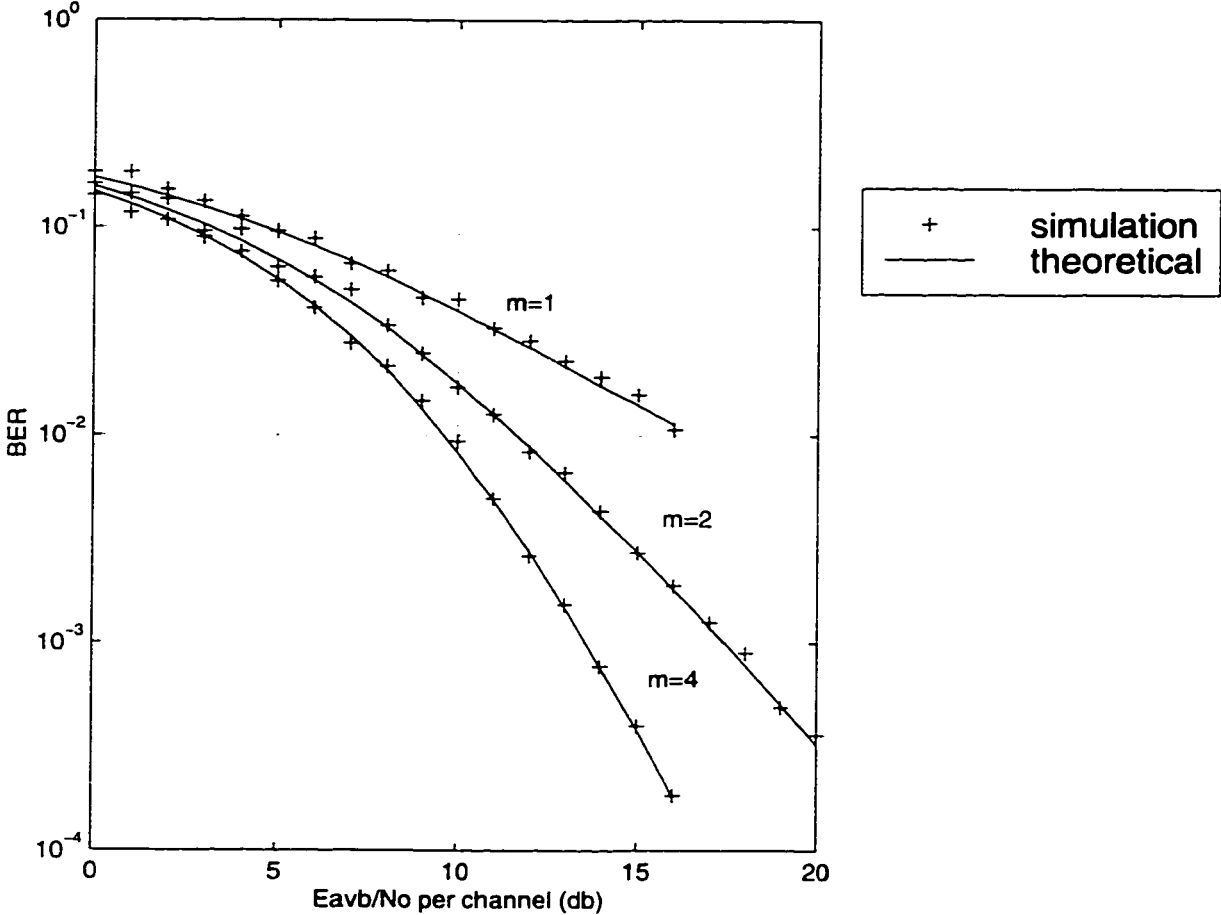


Figure 3.3: Performance of 16-QAM in Nakagami fading channel with different Nakagami parameter ($m = 1, 2, 4$)

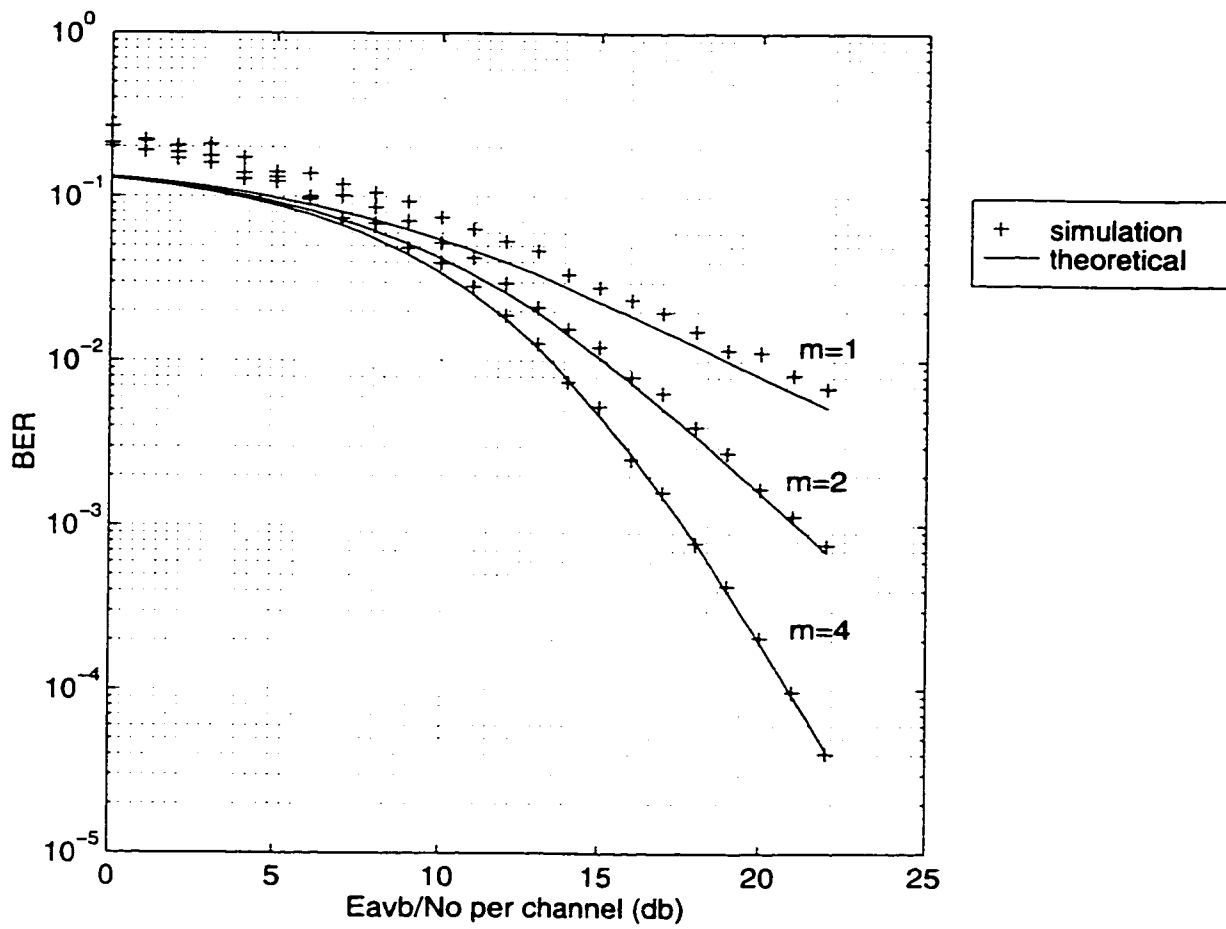


Figure 3.4: Performance of 64-QAM in Nakagami fading channel with different Nakagami parameter ($m = 1, 2, 4$)

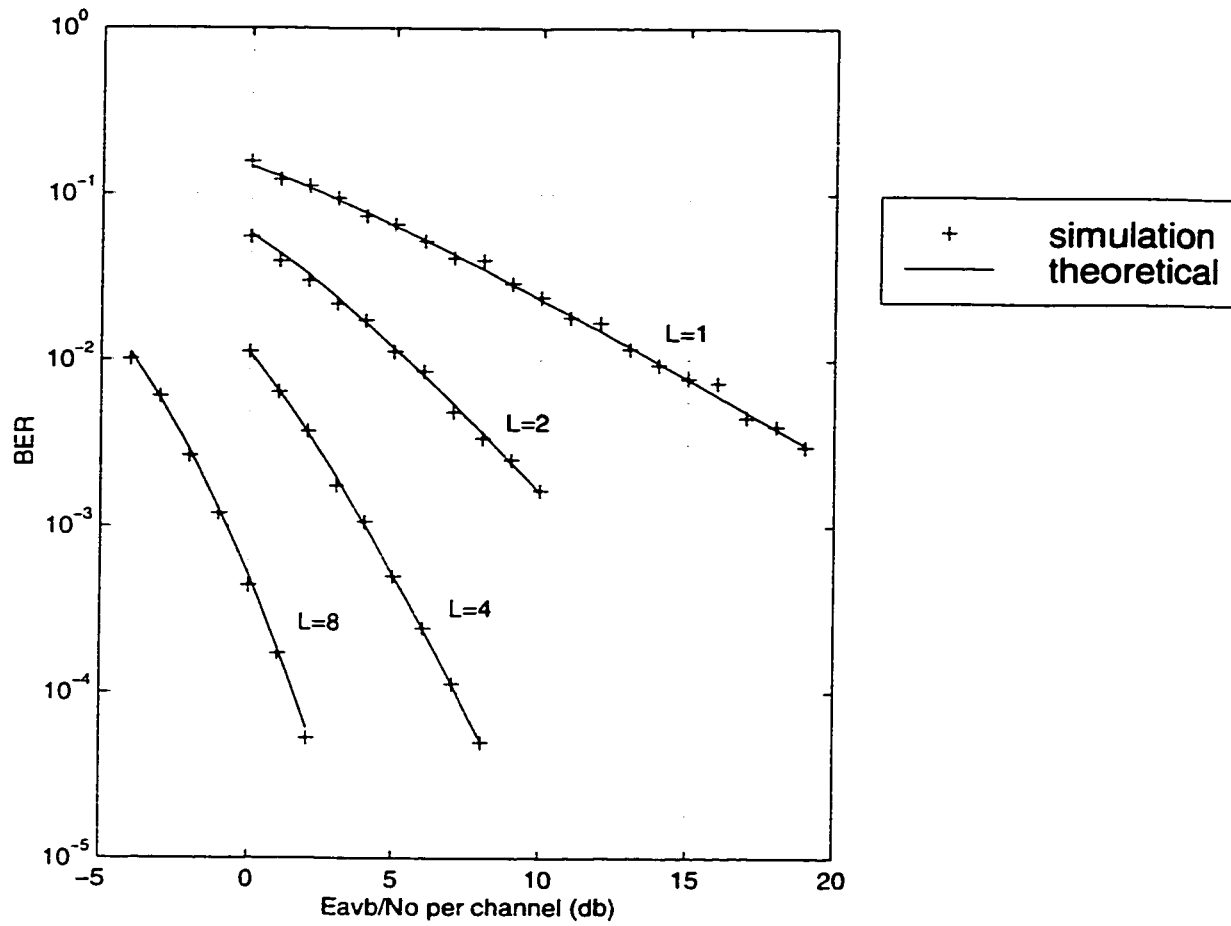


Figure 3.5: Performance of 4-QAM with MRC in Nakagami fading channels, ($m = 1$)

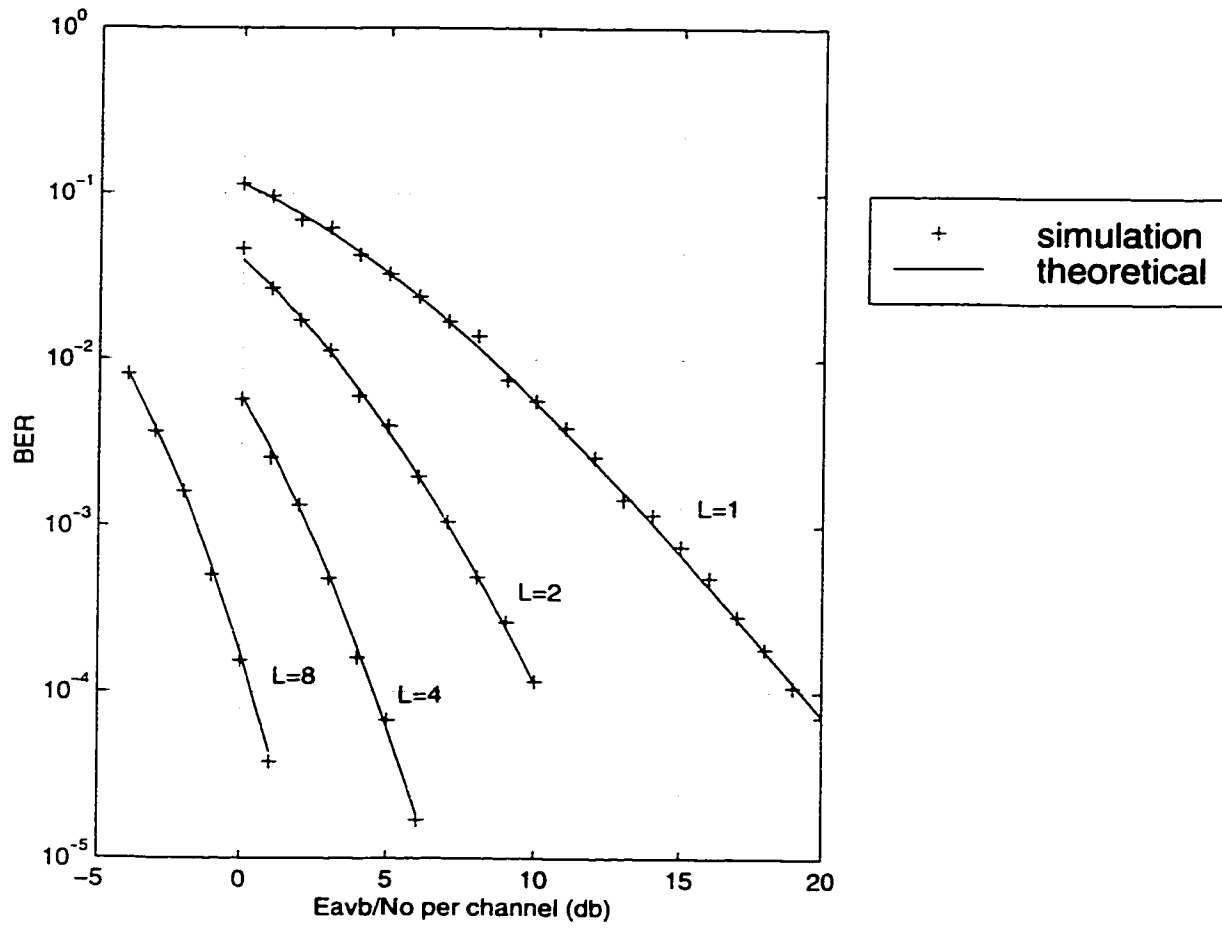


Figure 3.6: Performance of 4-QAM with MRC in Nakagami fading channels, ($m = 2$)

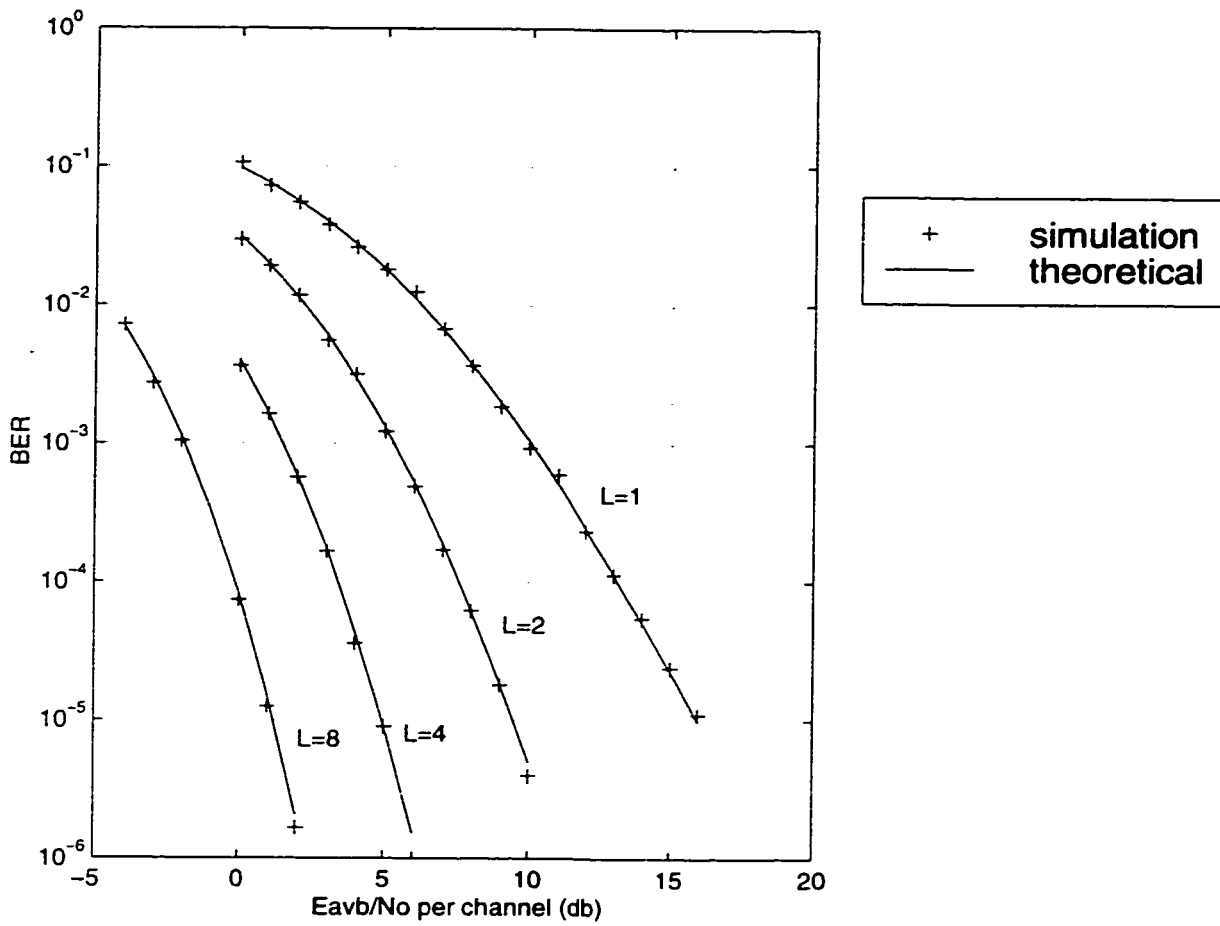


Figure 3.7: Performance of 4-QAM with MRC in Nakagami fading channels, ($m = 4$)

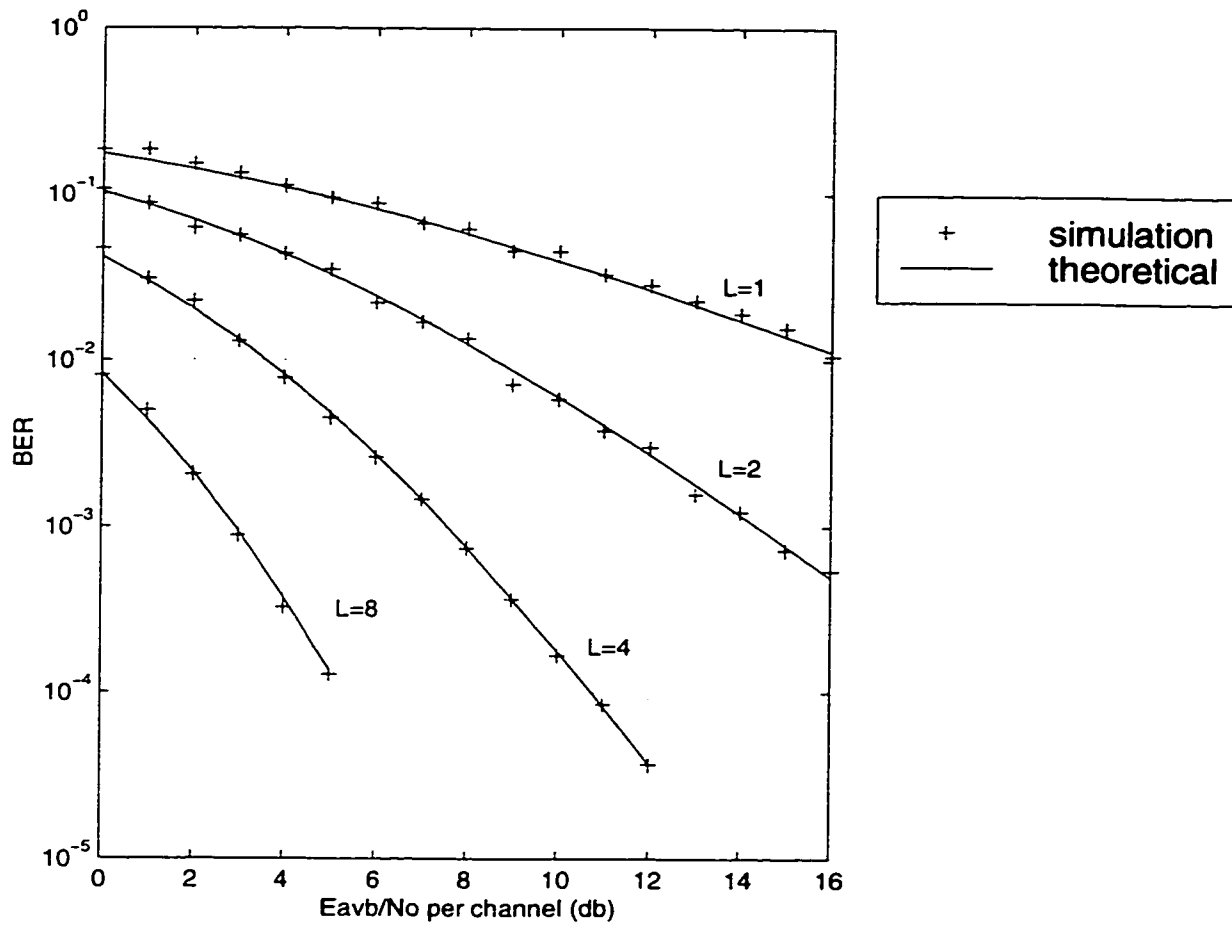


Figure 3.8: Performance of 16-QAM with MRC in Nakagami fading channels, ($m = 1$)

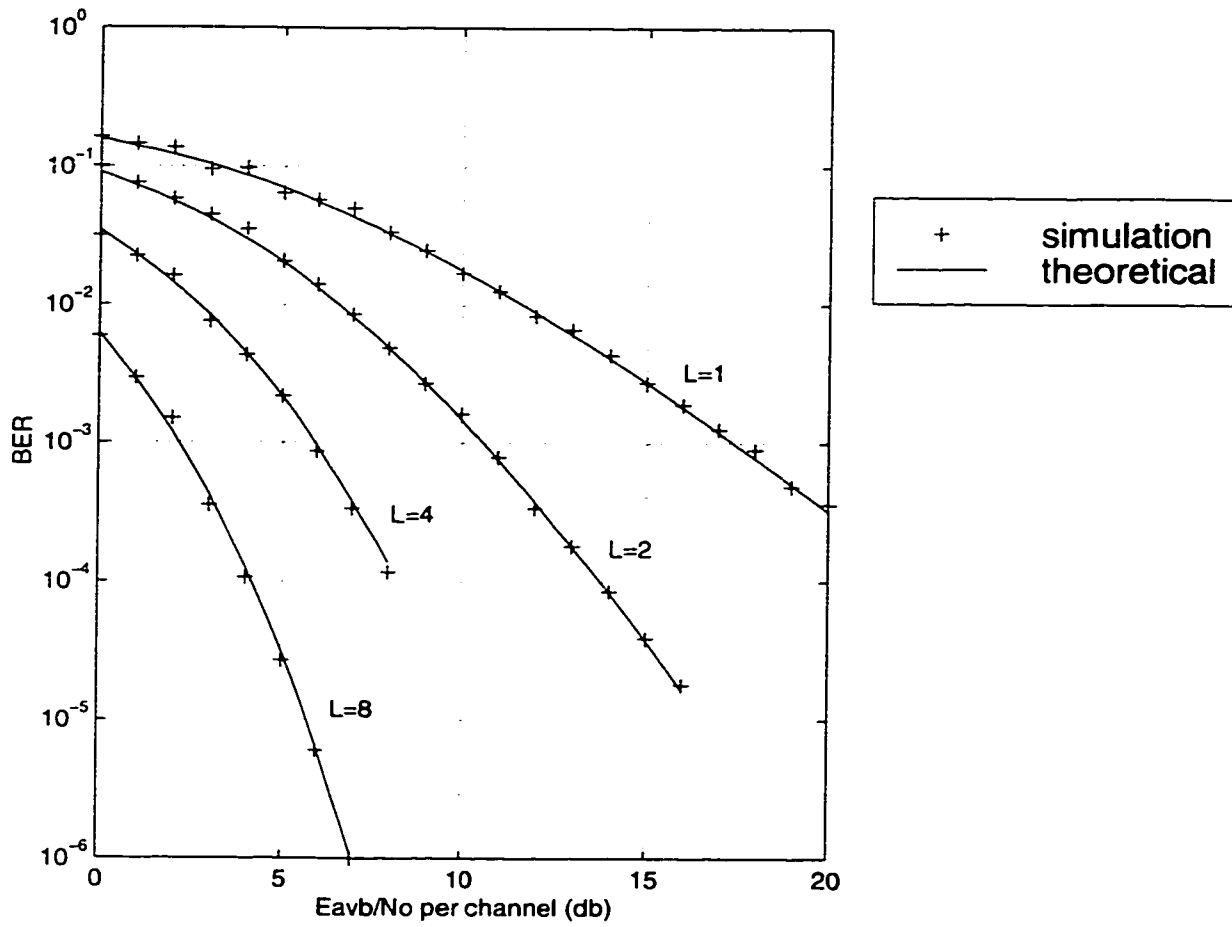


Figure 3.9: Performance of 16-QAM with MRC in Nakagami fading channels, ($m = 2$)

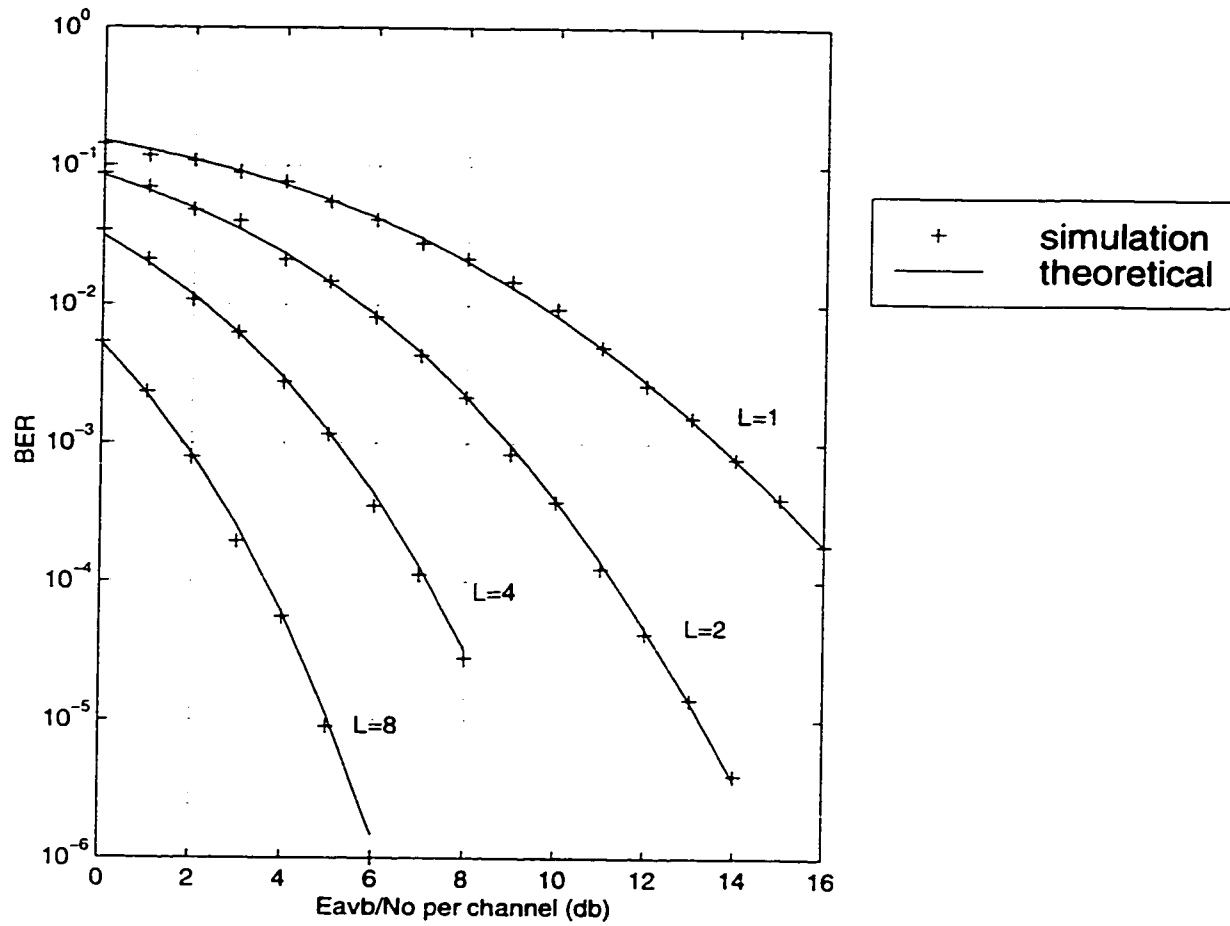


Figure 3.10: Performance of 16-QAM with MRC in Nakagami fading channels, ($m = 4$)

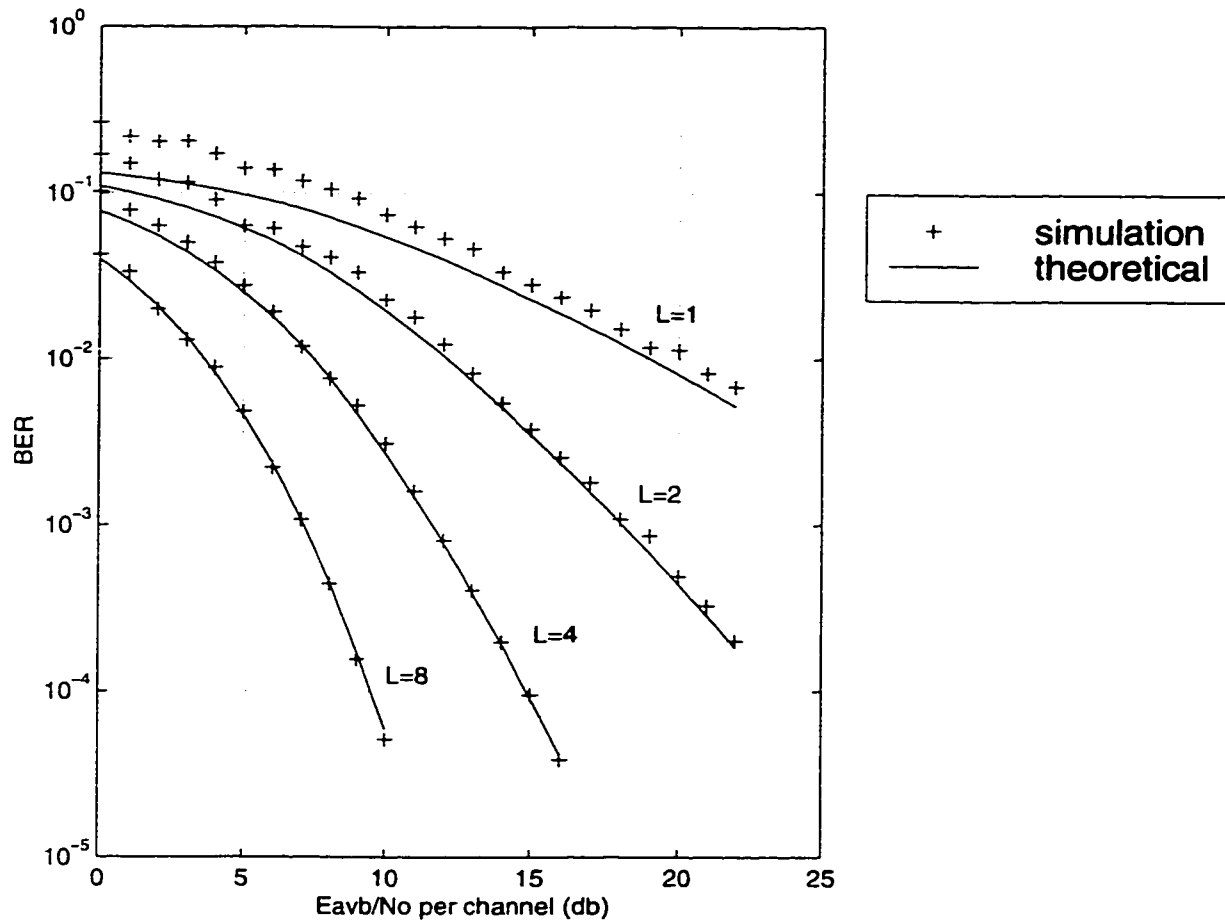


Figure 3.11: Performance of 64-QAM with MRC in Nakagami fading channels, ($m = 1$)

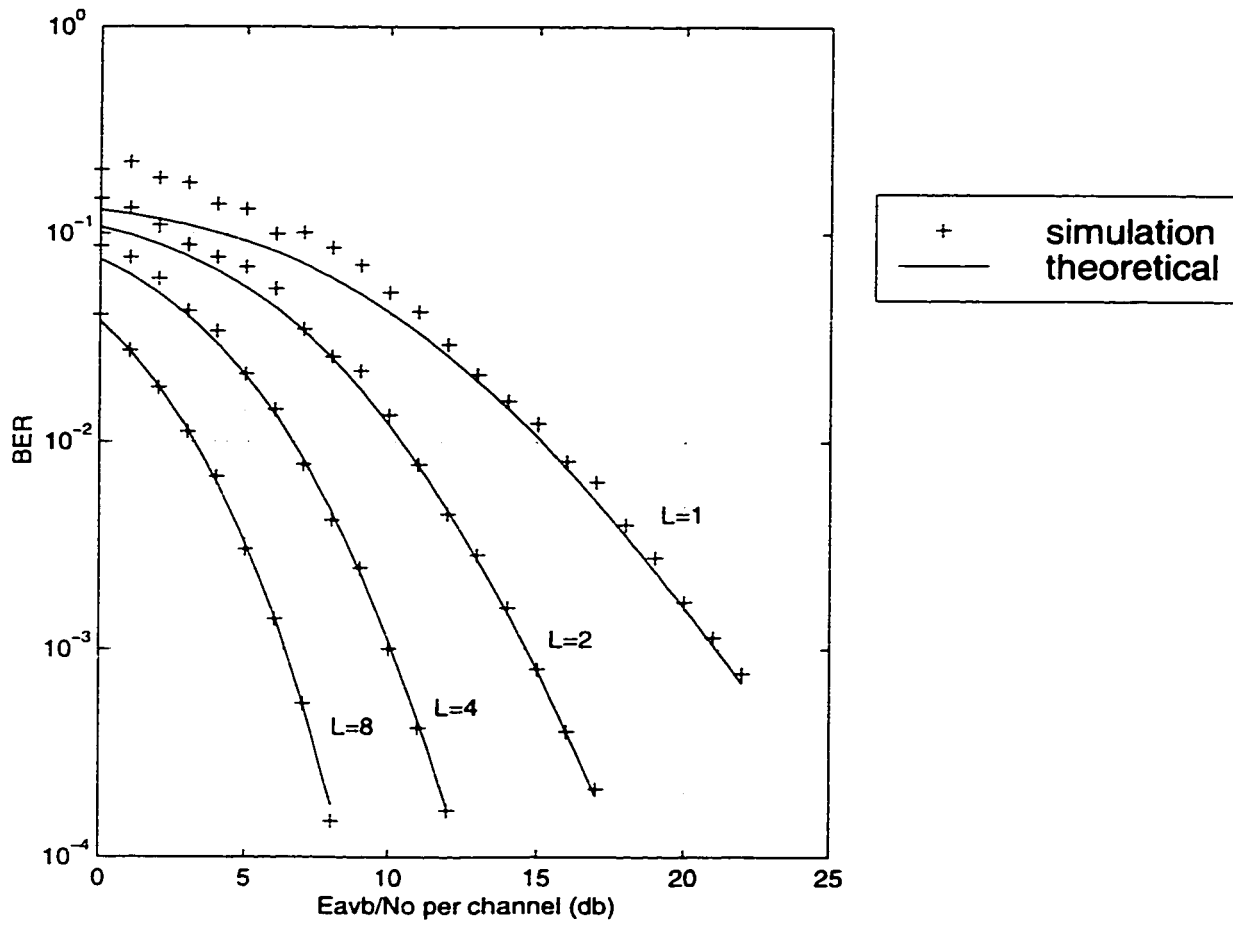


Figure 3.12: Performance of 64-QAM with MRC in Nakagami fading channels, ($m = 2$)

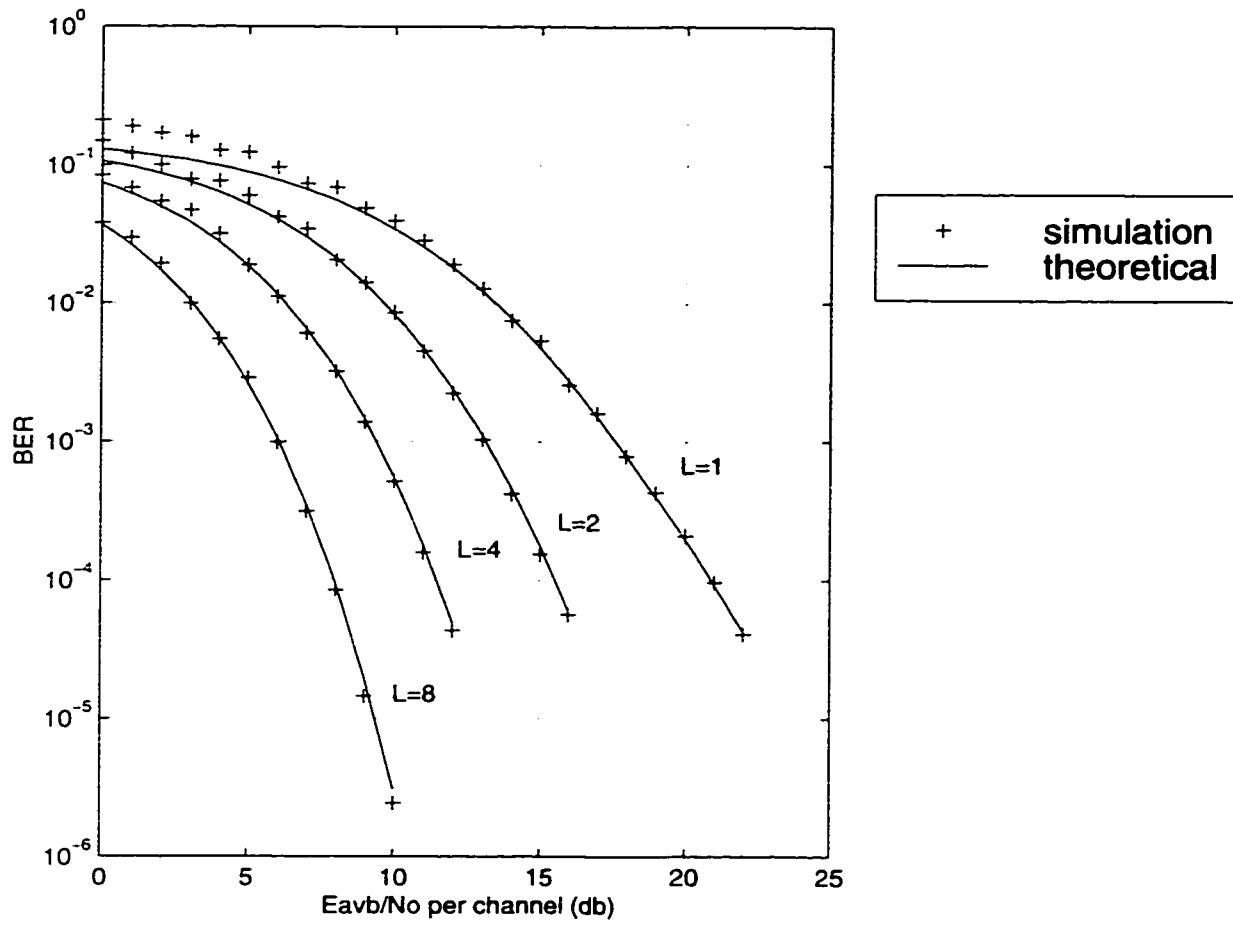


Figure 3.13: Performance of 64-QAM with MRC in Nakagami fading channels, ($m = 4$)

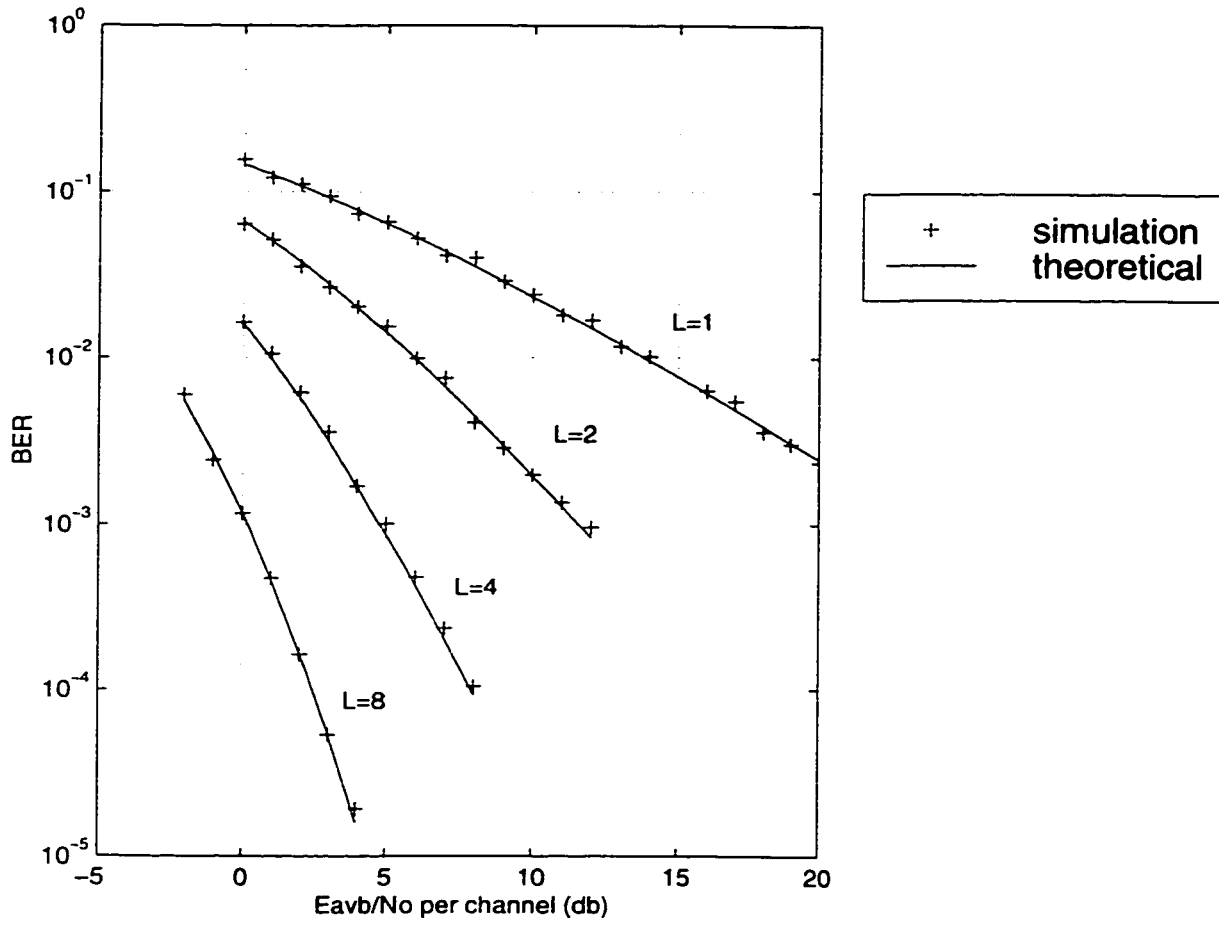


Figure 3.14: Performance of 4-QAM with EGC in Nakagami fading channels, ($m = 1$)

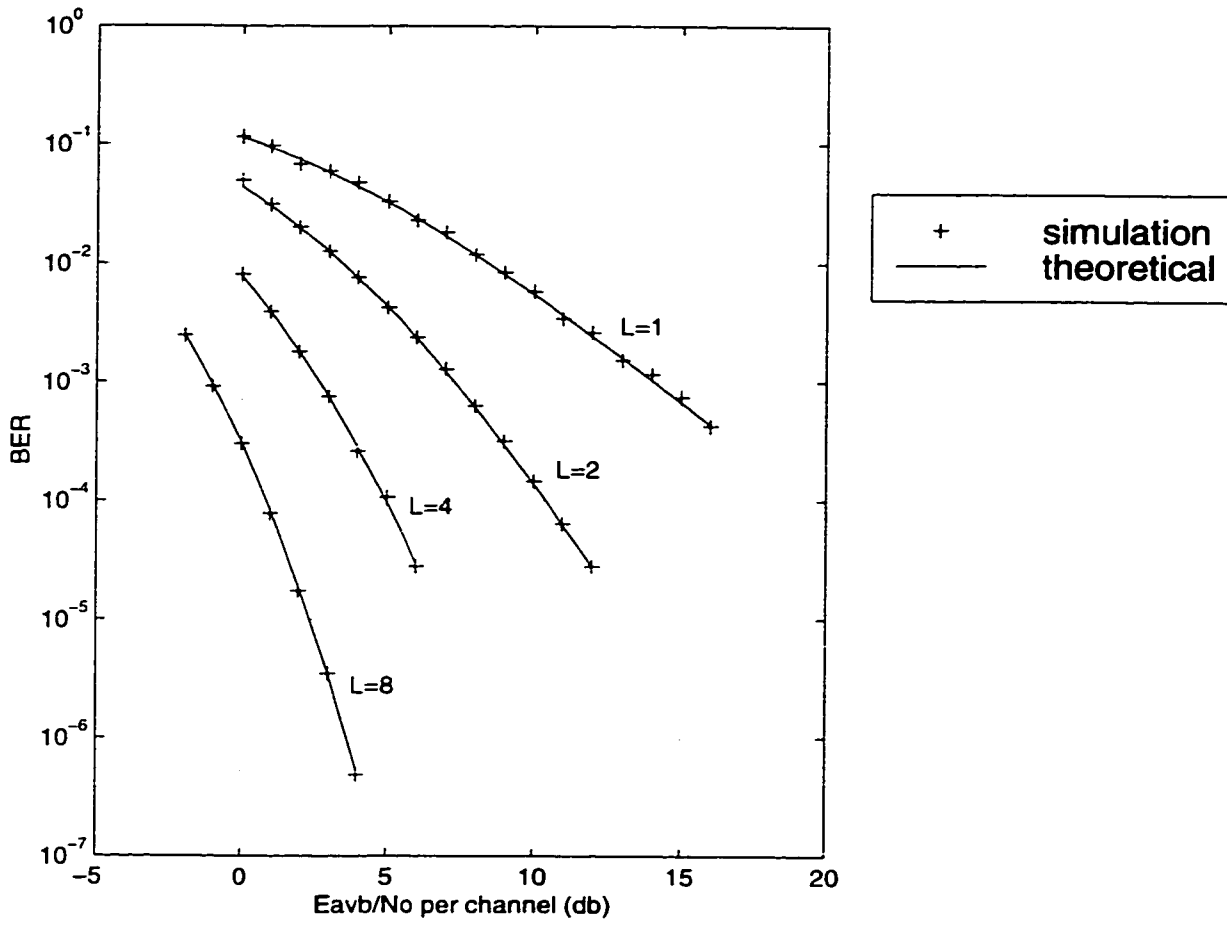


Figure 3.15: Performance of 4-QAM with EGC in Nakagami fading channels, ($m = 2$)

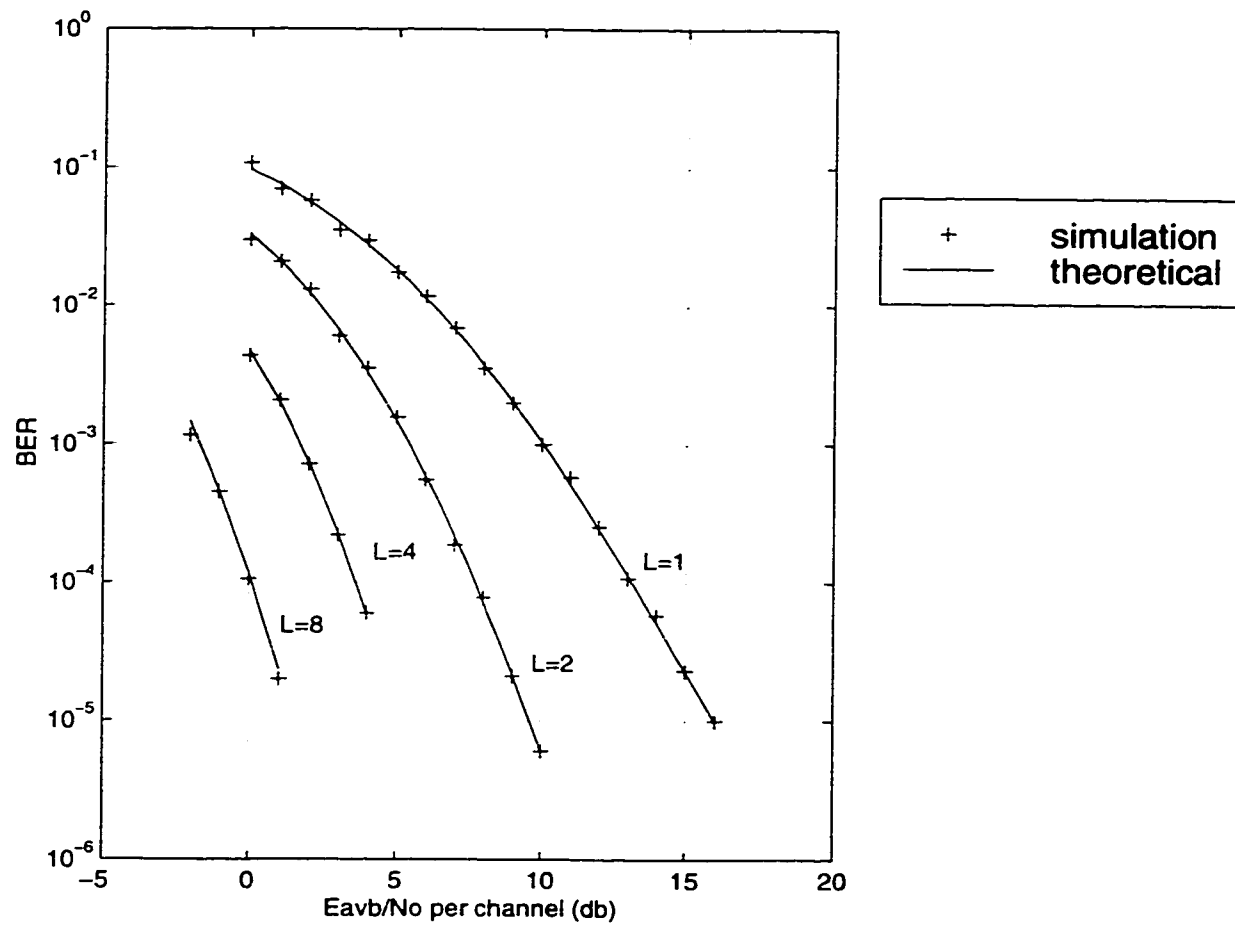


Figure 3.16: Performance of 4-QAM with EGC in Nakagami fading channels, ($m = 4$)

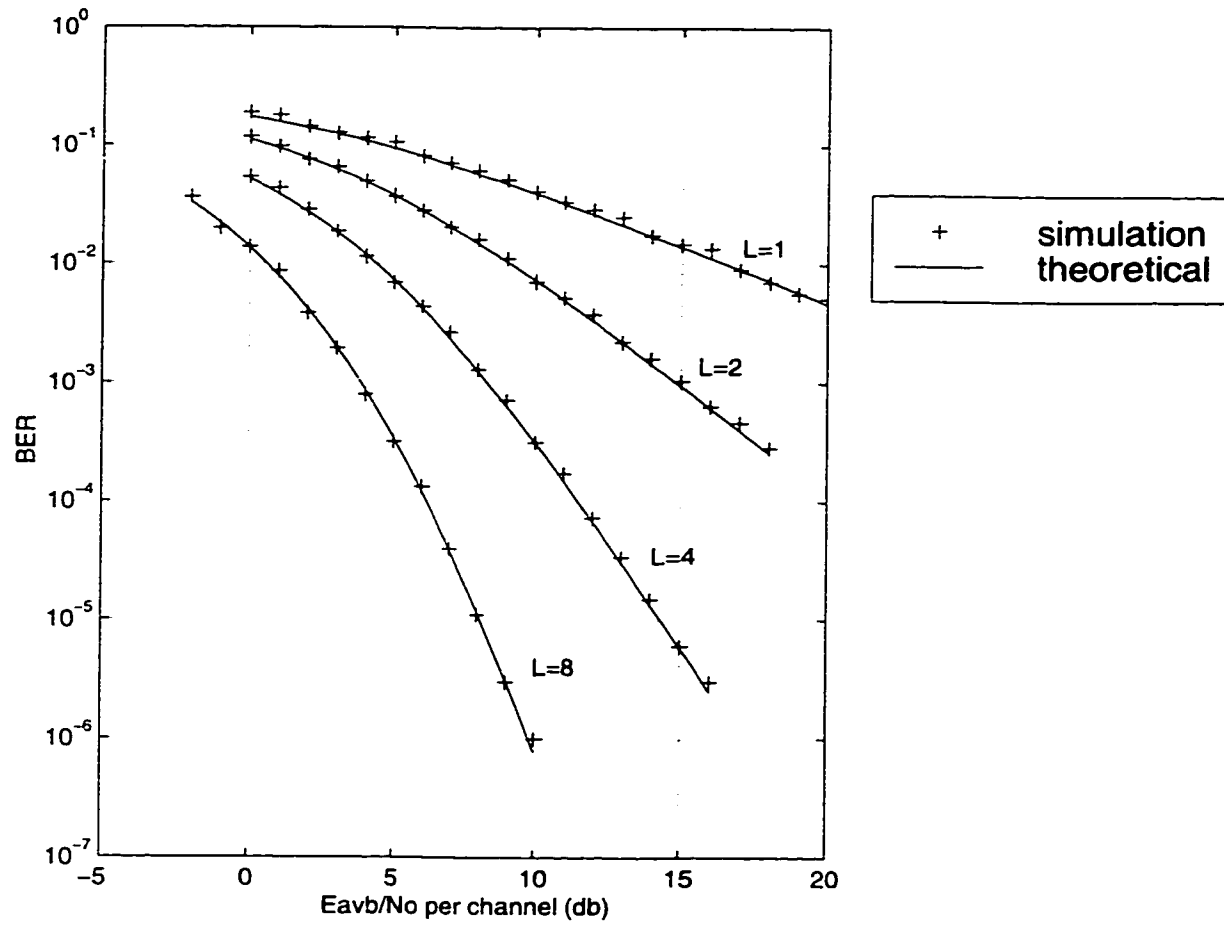


Figure 3.17: Performance of 16-QAM with EGC in Nakagami fading channels, ($m = 1$)

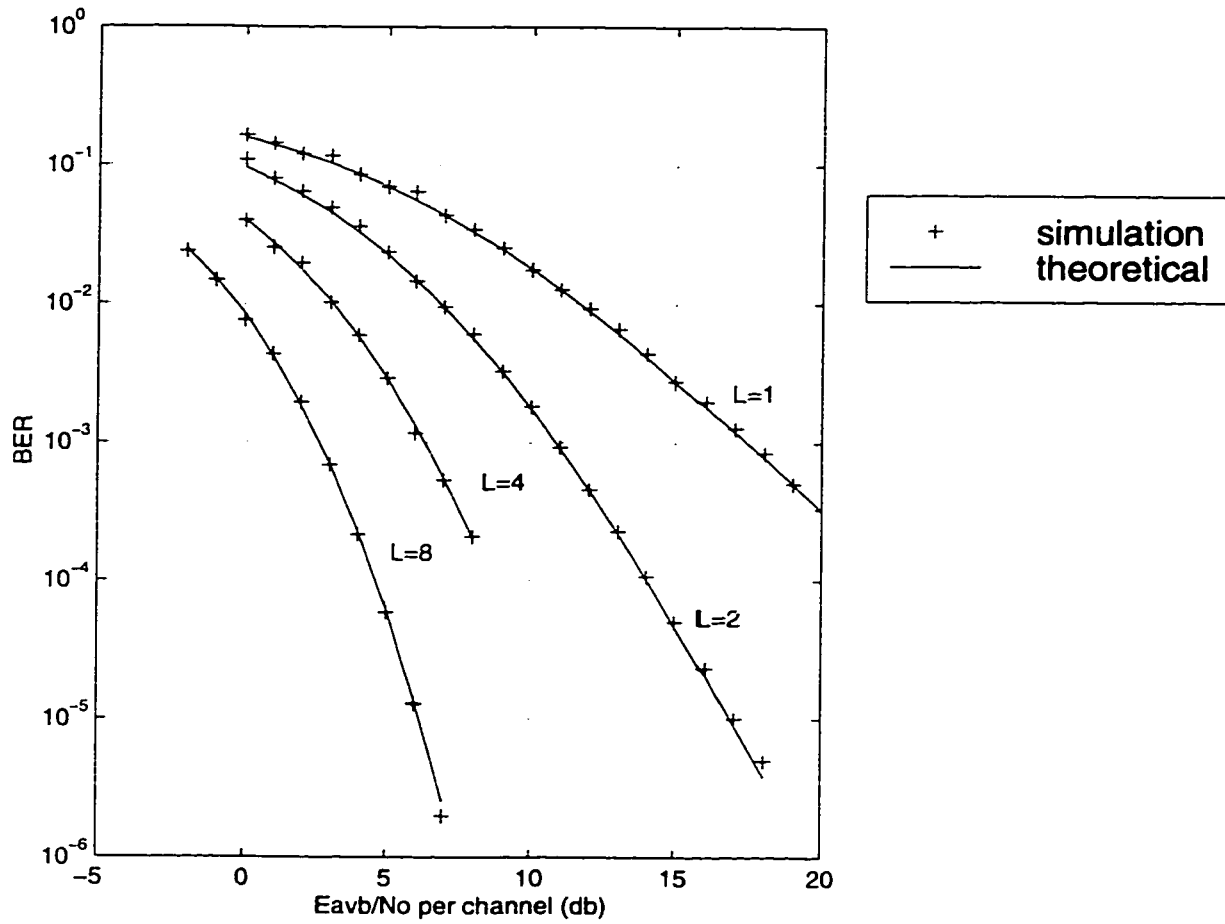


Figure 3.18: Performance of 16-QAM with EGC in Nakagami fading channels, ($m = 2$)

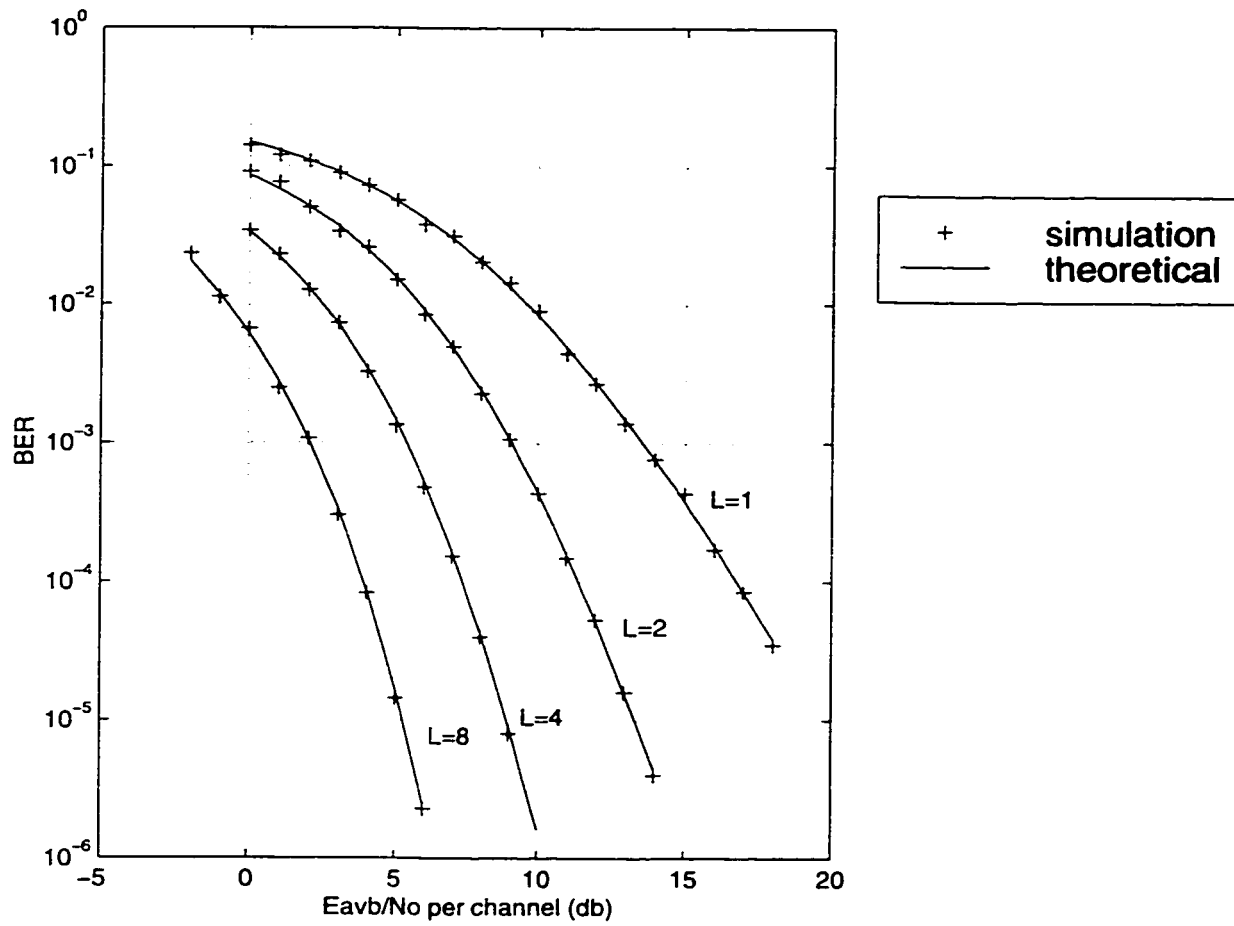


Figure 3.19: Performance of 16-QAM with EGC in Nakagami fading channels, ($m = 4$)

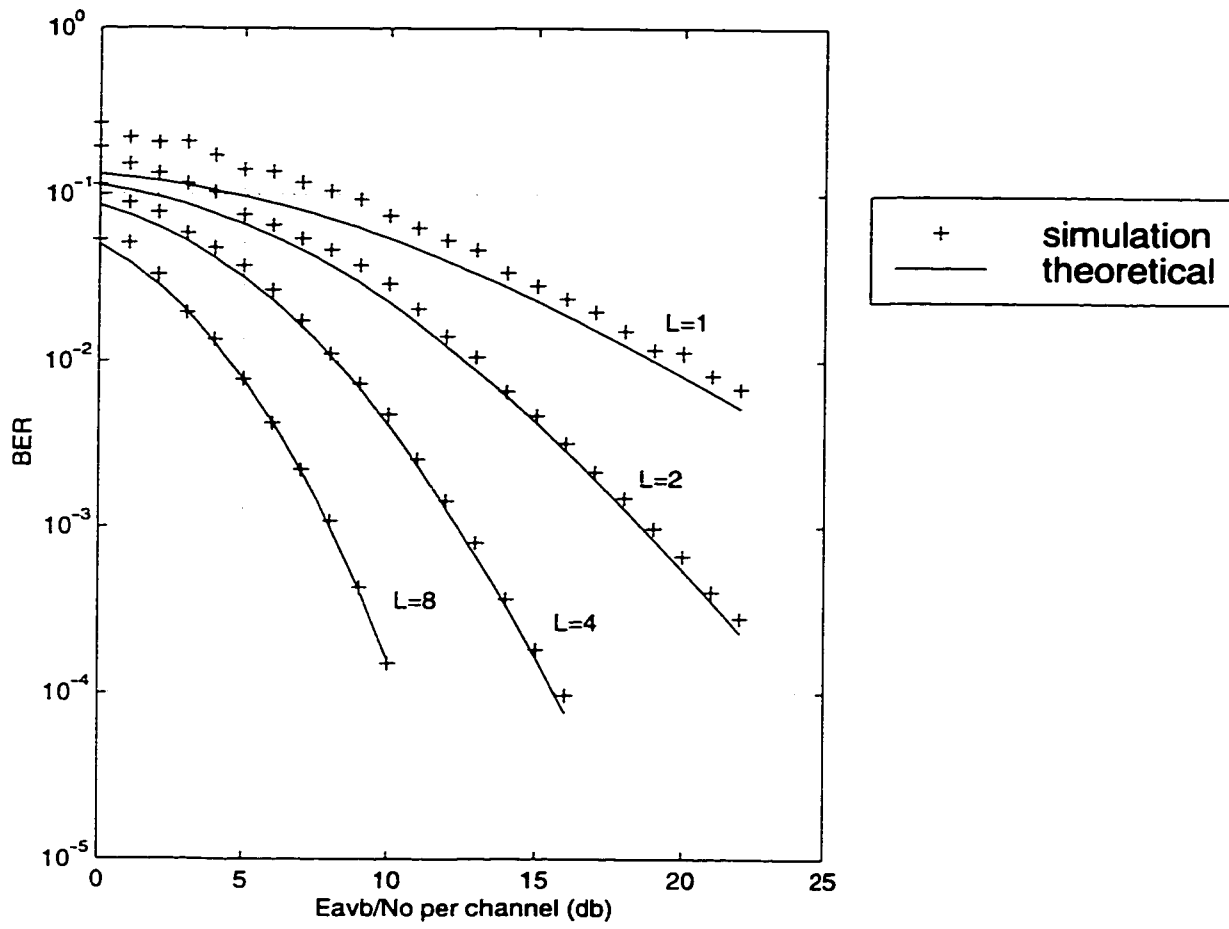


Figure 3.20: Performance of 64-QAM with EGC in Nakagami fading channels, ($m = 1$)

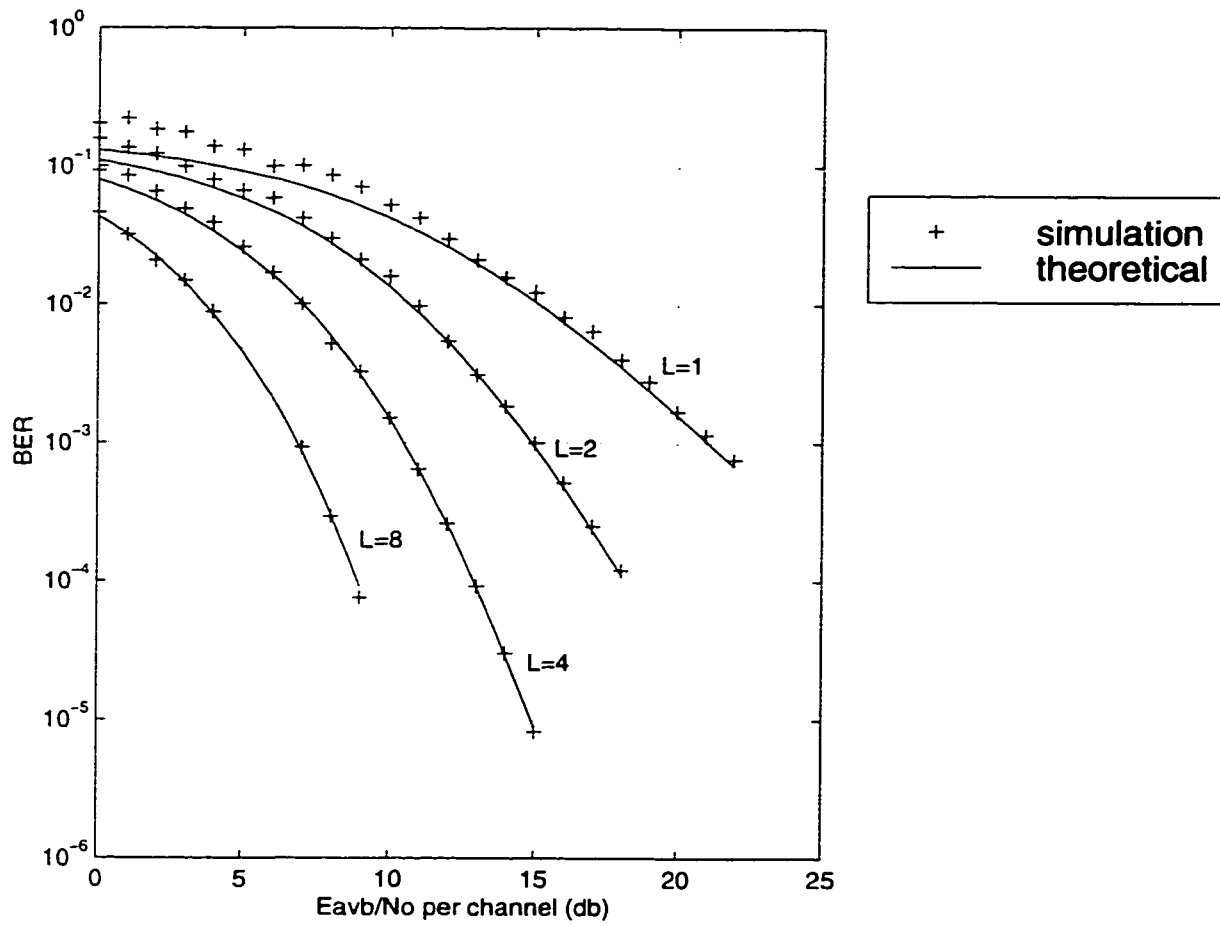


Figure 3.21: Performance of 64-QAM with EGC in Nakagami fading channels, ($m = 2$)

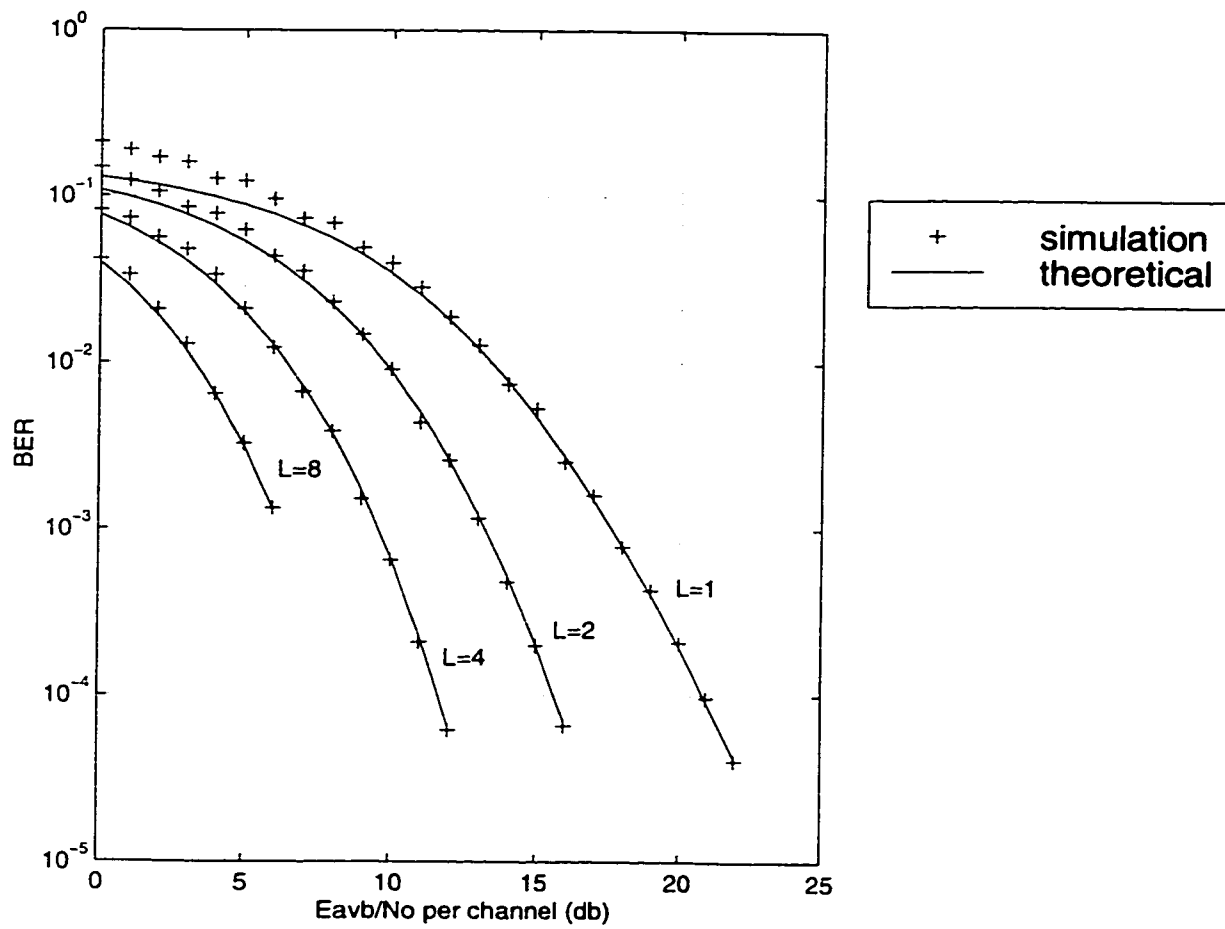


Figure 3.22: Performance of 64-QAM with EGC in Nakagami fading channels, ($m = 4$)

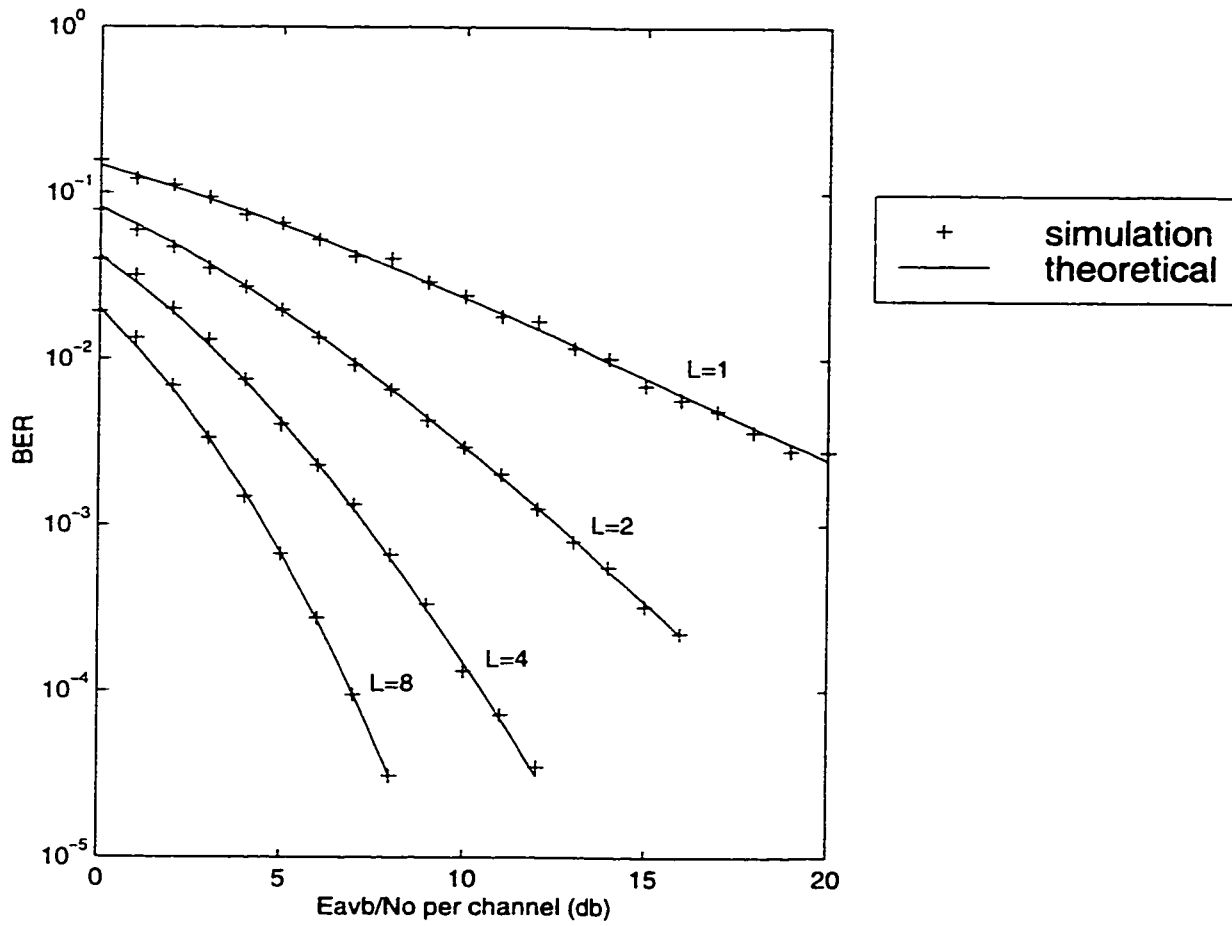


Figure 3.23: Performance of 4-QAM with SC in Nakagami fading channels, ($m = 1$)

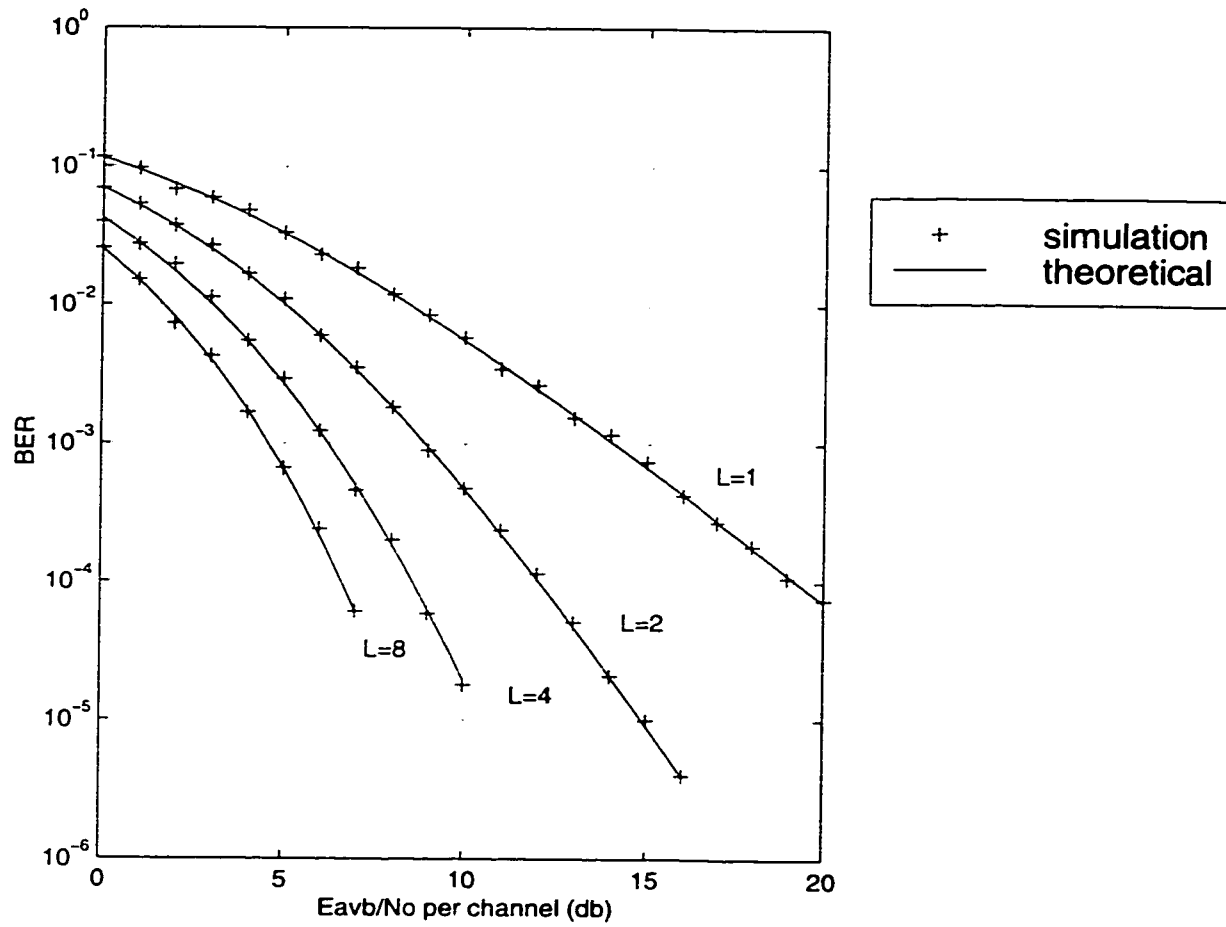


Figure 3.24: Performance of 4-QAM with SC in Nakagami fading channels, ($m = 2$)

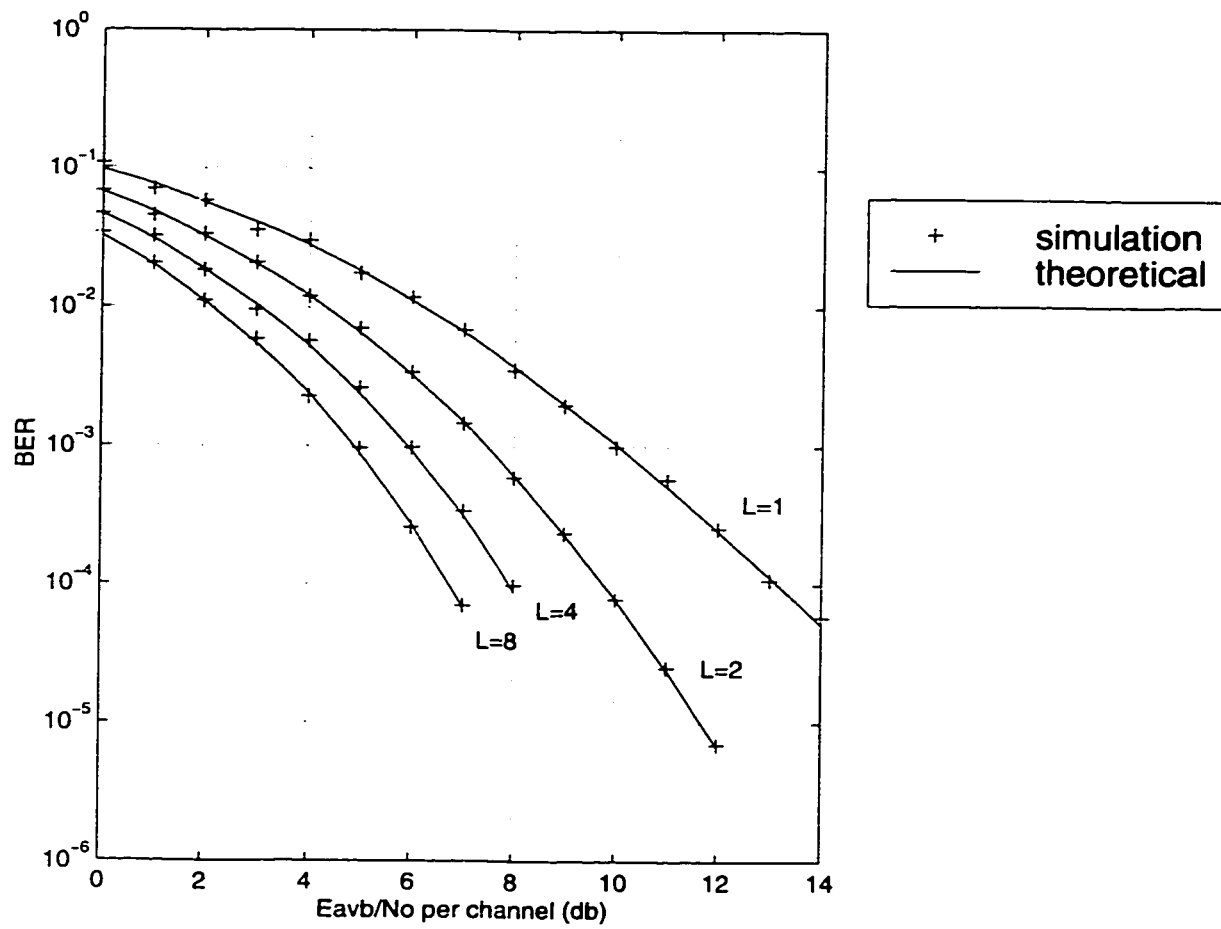


Figure 3.25: Performance of 4-QAM with SC in Nakagami fading channels, ($m = 4$)

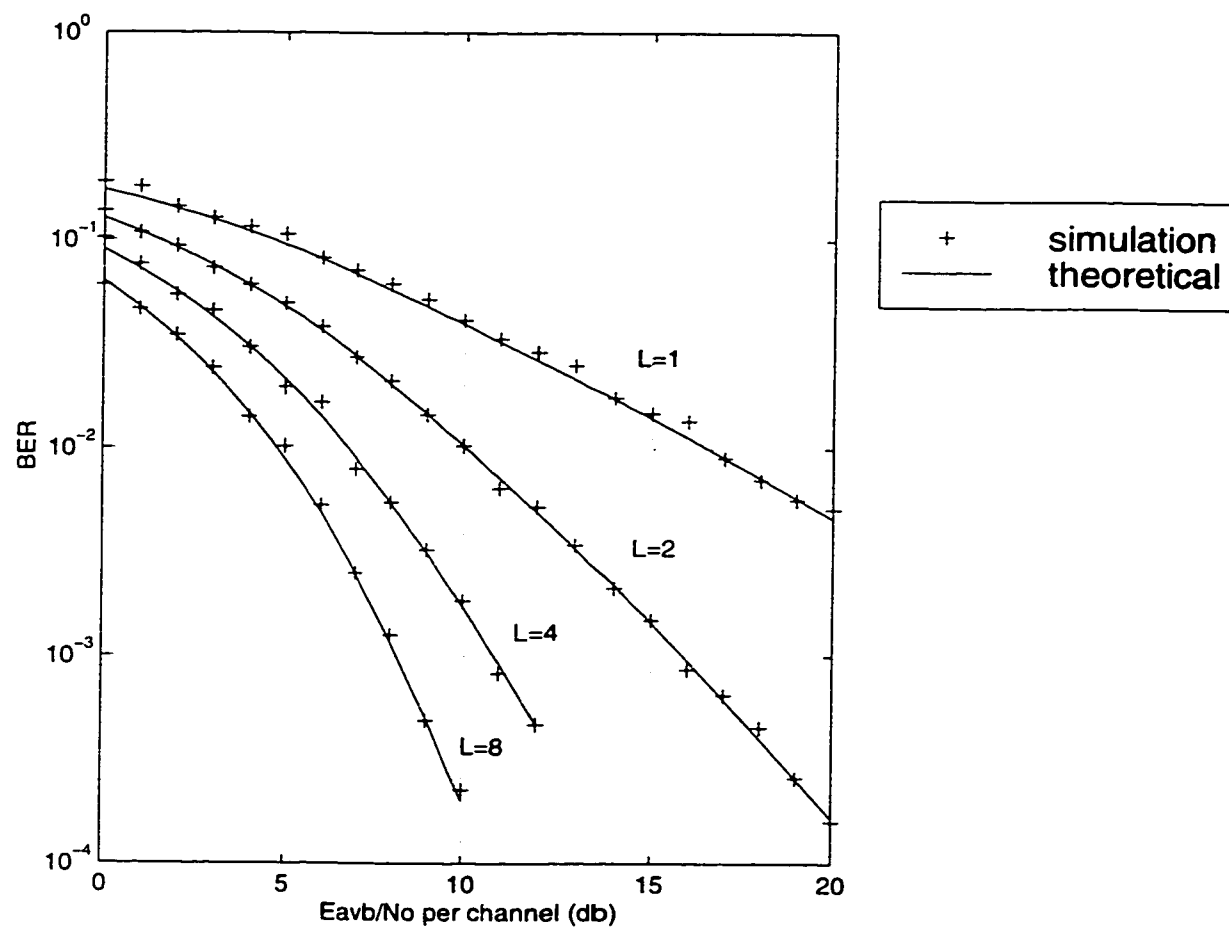


Figure 3.26: Performance of 16-QAM with SC in Nakagami fading channels, ($m = 1$)

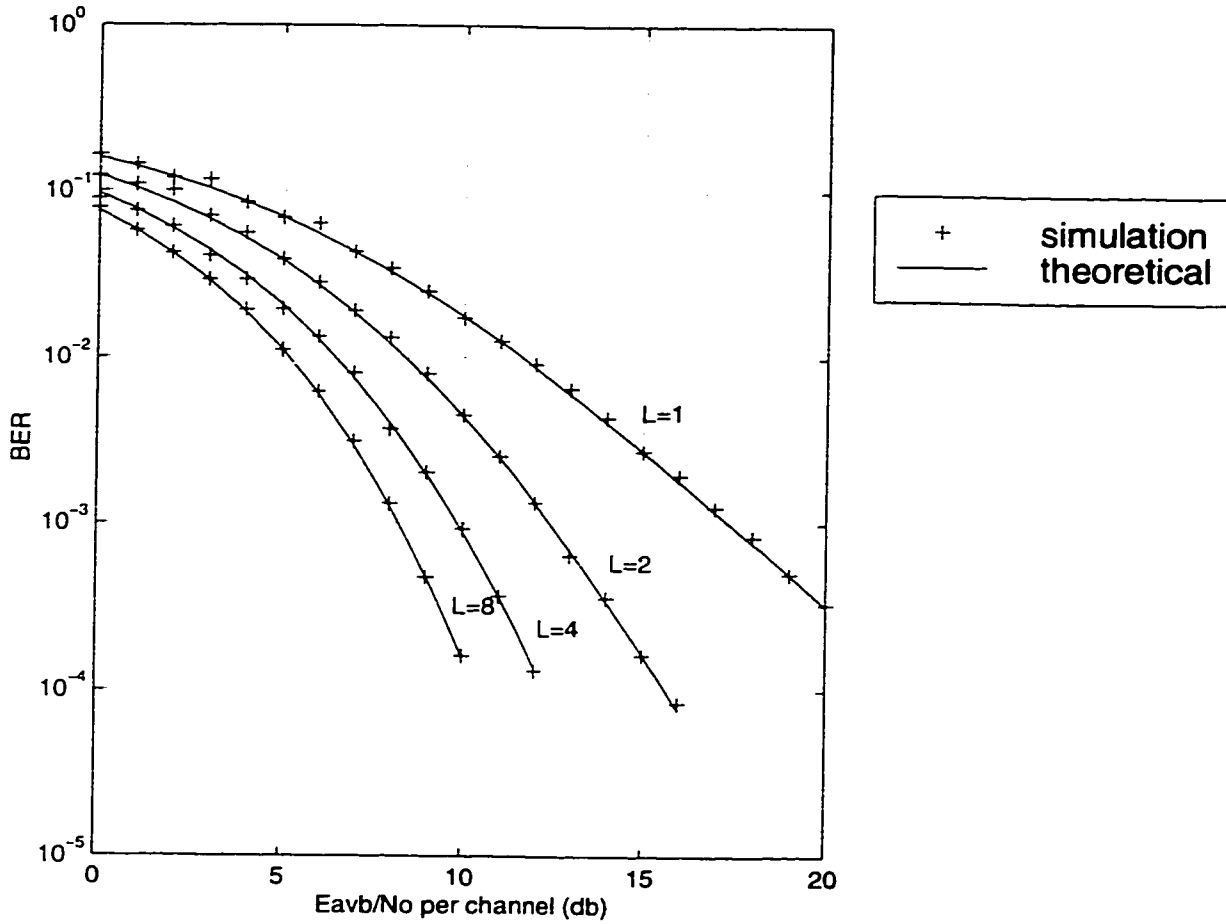


Figure 3.27: Performance of 16-QAM with SC in Nakagami fading channels, ($m = 2$)

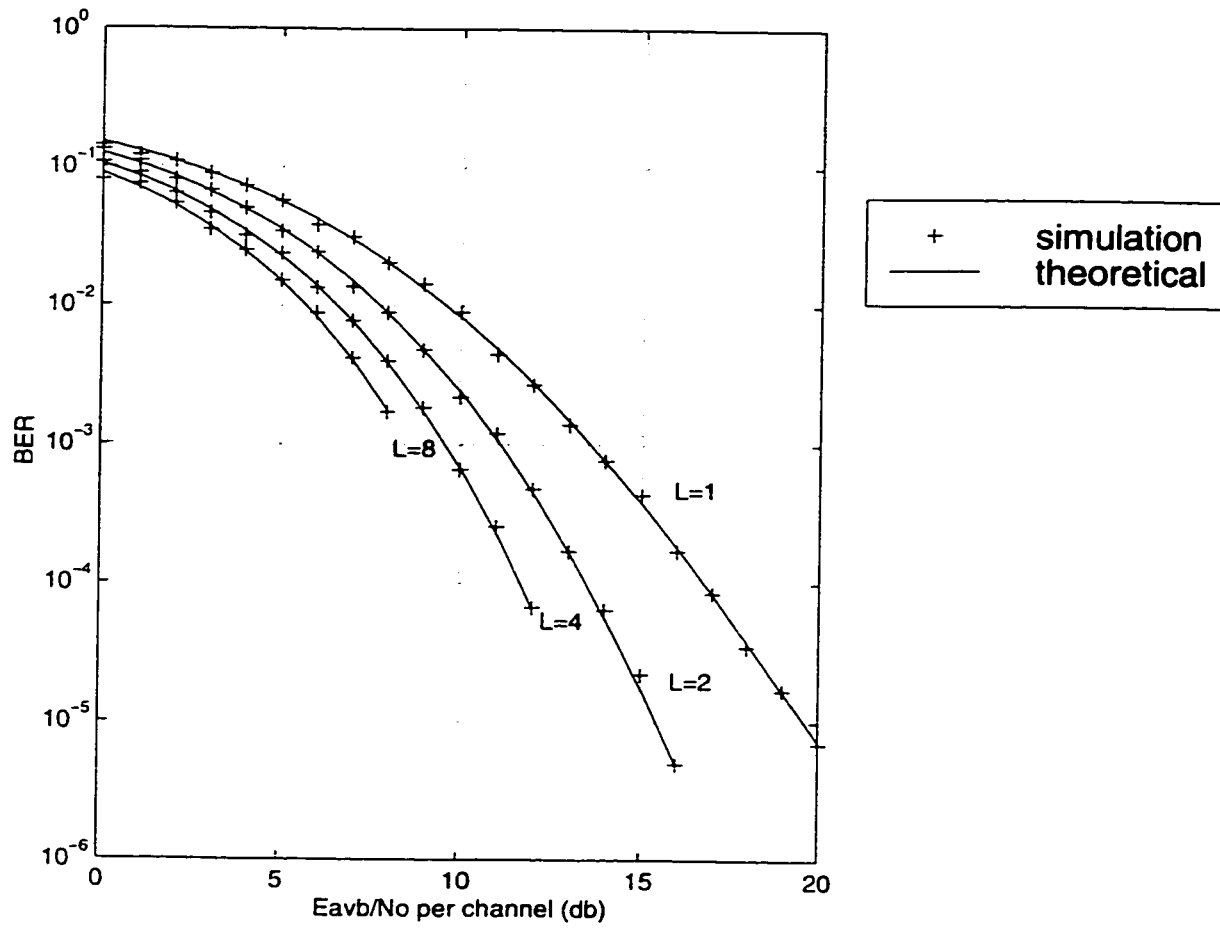


Figure 3.28: Performance of 16-QAM with SC in Nakagami fading channels, ($m = 4$)

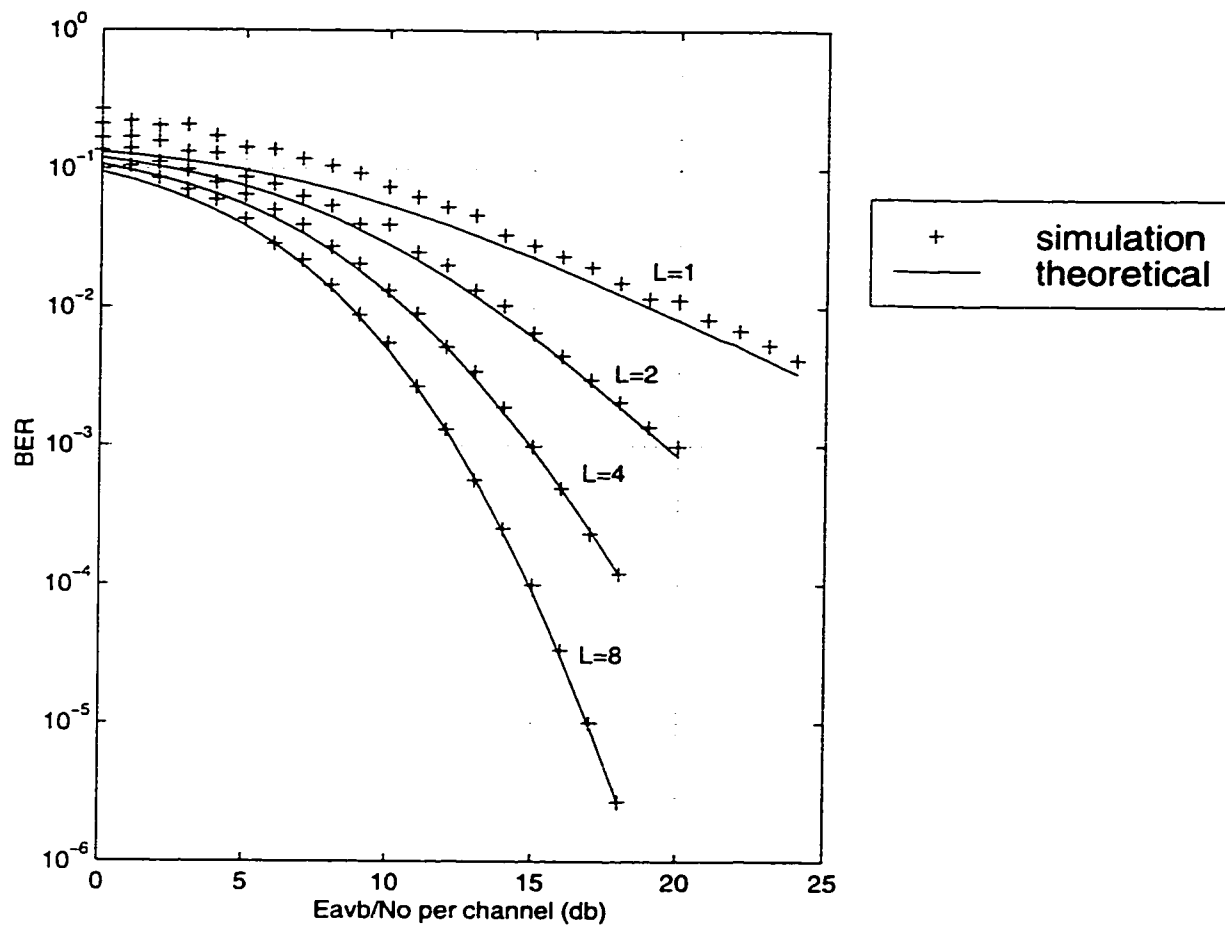


Figure 3.29: Performance of 64-QAM with SC in Nakagami fading channels, ($m = 1$)

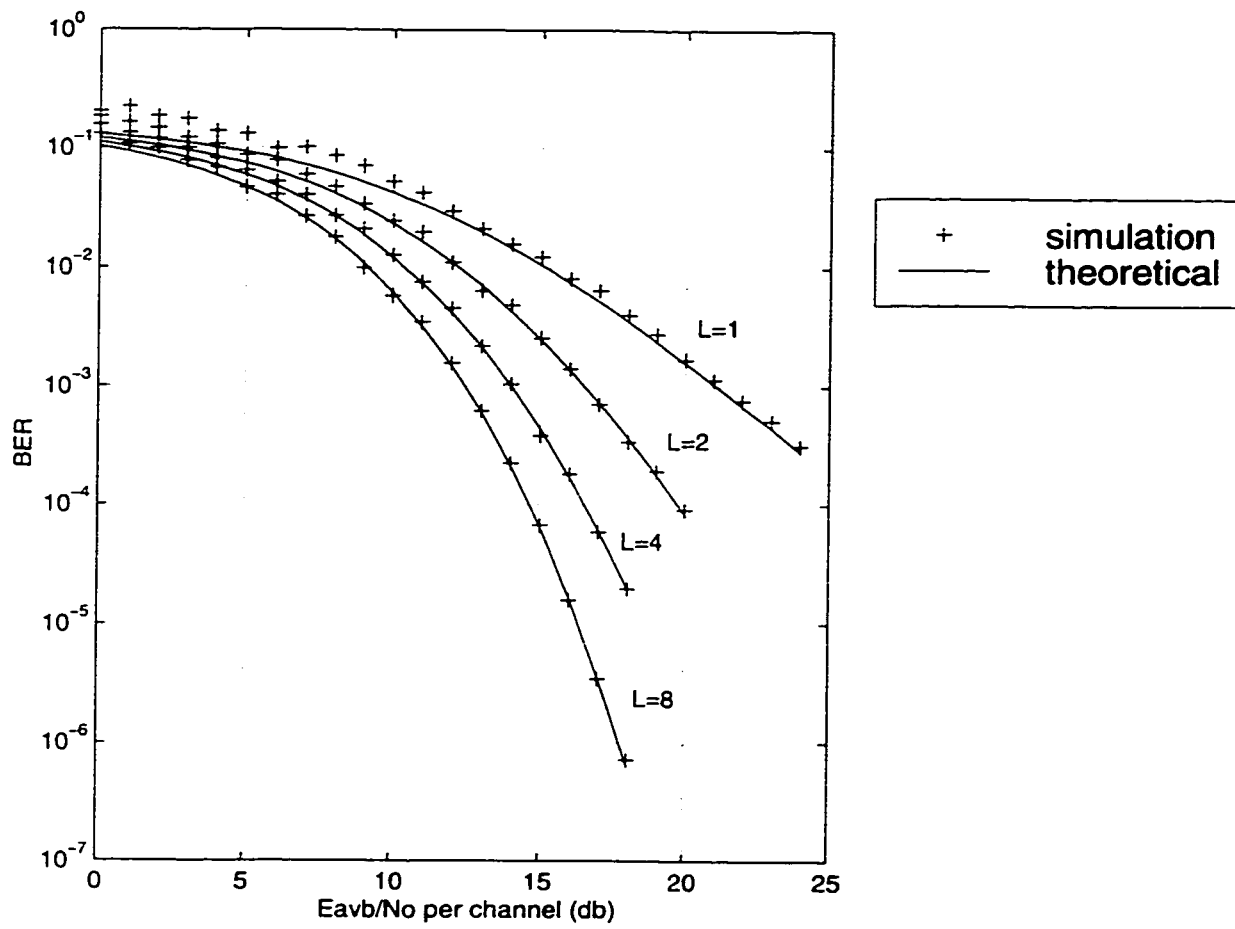


Figure 3.30: Performance of 64-QAM with SC in Nakagami fading channels, ($m = 2$)

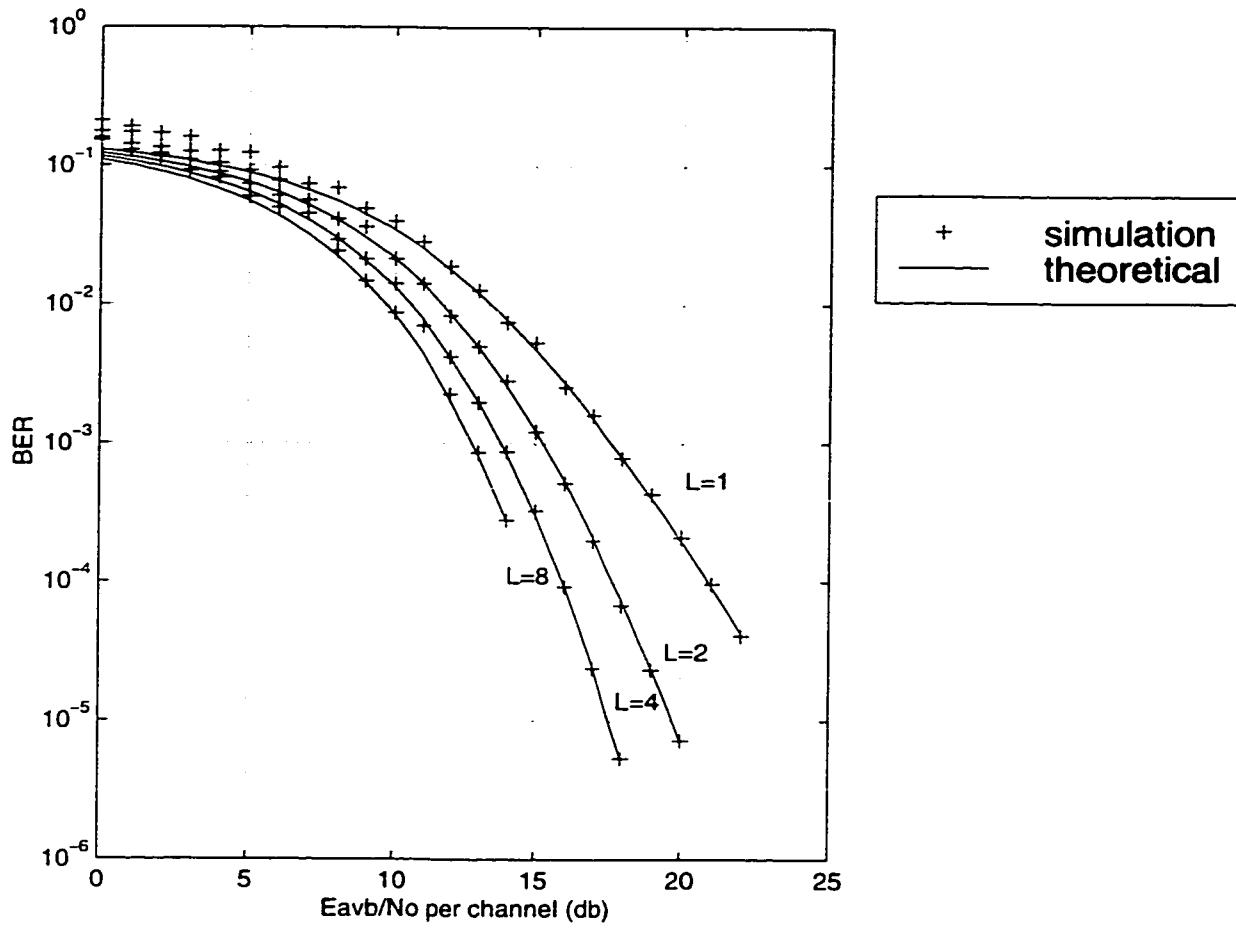


Figure 3.31: Performance of 64-QAM with SC in Nakagami fading channels, ($m = 4$)

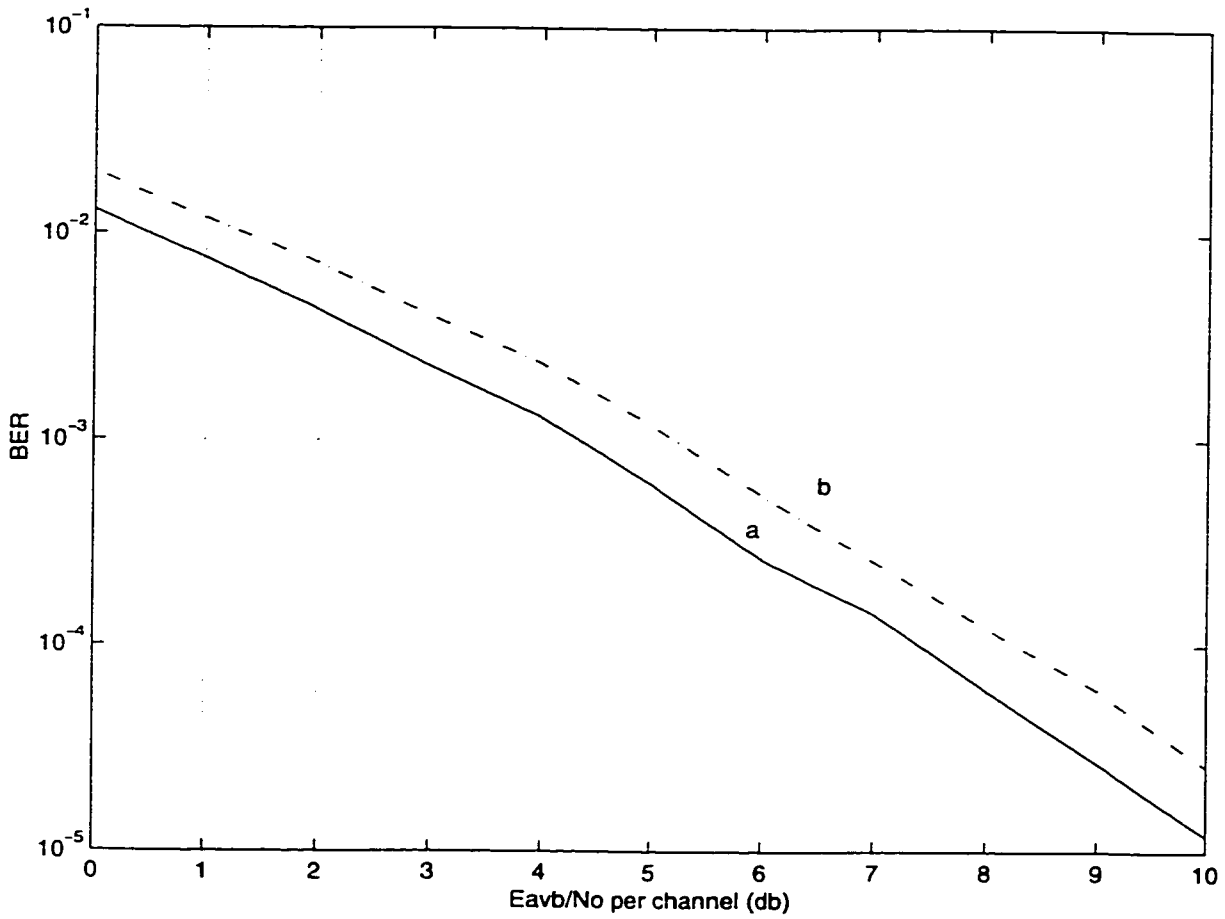


Figure 3.32: Performance of 4-QAM with GSC in Nakagami fading channels, ($m = 1, L = 4$) a- $L_c = 3$, b- $L_c = 2$

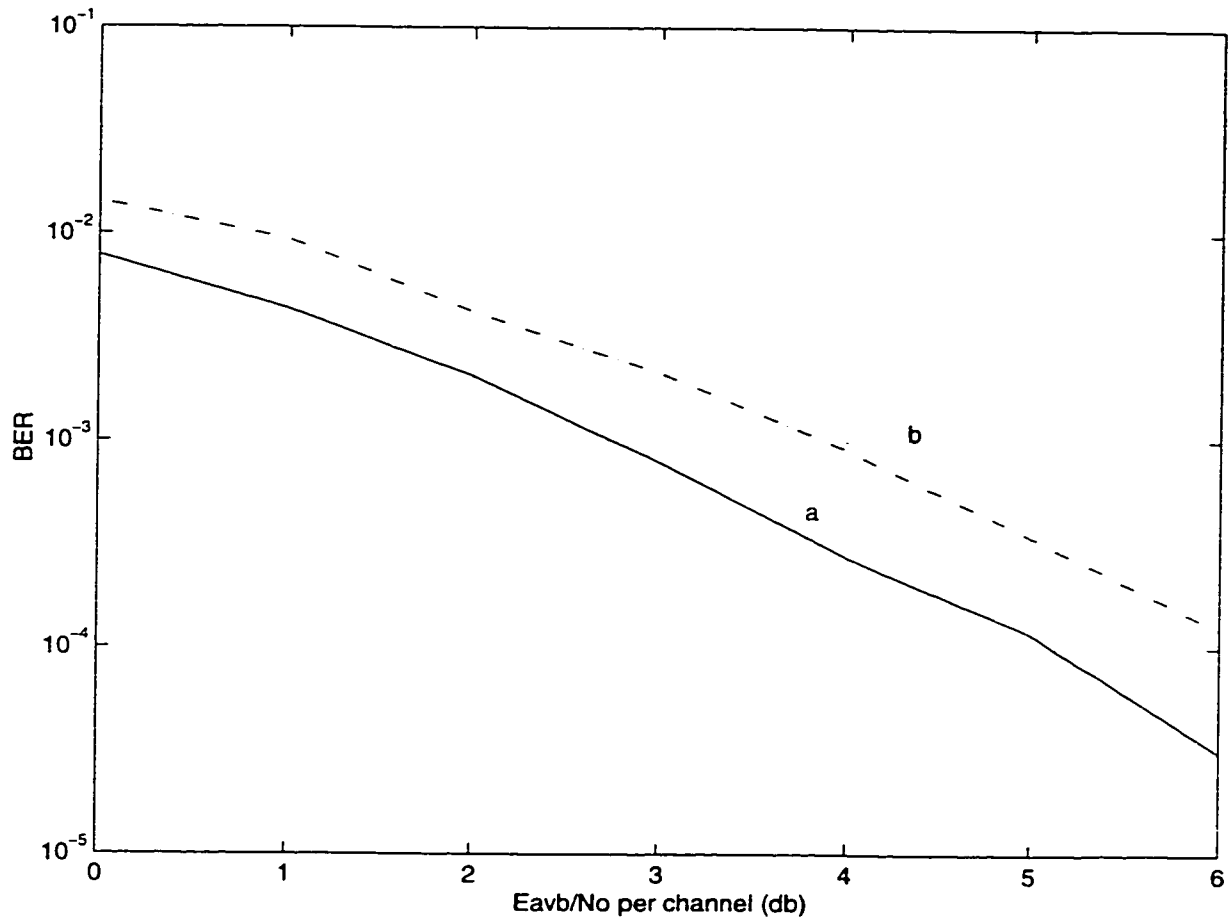


Figure 3.33: Performance of 4-QAM with GSC in Nakagami fading channels, ($m = 2, L = 4$) a- $L_c = 3$, b- $L_c = 2$

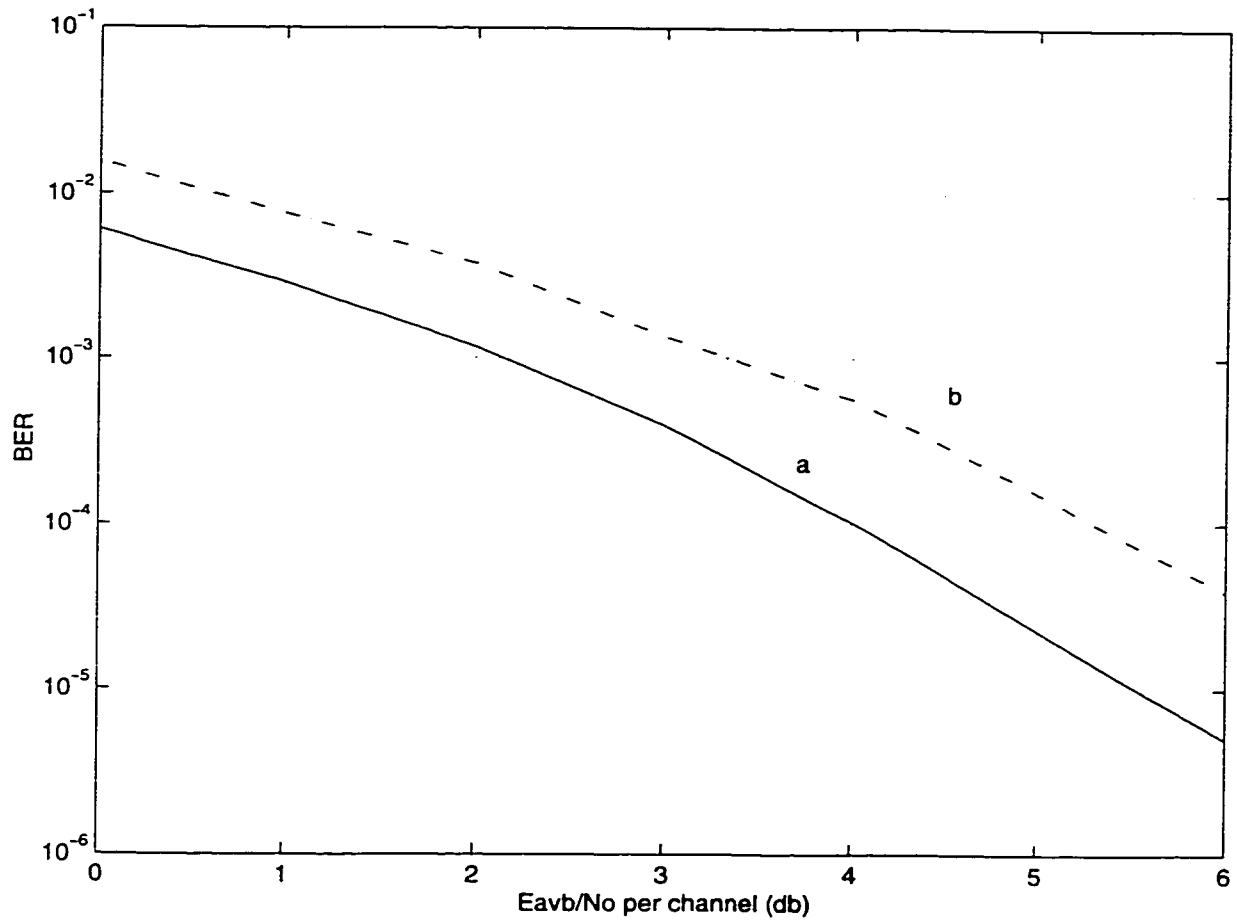


Figure 3.34: Performance of 4-QAM with GSC in Nakagami fading channels, ($m = 4, L = 4$) a- $L_c = 3$, b- $L_c = 2$

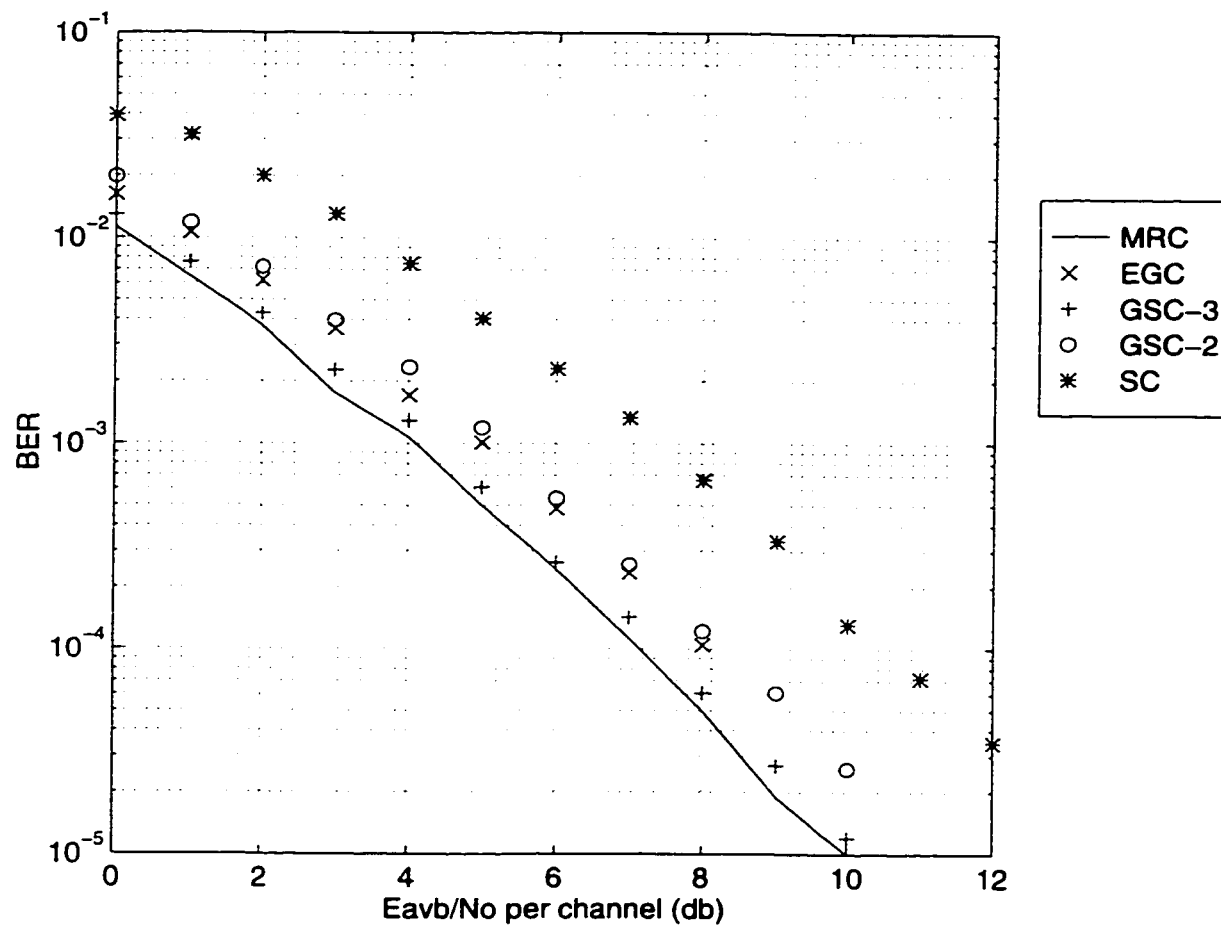


Figure 3.35: Performance of 4-QAM with different diversity Schemes in Nakagami fading channels, ($m = 1, L = 4$)

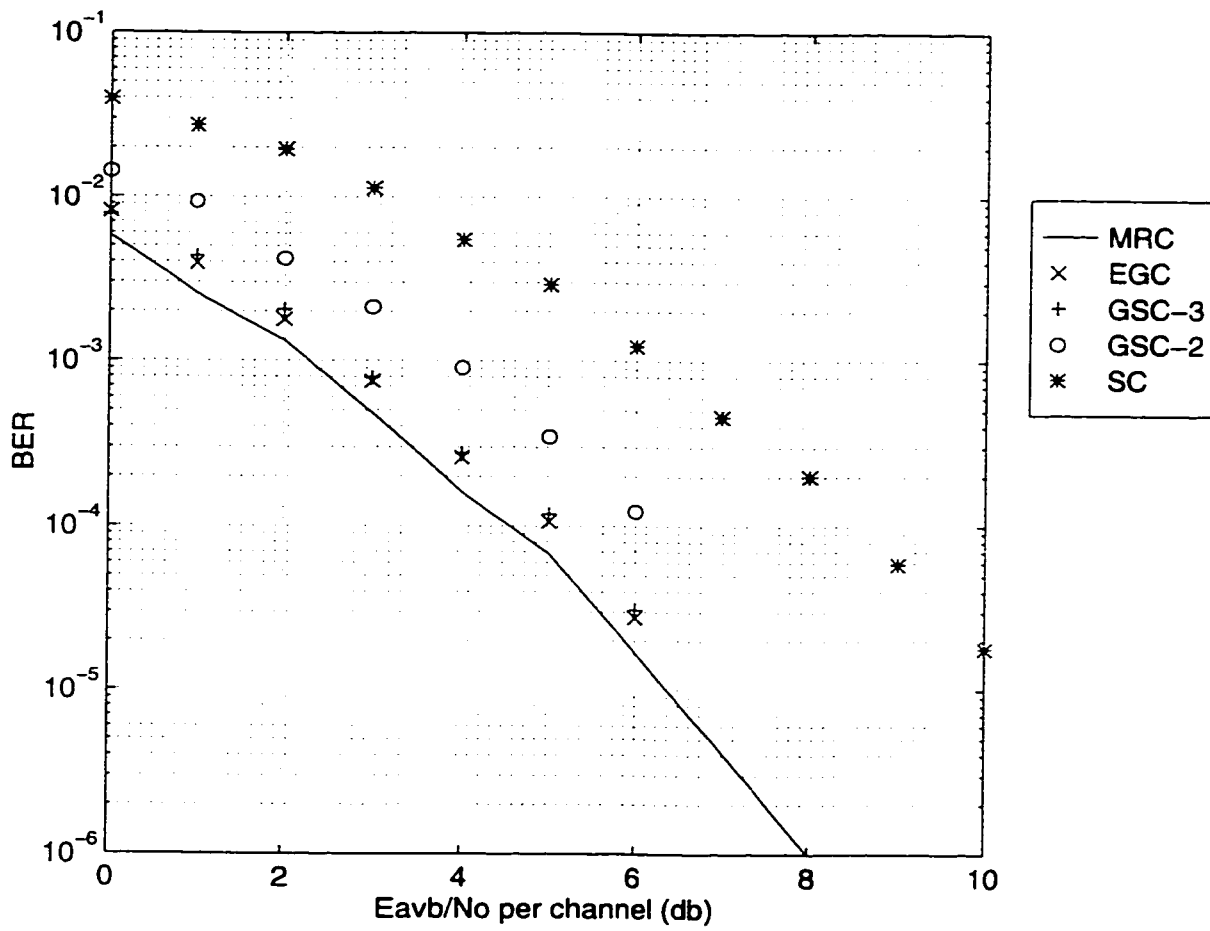


Figure 3.36: Performance of 4-QAM with different diversity Schemes in Nakagami fading channels, ($m = 2, L = 4$)

3.3 Observations and Discussion

3.3.1 Matching between Theoretical and Simulation

- Figure 3.1 shows that there is a match between the simulation points (*) which represent different families of the Nakagami distribution and the corresponding theoretical curves (solid line).
- The performance of M-QAM without/with different diversity schemes over Nakagami fading channels which is derived in chapter 3 is confirmed by simulation in Figure 3.2 - Figure 3.31 for different Nakagami parameter m , different size of M , and different number of branches L .

3.3.2 General Observation

- Large m models less fading conditions. Consequently, the performance improves with increasing m as shown in all figures.
- As the number of branches increases the performance gets better because the number of received signals which suffer from deep fade which is the main reason of the degradation of the performance will be reduced.
- The maximum gain achieved by diversity is for $L = 2$ and as the number of branches increase the gain will increase but at slower rate. It should be noted that the complexity also increases with increasing L , so it may not be worth going to very high values of L .
- For the same order of diversity, the SNR gain offered by diversity with

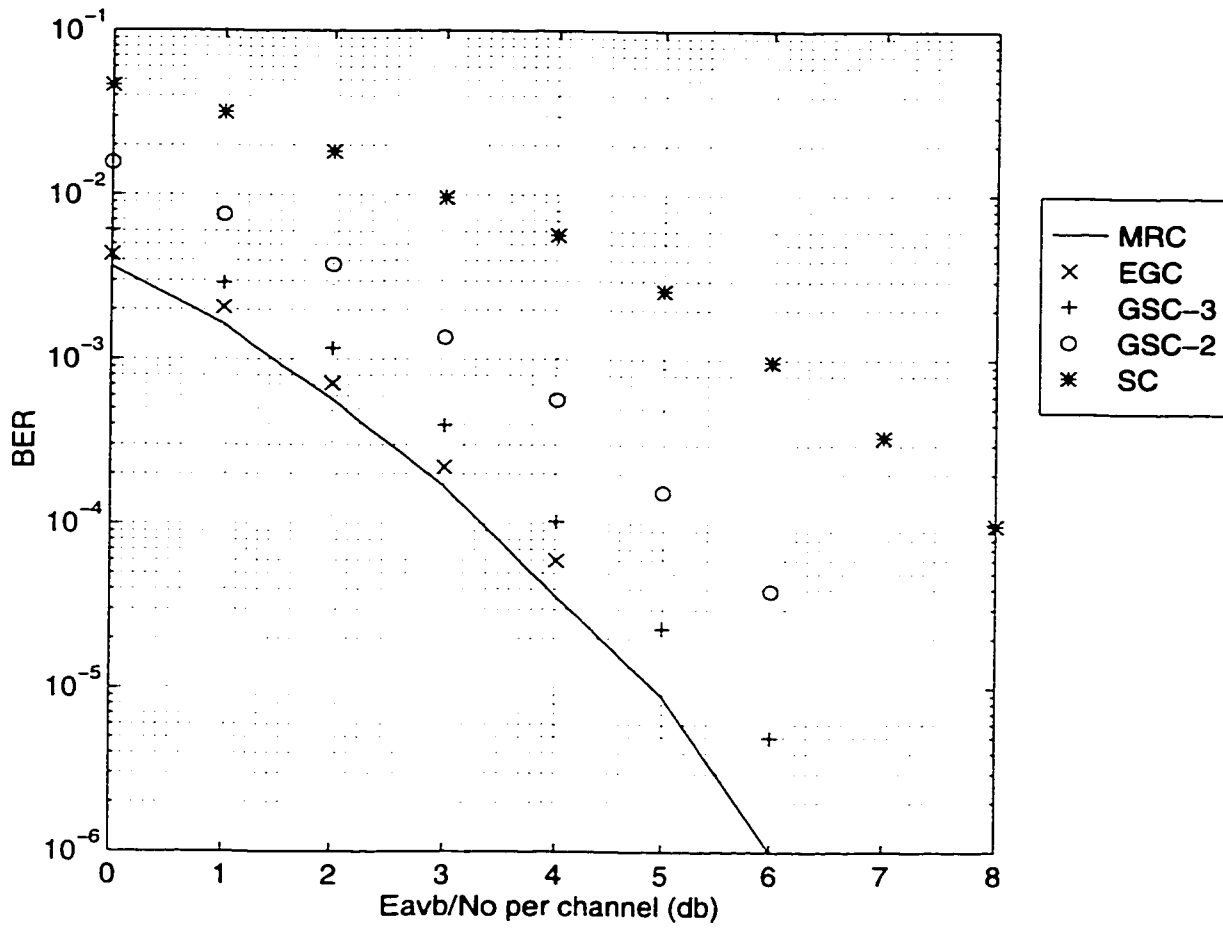


Figure 3.37: Performance of 4-QAM with different diversity Schemes in Nakagami fading channels, ($m = 4, L = 4$)

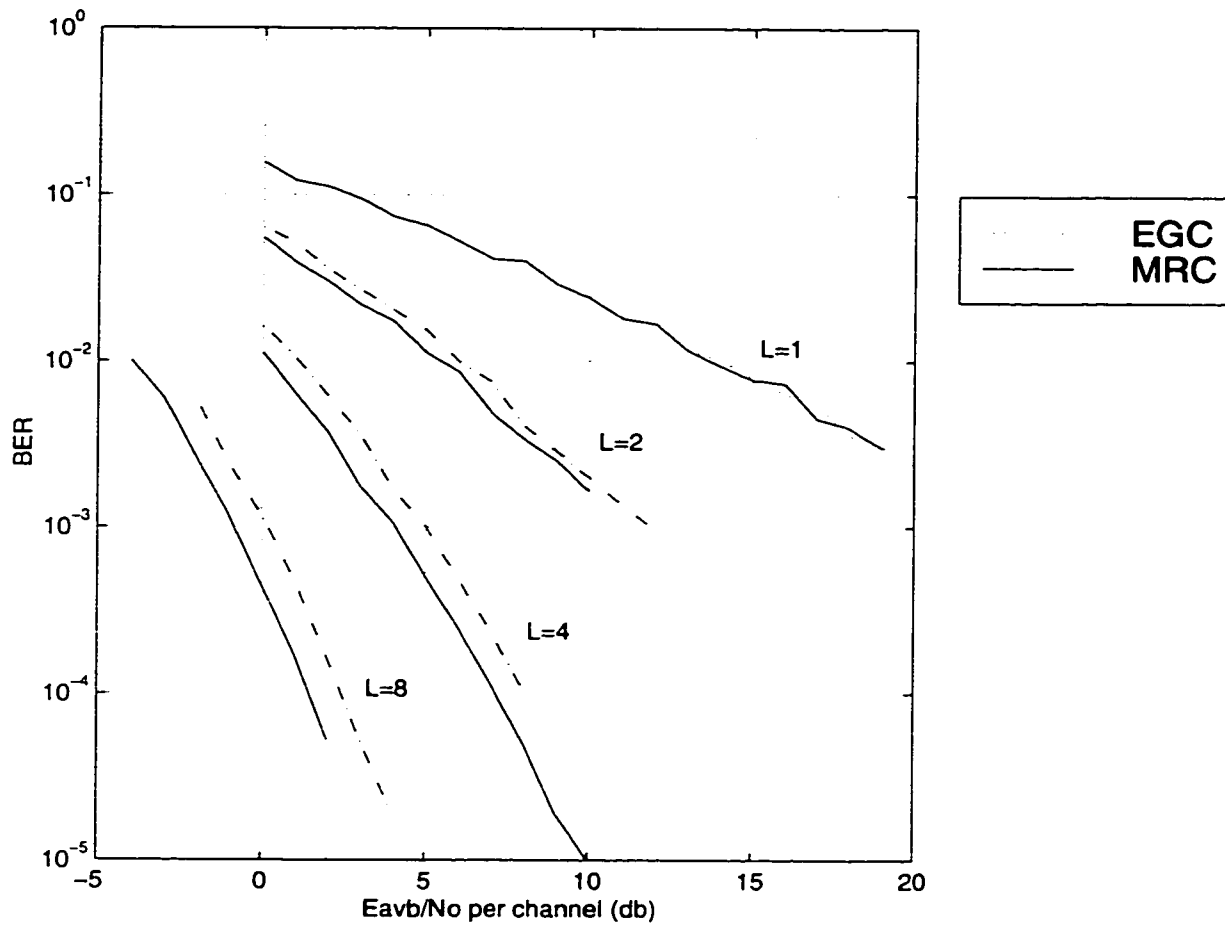


Figure 3.38: Performance of 4-QAM with MRC and EGC over Nakagami fading channels, ($m = 1$)

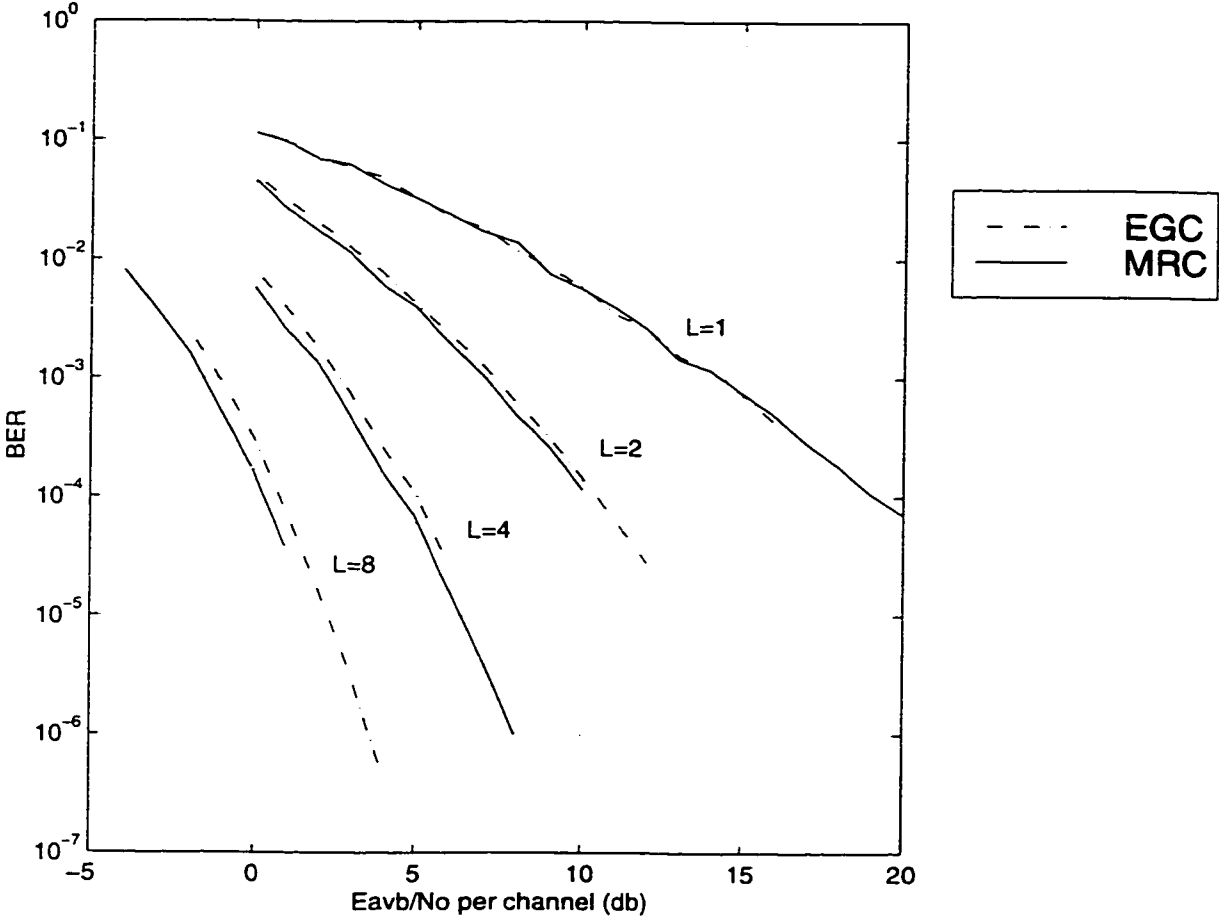


Figure 3.39: Performance of 4-QAM with MRC and EGC over Nakagami fading channels, ($m = 2$)

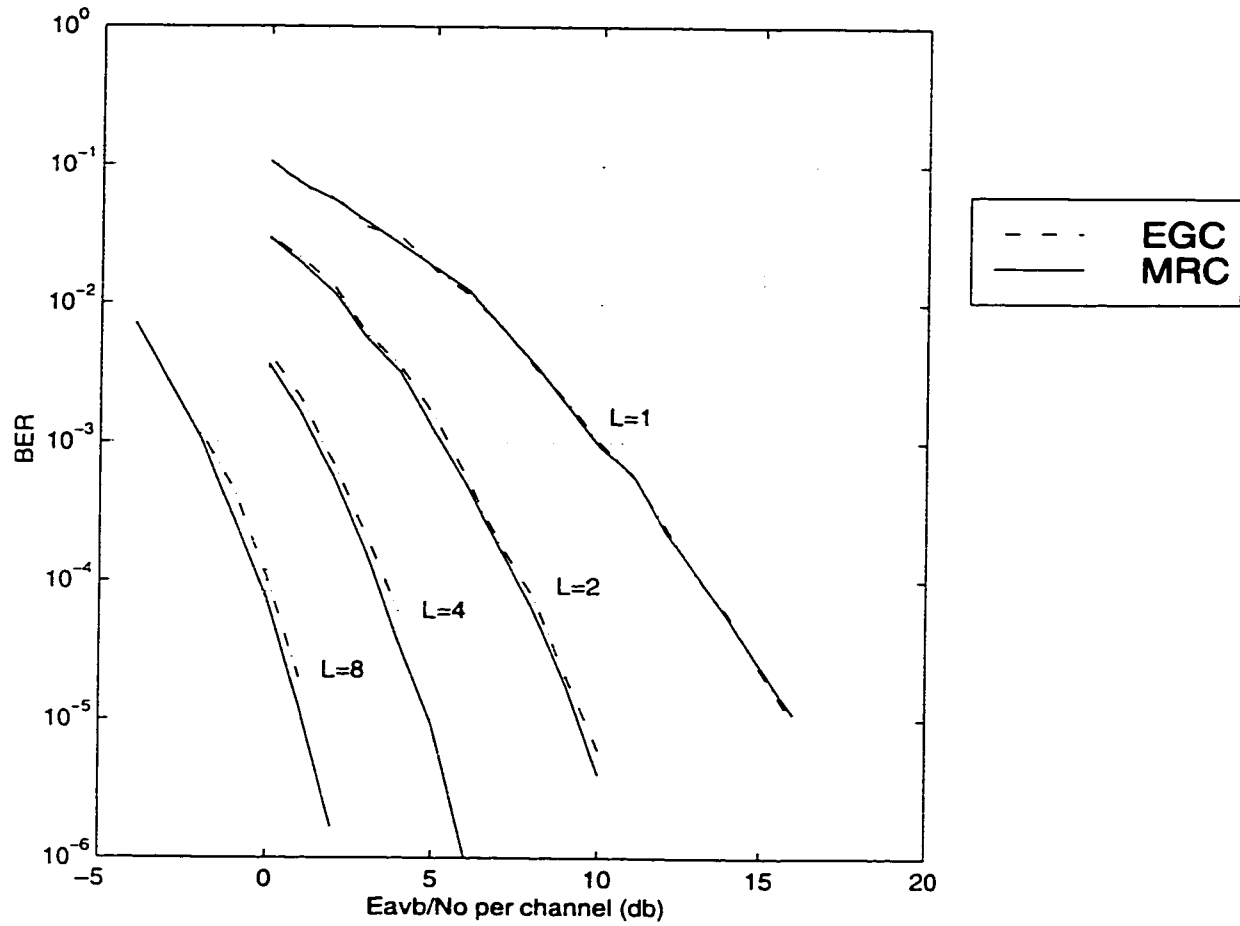


Figure 3.40: Performance of 4-QAM with MRC and EGC over Nakagami fading channels, ($m = 4$)

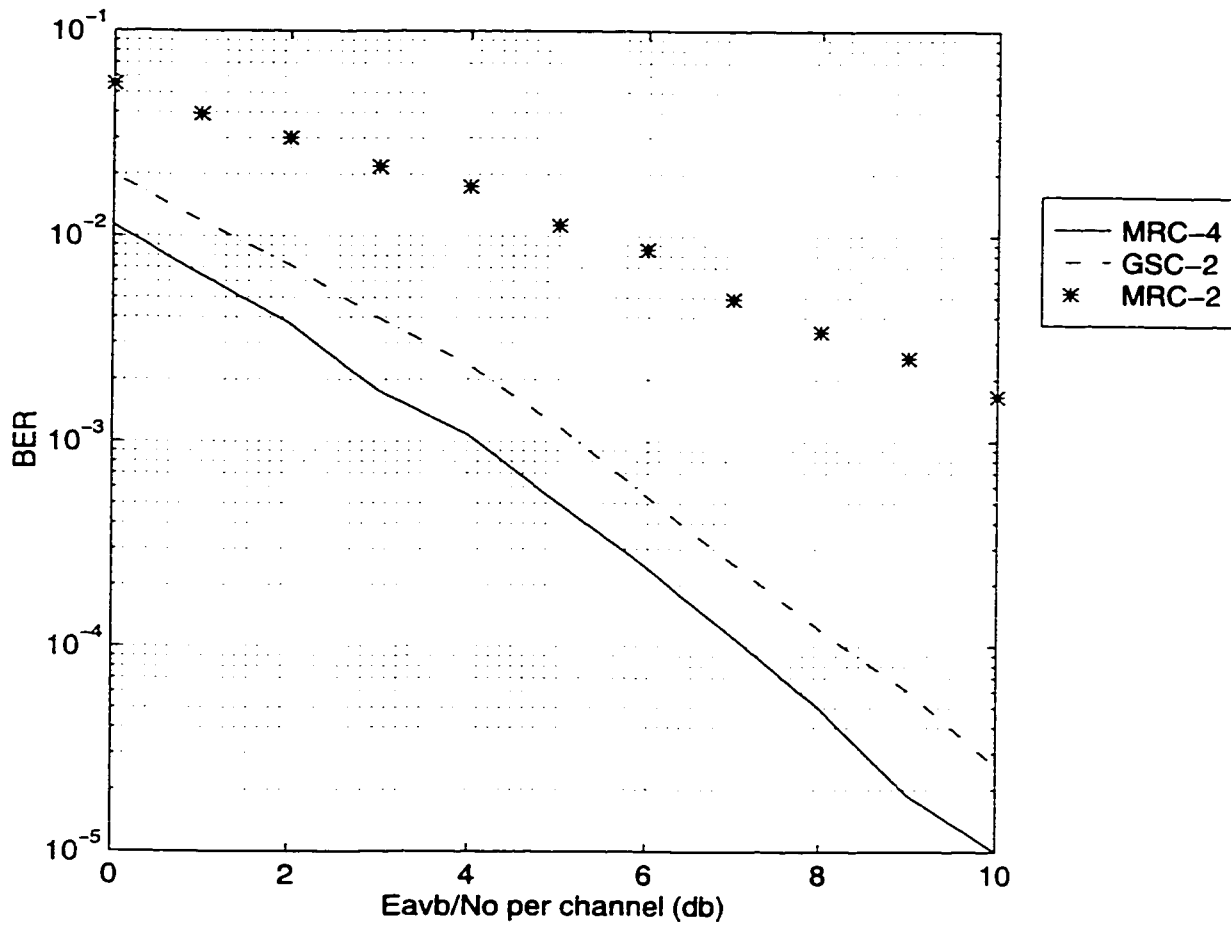


Figure 3.41: Performance of 4-QAM with MRC and GSC over Nakagami fading channels, ($m = 1$)

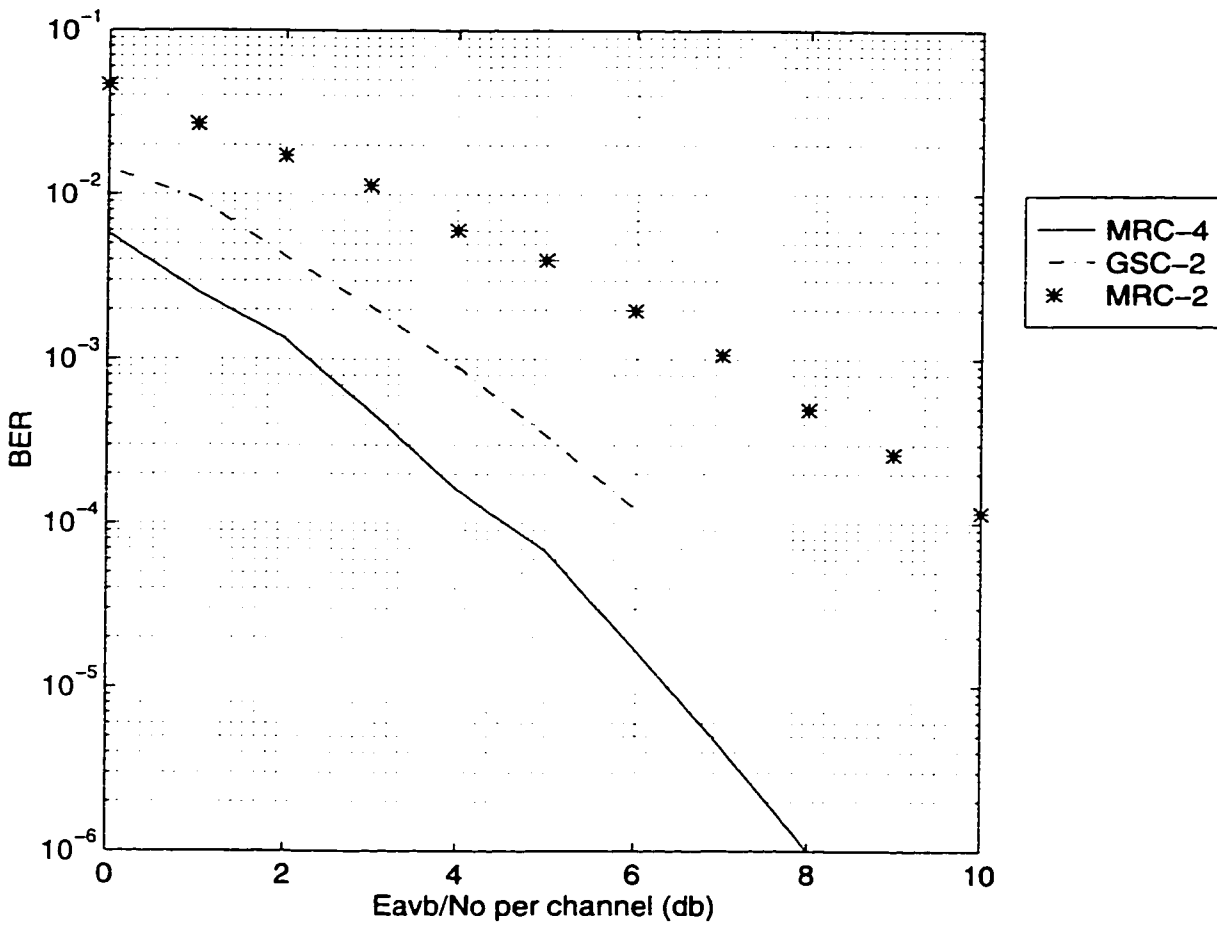


Figure 3.42: Performance of 4-QAM with MRC and GSC over Nakagami fading channels, ($m = 2$)

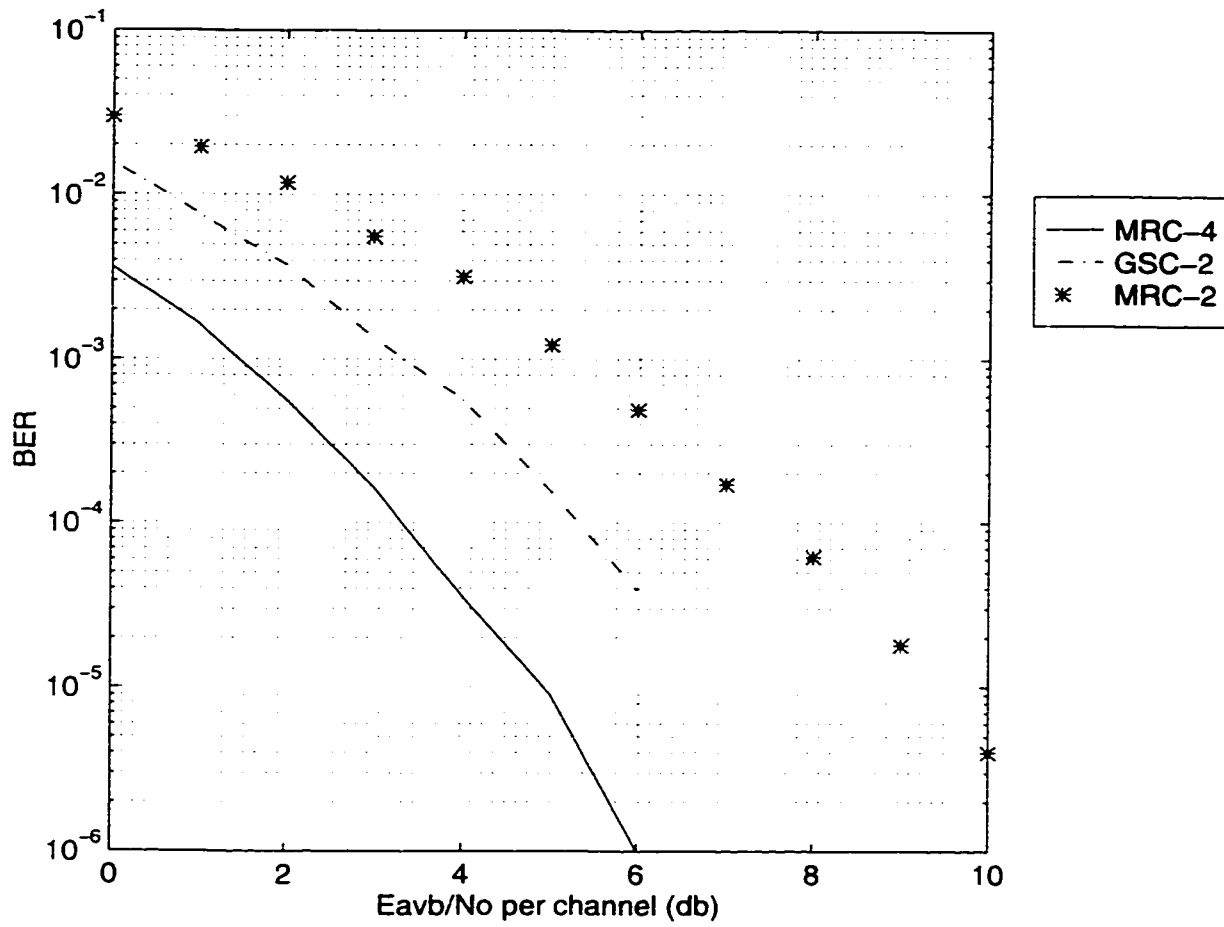


Figure 3.43: Performance of 4-QAM with MRC and GSC over Nakagami fading channels, ($m = 4$)

respect to the single channel receiver decreases as the fading becomes less severe (large m).

3.3.3 Comparison of MRC, EGC, SC, and GSC

The performance of 4-QAM with MRC, EGC, SC, GSC-2, and GSC-3 over Nakagami- m channel is shown in Figure 3.35 - Figure 3.37 for a constant number of available branches $L = 4$. The case $m = 1$ corresponds to Rayleigh fading. The cases $m = 2$ and $m = 4$ represent less severe fading conditions than Rayleigh. These figures show the followings:

- MRC has the best performance (optimum), however, it is more complex than the other schemes, while SC is poorer than other schemes in terms of performance but it is the simplest to implement.
- The performance of GSC ranges between the performance of MRC and SC. As the number of branches to be combined in GSC increases the performance gets better however the complexity increases.
- As the fading increases (less m) the performance of GSC gets closer to MRC performance while EGC performance gets poorer and this will be explained in the next paragraph.

Figure 3.38 - Figure 3.40 compare the performance of MRC and EGC with 4-QAM signals over Nakagami- m channel for different fading conditions and different number of branches. From these figures the following results are obtained :

- The performance of EGC is close to MRC performance, for example the difference is less than 1 dB for $L = 8$. Jake [40] stated that the difference is only 1.05 db in the limit of an infinite number of branches for Rayleigh channel.
- As the fading increases (less m), the difference in the performance of MRC and EGC also increases because EGC combines noisy branches (small amplitudes) and good branches (large amplitudes) with same gain while in MRC each branch is multiplied by its gain (amplitude) then all branches are combined so the effect of a noisy branch (small amplitude) on the output SNR is reduced and the effect of a good channel increases.

Comparison of the performance of MRC and GSC with 4-QAM signals over a Nakagami- m channel for different fading conditions is shown in Figure 3.41- Figure 3.43. These figures show the followings :

- The gain of optimum MRC over GSC is constant independent of SNR because both MRC and GSC provide an average BER inversely proportional to the L^{th} power of SNR.
- The amount of gain of GSC improves as the number of branches to be combined approaches L (which is in our simulation $L = 4$) since it takes advantage of the higher amount of diversity available.
- The amount of gain of GSC varies inversely with the severity of the fading. That is, for the more severe fading cases (small m), the suboptimum GSC scheme is closer to the optimum MRC scheme. The reason

is explained in the following argument. For channels with high amount of fading the combined branches are noisy and since GSC ignores the branches with lowest SNR's it is able to approach the performance of MRC. On the other hand, for channels with low amount of fading the combined branches are good and since The GSC is disregarding information carried in some of these branches it loses more gain compared to the gain achieved for high amount of fading.

- The performance of GSC-2 is better than MRC-2 since the GSC chooses the largest two.

Chapter 4

CONCLUSIONS AND RECOMMENDATION FOR FUTURE WORK

4.1 Conclusions

In this work we have considered the performance of MQAM scheme over Nakagami fading channels. MQAM was selected because it is a good candidate modulation scheme for future generation of wireless communication systems since it has better spectral efficiency than the ones used now. The combination (MQAM, Nakagami) has not been studied before. A Nakagami channel serves as a general model for fading channels; Rayleigh, Rice, and one-sided gaussian can be viewed as special cases of Nakagami-m distribution. Different family of the Nakagami distributions were presented and our simulations show perfect match.

Diversity is one of most widely applied techniques to mitigate fading, and hence the performance of the system under diversity has been investigated.

The diversity schemes considered are MRC, EGC, SC and GSC.

Therefore, in the Thesis, the performance of M-QAM over Nakagami fading channel with/without diversity schemes has been derived. In particular we have achieved the following :

- Derived the symbol error probability of MQAM over Nakagami channels with and without diversity.
- Simulated the symbol error probability of MQAM over Nakagami channels with and without diversity and verified the theoretical results derived in this work.
- Simulated the performance of MQAM over Nakagami channels with GSC diversity scheme.
- Studied the effect of different parameters, namely the Nakagami parameter m , the number of diversity channels L and the size of modulation M on the system performance.

The analytical results for the bit error rate performance derived have been validated through computer simulations. In general it can be observed in all the Figures presented that

- For large m , which implies less fading, the BER gets better.
- As the number of channel branches L is increased, the BER gets better, this can be explained thus; there is low probability of deep fade as L increases

- It is clear that the largest incremental gain is obtained in going from single to double diversity. The gain diminishes as the order of diversity increases
- For the diversity schemes considered, the MRC achieves the best performance. In fact, its is the optimal combining scheme for equal energy branches, while the SC has the least performance.
- The performance of GSC ranges between that of MRC and SC.
- For very large L , the performance of EGC is close to that of MRC, for $L=8$, the difference is about 1 dB. Jakes reported 1.05 dB in the limit of an infinite number of branches.
- The performance of GSC-2 is better than MRC-2, since GSC selects the largest two.

4.2 Recommendations for Future work

- Analysis of the performance of M-QAM with GSC over Nakagami fading channels.
- The effect of coding on the performance of M-QAM over Nakagami fading channels.
- The performance of M-QAM over fast or frequency selective Nakagami fading .

- In practice, the measurement of the SNR at the channel output may be difficult or very expensive and as such, the branch with the largest signal-plus-noise (S+N) is used instead. Therefore, a selection diversity system based on SNR may not accurately reflect the performance of more commonly implemented selection diversity systems. The effect of choosing the largest S+N on the performance of different modulation schemes (i.e M-QAM) over Nakagami fading channels can be studied .
- The effect of correlation between the diversity branches on the performance of M-QAM over Nakagami fading channels.
- The effect of channel estimation error on the performance of M-QAM.

Bibliography

- [1] John G. Proakis, *Digital Communications*, NY : McGraw-Hill, New York, second edition, 1989.
- [2] P. A. Bello, "Characterization of randomly time-variant linear channels", *IEEE Trans. Commun Syst*, CS-11(4):360–393, December 1963.
- [3] W. Braun and U. Dersch, "A physical Mobile Radio Channel Models", *IEEE Trans on Veh. Tech.*, VT40(1):472–482, May 1991.
- [4] IEEE Veh. Technl. Soc. Committee on Radio Propagation. *IEEE Trans. Veh. Technl.*, 37:57–60, February 1988.
- [5] U. Charash, "*A study of multipath reception with unknown delays*", PhD thesis, University of California, Berkeley, 1974.
- [6] U. Charash, "Reception through Nakagami fading multipath channels with random delays", *IEEE Trans. Commun Syst*, COM-27:657–670, April 1979.
- [7] H. B. James and P. I. Wells, "Some tropospheric scatter propagation measurements near the radio-horizon", *Proc. IRE*, pages 1336–1340, October 1955.

- [8] G. R. Sugar, "Some fading characteristics of regular VHF ionospheric propagation", *Proc. IRE*, pages 1432–1436, October 1955.
- [9] S. Basu, E. M. Mackenzie, E. Costa, P. F. Fougere, H. C. Carlson, and H. E. Whitney, "250 MHz/GHz scintillation parameters in the equatorial, polar, and aural environments", *IEEE J. Select. Areas Commun.*, SAC-5:102–105, Feb 1987.
- [10] T. L. Staley, R. C. North, W. H. Ku, and J. R. Zeidler, "Performance of coherent MPSK on frequency selective slowly fading channels", *Proc. IEEE Veh. Technol. Conf.*, VTC'96:784–788, April 1996.
- [11] T. L. Staley, R. C. North, W. H. Ku, and J. R. Zeidler, "Channel estimated-based error probability performance prediction for multichannel reception of linearly modulated coherent systems on fading channels", *Proc. IEEE Mil. Commun. Conf. MILCOM'96*, October 1996.
- [12] T. L. Staley, R. C. North, W. H. Ku, and J. R. Zeidler, "Probability of error evaluation for multichannel reception of coherent MPSK over Ricean fading channels", *Proc. IEEE Int. Conf. on Commun. ICC'97*, pages 30–35, June 1997.
- [13] Gordon L. Stuber, *Principles of Mobile Communications*, Upper Saddle, NJ: Kluwer Academic, 1996.
- [14] K. A. Stewart, G. P. Labedz, and K. Sohrabi, "Wideband channel measurements at 900 MHz", *Proc. IEEE Veh. Technol. Conf. VTC'95*, pages 236–240, July 1995.

- [15] R. J. C. Bultitude, S. A. Mahmoud, and W. A. Sullivan, "A comparison of indoor radio propagation characteristics at 910 MHz and 1.75 GHz", *IEEE J. Select. Areas Commun*, SAC-7:20–30, January 1989.
- [16] T. S. Rappaport and C. D. McGillem, "UHF fading in factories", *IEEE J. Select. Areas Commun*, SAC-7:40–48, January 1989.
- [17] G. H. Munro, "Scintillation of radio signals from satellites", *J. Geophys. Res*, 68, April 1963.
- [18] P. D. Shaft, "On the relationship between scintillation index and Rician fading", *IEEE Trans. Commun.*, COM-22:731–732, May 1974.
- [19] M. Nakagami, *The m-distribution a General Formula of Intensity Distribution of Rapid Fading in statistical methods in radio wave propagation*. Hoffman ed. Oxford: England, 1960.
- [20] H. Suzuki, "A Statistical Model for Urban Multipath Propagation", *IEEE Transaction on Communications*, COM-25(7):673–690, July 1977.
- [21] P. J. Crepeau, "Coding Performance on Generalized Fading Channels". *MIL-COM'88 conference proceedings*, 23-26:15.1.1–15.1.7, October 1988.
- [22] A. H. Aghvami, "Digital modulation techniques for mobile and personal communication systems", *Electronics and communication Engineering Journal*, pages 125–132, June 1993.
- [23] Seiichi Sampi, "*Applications of Digital wireless Technologies to Global Wireless Communications*", Upper Saddle,NJ: Prentice Hall, 1997.

- [24] Murota K. and Hirade K, "GMSK Modulation for Digital Mobile Radio Telephony ", *IEEE trans. in comm.*, COM-29(7):1044–1050, July 1980.
- [25] Kinoshita K. et al, "Evaluation of 16 Kbits/s Digital Voice Transmission ", *IEEE trans. in comm.*, VT-33(4):321–326, November 1984.
- [26] Honma K. et al, "On a Method of Constant Envelope Modulation for Digital Mobile Communications ", *IEEE ICC 80*, pages 24.1.1–24.1.5, June 1980.
- [27] Akaiwa Y. et al, "Performance of Baseband Bandlimited multi-level FM with Discriminator detection for Digital Mobile Telephony", *Trans. IECE Japan*, E64:463–469, July 1981.
- [28] F.D Jager and Dekker C.B, "Tamed Frequency Modulation, A Novel Method to Achieve Spectrum Economy in Digital Transmission ", *IEEE trans. in comm.*, COM-26(5):532–542, May 1978.
- [29] Akaiwa Y. and Nagata Y, "Highly Efficient Digital Mobile Communications with a Linear Modulation Method ", *IEEE Journal on Selected Areas in comm.*, 5(5):890–895, June 1987.
- [30] Feher Kamilo, "*Wireless Digital Communications, Modulation and Spread Spectrum applications* ", Upper Saddle,NJ: Prentice Hall, 1995.
- [31] RCR, "Digital Cellular telecommunication systems", *RCR*, STD-27, April 1991.

- [32] EIA, "Dual-mode subscriber equipment compatibility specification", *EIA specification IS-54*, 2215, May 1990.
- [33] Bateman A, "Feedforward Transparent Tone-in-Band its Implementation and Applications", *IEEE trans. Veh. Tech.*, 39(3):235–243, August 1990.
- [34] Hanzo et al, "A Subband Coding BCH Coding and 16QAM System for Mobile Radio Speech Applications", *IEEE trans. Veh. Tech.*, 39(4):327–339, November 1990.
- [35] RCR, "Digital MCA System", *RCR*, STD-32, November 1992.
- [36] RCR, "Digital Public Private Mobile Radio Systems", *RCR*, STD-29, December 1993.
- [37] Davidson A. and Marturano L, "Impact of Digital Techniques on Future LM Spectrum Requirement", *IEEE Veh. Tech. Soc. News*, pages 14–30, May 1993.
- [38] S. Sampei and Sunaga T, "Rayleigh Fading Compensation for QAM in Land Mobile Radio Communications", *IEEE trans. Veh. Tech.*, 42(2):137–147, May 1993.
- [39] S. Sampei, "Performance of trellis coded 16-QAM/TDMA system for land mobile communications", *Proc. IEEE Conf. on Commun*, pages 1953–1957, June 1990.

- [40] Williams C. Jakes, *Microwave Mobile Communication*, J. Wiley and son, New York, 1974.
- [41] W. Lee, *Mobile Communications Engineering*, NY : McGraw-Hill, New York, 1982.
- [42] M. Schwartz, W. R. Bennett, and S. Stein, *Communication Systems and Techniques*, NY:McGraw-Hill, New York, 1966.
- [43] D. Brennan, "Linear diversity combining techniques", *Proc. IRE*, 47:1075–1102, June 1959.
- [44] N. Kong, T. Eng and L. B. Milstein, "A selection combining scheme for RAKE receivers", *Proc. IEEE Int. Conf*, pages 426–429, November 1995.
- [45] T. Eng, N. Kong and L. B. Milstein, "Comparison of diversity combining techniques for rayleigh fading channels", *IEEE Trans. Commun*, 44:1117–1129, Sept 1996.
- [46] N. Kong and L. B. Milstein, "Combined average SNR of a generalized diversity selection combining scheme", *Proc. IEEE Int. Conf. Commun*, ICC98:1556–1560, June 1998.
- [47] A. H. Wojnar, "Unknown Bounds On Performance in Nakagami Channels ", *IEEE trans. on Comm.*, COM-34(1):20–25, Jan 1986.

- [48] Miyagaki Y. Morninaga N. and Namekkawa T, "Error probability characteristics for CPSK signals through m-distributed fading channel", *IEEE Trans on com*, COM-26(1):88-100, January 1978.
- [49] V. Aalo and S. Pattaramali, " Average Error Rate for Coherent MPSK Signals in Nakagami FAding Channels", *Electronic Letters*, 32(17):1538-1539, August 1996.
- [50] G. Fedele, "Error Probability for detection of M-DPSK Signals in Slow Non-Selective Nakagami FAding ", *Electronics Letters*, 30(8):620-621, April 1994.
- [51] M. Tanda, "Bit Error Rate of DQPSK Signals in Slow Nakagami Fading ", *Electronic Letters*, 29(5):431-342, March 1993.
- [52] E. K. Al-hussaini and A. A. M. Al-bassiouni, "Performance of MRC diversity systems for the detection signals with Nakagami fading", *IEEE Trans on Comm.*, COM-33(12):1315-1319, December 1985.
- [53] T. Eng and L. B. Milstein, "Coherent DS-CDMA performance in Nakagami multipath fading", *IEEE Trans on Comm.*, COM-43(2/3/4):1134-1143, Febr/March/April 1995.
- [54] G. Eftymoglou V. Aalo and H. Helmken, "Performance analysis of coherent DS-CDMA systems in Nakagami fading with arbitrary parameters", *IEEE Trans on Veh. Technol.*, VT-46:289-297, 1997.

- [55] C. Tellambura A. Annamala and V. K. Bhargava, "Efficient Computation of MRC Diversity Performance in Nakagami Fading Channel with arbitrary parameters", *Electronics Letter*, 34(12):1189–1190, June 1998.
- [56] V. A. Aalo, "Performance of maximal-ratio diversity systems in correlated Nakagami-fading environment", *IEEE Trans on Comm.*, COM-43:2360–2369, Aug 1995.
- [57] G. Fedele and M. M. Rao, "MRC performance of binary signals in Nakagami fading with general branch correlation", *IEEE Trans on Comm.*, COM-47(1):44–52, January 1999.
- [58] Q. T. Zhang, "Maximal-Ratio combining over Nakagami fading channels with an arbitrary branch covariance matrix", *IEEE Trans on Veh Tech.*, 48(4):1141–1150, July 1999.
- [59] N. C. Beaulieu A. A. Abudayya, "Analysis of equal gain diversity on Nakagami fading channels", *IEEE Trans on Comm.*, COM-39(2):225–233, February 1991.
- [60] N. C. Beaulieu, "An infinite series for the computation of the complementary probability distribution function of a sum of independent random variables", *IEEE Trans on Comm.*, COM-38:1463–1474, Sept 1990.
- [61] J. F. Weng and S. H Leung, "Bit error Probability of MDPSK in Nakagami Fading Channels", *Electronics letters*, 33(20):1675–1676, September 1997.

- [62] J. F. Weng and S. H. Leung, "Analysis of DPSK with equal gain combining in Nakagami fading channels", *Electronics Letters*, 33(8):654–656, April 1997.
- [63] M. A. Blanco, "Diversity receiver performance in Nakagami fading", *Proceedings of IEEE Southeastern Conf*, pages 529–532, 1983.
- [64] Ramesh Sannegowda and V. Aalo, "Performance of Selection Diversity Systems in a Nakagami Fading environment ", *IEEE 94*, 1(1):190–195, January 1994.
- [65] G. Fedele, "Error probability for diversity detection of binary signals over Nakagami fading channels", *PIMRC*, pages 607–611, 1994.
- [66] E. K. Al-hussaini and A. M. Al-bassiouni, "Performance of an ideal switched diversity receiver for NCFSK signals with Nakagami fading", *Trans. IECE*, E-65(12):750–751, December 1982.
- [67] O. C. Ugweje and V. A. Aalo, "Performance of selection diversity system in correlated Nakagami fading", *IEEE*, 1997.
- [68] A. S. Krishnamoorthy and M. Parthasarathy, "A multivariate gamma-type distribution", *Annals Math Statist*, 22:549–557, 1951.
- [69] M. K. Simon and M. S. Alouini, "A unified approach to the performance analysis of digital communication over generalized fading channels", *Proceedings of IEEE*, 86(9):1860–1877, September 1998.

- [70] M. K. Simon and M. S. Alouini, "A unified approach to the probability of error for noncoherent and differentially coherent modulations over generalized fading channels", *IEEE Trans on Comm*, 46(12):1625–1638, December 1998.
- [71] M. K. Simon and M. S. Alouini, "A unified performance analysis of digital communication with dual selective combining diversity over correlated Rayleigh and Nakagami-m fading channels", *IEEE Trans on Comm*, 47(1):33–43, January 1999.
- [72] M. K. Simon and M. S. Alouini, "Performance of coherent receivers with hybrid SC/MRC over Nakagami-m fading channels", *IEEE Trans on Veh. Tech.*, 48(4):1155–1164, July 1999.
- [73] J. W. Craig, "A new simple and exact result for calculating the probability of error for two-dimensional signal constellations", *Proc. IEEE Milit. Comm. Conf. MILCOM'91*, pages 571–575, Oct. 1991.
- [74] S. Sampi and T. Sunaga, "Performance of multi-level QAM with post-detection maximal ratio combining space diversity for digital land-mobile radio communications", *IEEE Trans. on Veh. Tech.*, 42(3):294–301, August 1993.
- [75] C. J. Kim, Y. S. Kim, G. Y. Jung and H. J. Lee, "BER analysis of QAM with MRC space diversity in Rayleigh fading channel", *Proc. PIM RC95*, pages 482–485, September 1995.

- [76] J. Lu, T. T. Tjhung and C. C. Chai, "Error probability performance of l-branch diversity reception of MQAM in Rayleigh fading", *IEEE Trans. on Comm*, 46(2):179–181, February 1998.
- [77] G. S. Mahrokh and A. Aghamohammadi, "On the error probability of linearly modulated signals on frequency-flat Ricean, Rayleigh and AWGN channels", *IEEE Trans. on Comm*, 43(2/3/4):1454–1466, Febr/March/April 1995.
- [78] Sandeep Chennakeshu and John B. Anderson, "Error Rates for Rayleigh Fading Multichannel Reception of MPSK Signals", *IEEE Trans on Comm.*, COM-43(2/3/4):338–346, Febr/March/April 1995.
- [79] M. S. Alouini, "*Adaptive and Diversity Techniques for Wireless Digital Communications over Fading Channels*", PhD thesis, California Institute of Technology, 1998.
- [80] I. S. Gradshteyn and I. M. Ryzhik, *Table of Integrals, Series, and Products*, San Diego, CA: Academic, 1994.
- [81] Gennaro Fedele, "Error Probability for Diversity Detection of Binary Signals Over Nakagami Fading Channel ", *IEEE 94*, 1(1):1–1, January 1994.